Stability Analysis of Caves in Gaziantep Region

M. Sc. Thesis
in
Civil Engineering
University of Gaziantep

Supervisor
Assist. Prof. Dr. Hanifi ÇANAKCI

by

Ahmet Ersin BİRCAN

T.C.
GAZİANTEP UNIVERSITY
GRADUATE SCHOOL OF
NATURAL and APPLIED SCIENCES
CIVIL ENGINEERING

Name of the thesis: Stability Analysis of Caves in Gaziantep Region

Name of the student: Ahmet Ersin BİRCAN

Exam date: 13.06.2007

Approval of the Graduate School of Natural and Applied Sciences

Prof. Dr. Sadettin ÖZYAZICI
Director

I certify that this thesis satisfies all the requirements as a thesis for the degree of Master of Science.

Assoc. Prof. Dr. Mustafa GÜNAL
Head of the Department

This is to certify that we have read this thesis and that in our opinion it is fully adequate, in scope and quality, as a thesis for the degree of Master of Science.

Assist. Prof. Dr. Hanifi ÇANAKCI
Supervisor

Examining Committee Members

Prof. Dr. Mustafa LAMAN ____________________

Assist. Prof. Dr. Hanifi ÇANAKCI ____________________

Assist. Prof. Dr. Hamza GÜLLÜ ____________________

Assist. Prof. Dr. Erhan GÜNEYİSİ ____________________

Assist. Prof. Dr. Mehmet GESOĞLU ____________________

Bu kitabı,
Eğitimim boyunca her türlü desteği severek veren
anneme, babama ve kız kardeşime
ithaf ediyorum.

ABSTRACT

STABILITY ANALYSIS OF CAVES IN GAZİANTEP REGION

BİRCAN, Ahmet Ersin
Master of Science in Civil Engineering
Supervisor: Assist. Prof. Dr. Hanifi ÇANAKCI
June 2007, 102 pages

Limestone, which can be easily shaped and used as dimension stone at the house construction, cover extensive area of Gaziantep. In the past, people living in the region had opened many stone mines. Due to the increasing of residential areas at the city, these mines started to be used as caves and now they exist in the urban areas, which cause danger. Some people are living over those caves and some are working in the caves. The objective of this work is to investigate the collapse risk potential of existing caves in the city center. The caves were modeled using geometrical dimensions and geotechnical properties of the rock. Totally, 15 caves were analyzed using Plaxis finite element code V8, 2D program. A 300 kPa foundation load applied to roof of the cave. The results from the analysis showed that all the investigated caves are safe against failure under existing studied conditions.

Key words: Stability Analysis, PLAXIS, Caves, Limestone, Factor of safety

ÖZET

GAZİANTEP BÖLGESİNDEKİ MAĞARALARIN STABİLİTE ANALİZLERİ

BİRCAN, Ahmet Ersin
Yüksek Lisans Tezi, İnşaat Mühendisliği
Tez Yöneticisi: Yrd. Doç. Dr. Hanifi ÇANAKCI
Haziran 2007, 102 Sayfa

Kolayca şekil alabilen ve kesme taş olarak ev yapımında kullanıma uygun olan kireştaşı, Gaziantep bölgesinin geniş bölümünü kapsamaktadır. Bu amaçla geçmişte bölge insanları birçok taş ocakları açmışlardır. Şehirde yerleşim alanlarının artmasıyla, bu ocaklar mağara olarak günümüzde insanların yaşadığı alanların ortasında tehlike oluşturacak şekilde bulunmaktadırlar. Bazı insanlar bu mağaraların üzerinde inşa edilen evlerde yaşamakta, bazıları ise bu mağaraların içlerinde çalışmaktadırlar. Bu çalışmanın amacı şehir merkezinde bulunan mevcut mağaraların göçmeye karşı risk değerlendirilmelerinin yapılmasıdır. Mağaraların geometrik ölçüleri ve kayanın geoteknik özellikleri kullanılarak modellemeler yapıldı. Toplam olarak 15 mağaranın, sonlu elemanlar yöntemine göre çalışan Plaxis V8, 2D programıyla, analizleri gerçekleştirildi. Mağara tavanının üzerine 300 kPa yük uygulandı. Analiz sonuçları, incelenen tüm mağaraların, mevcut çalışma koşulları altında göçmeye karşı güvenli olduğunu göstermiştir.

Anahtar kelimeler: Stabilite Analizleri, PLAXIS, Mağaralar, Kireçtaşı, Güvenlik katsayısı

ACKNOWLEDGEMENTS

I would like to express my gratefulness to Assist. Prof. Dr. Hanifi ÇANAKCI for his advices, support and patience at each step of this study. It has always been a pleasure to work with such academicians.

I would like to express my warmest and deepest appreciation to my sister, Müjde for her unconditional support at any time throughout my education.

I should also thank to my mother and father from whom I have always received spiritual and remarkable support who made me strong all the time.

My special thanks are extended to Dr. Mustafa ŞAHMARAN, Tahir KIMILDAR from STFA Construction Inc. and Müge İNANIR from GEOGRUP Construction Inc. for answering my questions each time whenever I need their help.

TABLE OF CONTENTS

LIST OF FIGURES

LIST OF SYMBOLS

E	Young's Modulus
Φ	Internal angle of friction
c	Cohesion
K_0	Coefficient of Lateral Earth Pressure
E_{RM}	Deformation modulus of a rock mass
UCS	Unconfined compressive strength
σ_{ucs}	Unconfined compressive strength of rock
R_N	Schmidt Hammer Value of N-type
R_L	Schmidt Hammer Value of L-type
GSI	Geological strength index
D	The disturbance factor
Tmf	Fırat formation
Tmga	Gaziantep Formation
σ_N	Actual normal stress
ΣMsf	Total multiplier
τ_{max}	Maximum value of shear stress
τ	Value of shear stress
τ_{rel}	Relative shear stress
c_r	Reduced Cohesion
Φ_r	Reduced internal angle of friction

LIST OF TABLES

CHAPTER 1

INTRODUCTION

1.1 General

Gaziantep province extends over a territory of 7,642 km^2. Its population is 1,293,849 according to the provisional results of the Population Census of 2000. Besides central district, its peripheral districts are Araban, İslahiye, Kargamış, Nizip, Nurdağı, Oğuzeli, Şahinbey, Şehitkamil and Yavuzeli **(www.gap.gov.tr)**.

The province of Gaziantep, which has kept its geographical importance for years, was used to be on the Silk Way in the past, and is situated on the border of the Mediterranean Region, South East Anatolia, and Syria. Now Gaziantep is the most developed province of all Southeastern Anatolia in terms of industrial and commercial activities. Because of this reason, the city takes a lot of emigrants from other parts of Turkey which makes the city to have to enlarge and construct new living areas for those people. While Gaziantep is taking immigrants from other cities, it is getting harder for governments and municipalities to facilitate and organize the places for those people to live. So that people are constructing their own houses to the suitable places close by the city center sometimes legally sometimes illegally. Consequently, because of lack of information, some people are building their houses at a district where the caves present, and these caves could cause serious hazards at an event of subsidence.

In Gaziantep, there is a region which has caves situated close to surface. During the development of the city, many structures were constructed over these caves. They are generally single, two and three-story residential houses. Most of the structures were constructed without conducting any geotechnical investigation **(Çanakcı 2007).**

Moreover some people have their houses or working places in these caves. People living at that region are under danger and there is a problem due to the risk of collapsing of caves at these housing areas.

One of these caves, which is in Şahinbey Aydınbaba Region, collapsed suddenly on the 28 March 2003 in the evening. Nobody living in that part noticed any signs of subsidence before the event. With this subsidence, five houses were collapsed abruptly. Five people living in these houses were rescued, but one of them died.

In the second case, a cave located in Hamdi Kutlar Street, a busy road, collapsed on the 13th April 2005 with no reported injury to people or damage to the buildings. Both events triggered wide media interest and caused great concern among people.

After these tragic events, the danger of structures over caves is noticed. And the questions of the stability problem of these caves begin to take part in minds. This event was initiated this area to be on focus, and was selected as the investigation area.

The caves at shallow depths situated in the city center have a potential risk to collapse, and cause damage for people and structures being near these caves. There is a growing concern among public for the caves which has a potential to collapse suddenly. Therefore this study involves the stability analysis of these caves against failure. The results of this study may be used to prevent possible collapses that can occur in the future.

1.2 Objectives

Briefly the objectives can be set as:

a) To obtain geometry of caves and properties of cave rock.
b) To make a stability analysis of the caves using Plaxis V8 - 2D program.
c) To assess the risk of failure of the caves.

1.3 Organization of the Thesis

The thesis is divided into 5 chapters, which are arranged as follows;

Chapter 1 includes a general view of the study by establishing the problem, giving the objectives.

A literature review of the general properties of caves and the geology of Gaziantep are given in chapter 2.

In chapter 3, the computer programs used in this study was explained, and it is clarified how to gather the geotechnical parameters for analysis.

Chapter 4 includes the results of models and discussion is done.

Chapter 5 contains the conclusions drawn from this research work and the recommendations for future study are given.

CHAPTER 2

LITERATURE SURVEY

2.1 Introduction

In different parts of the world, man-made caves can cause problems for people living at city centers. One of them, from Nottingham city (UK) reported that hundreds of man-made artificial caves that had been cut into outcrops of Triassic Sherwood sandstone, by **Waltham (1993)**. Subsidence of some caves was reported. The author studied on the caused of the collapse of the Stanford Street crown hole along with previous collapses. Geotechnical properties of the Sherwood sandstone, especially the strengths of the saturated and dry states of the cave material were analyzed. The author states that intact rock strength is closely related to the degree of weathering. Unconfined compressive strength of the material decreases from over 30 MPa at depths greater than 10 m to around 1 MPa close to rock head. The collapse of the Stanford Street crown hole roof was mainly attributed to the loss of strength of sandstone (40-80%) due to saturation caused by leakage from water pipes.

Another study was done by **Çanakcı (2007)** for the collapsed caves in Gaziantep. This work is one of the most current and comprehensive investigation on caves in the city of Gaziantep. The study mainly focuses on an investigation of the possible causes for the collapse of man-made limestone caves, which are at a shallow depth, of various width and length. These caves were mainly excavated to provide work or storage space. He initiated this study after the events of the collapses of two shallow man-made caves, which triggered wide media coverage and caused great concern among people. The study clearly states that the existence of caves at shallow depths in the city center is a potential hazard for the structures over and around these caves. Therefore, the author suggests that the construction of any structures in the area should be done with special consideration. During his study, a total of 17 caves were identified and their dimensions were measured. Interviews with local people were conducted in order to gather more information about the caves. It is discovered that there are a lot of collapsed caves in the city. However, information on the time, cause and size of the collapsed caves were not documented. Almost all the collapsed caves were filled and rearranged as parks. In the study, main focus was made on two recently collapsed caves named Hamdi Kutlar (Figure 2.1.) and Karakabir (Figure 2.2.).

Figure 2.1. One of the collapsed caves at Hamdi Kutlar Street in Gaziantep

The author gives information about the collapsed caves after making an introduction. At this part of the work, the location, history, dimensions and the nearby structures of the caves were investigated and explained. After the section of the information on caves, he gave brief information about the geology of the site. Afterwards, he determined the geological and geotechnical properties of limestone and made a visual inspection on the collapsed caves. Potential causes of failure, which are loss of strength of the rock material due to saturation, discontinuities, weathering and vibrations were investigated and discussed. Finally it was concluded that the reduced strength of the limestone due to sewer pipe leakage and surface water combined with additional loads coming from traffic and structures were shown main reason for these collapses.

Figure 2.2. One of the collapsed caves called Karakabir in Gaziantep

One other study was done by **Waltham and Park (2002)**. They reported the existence of 59 lave tubes in Cheju Island, South Korea. At their study, the focus was made on three different causes for the failure of the tube roof, which are: subsidence of the thin roof during the flow of lave, minor earthquakes that are common on active

Figure 2.3. The housing above a cave in the study of Waltham and Park (2002)

volcanoes and weakening of the thin arches above the lava tubes by weathering affect. The authors mainly worked on three different locations, which are Manjang Gul, Sung Gul and Cheamchon Gul. At these locations, microgravity survey was found out to be the most useful method to verify the location of lava tubes during subsurface investigation. From their study, the entrance to a lava tube can be seen in Figure 2.3., where the entrance lies between the houses, and the cave was used as cool storage.

In the study, a notable feature of Manjang Gul location, which is the large size of its tube, was investigated. Much of it is 15 m wide and 10 m high, and some sections are 20 – 25 m wide. The entrance of the tube is through a simple natural collapse, about 12 m across, where the original tube rose slightly and the roof was less than 4 m thick. It is explained in the study that the cave is now a popular tourist site. The entrance of the cave is in a high level loop off the main tube, and there are two tubes merge at the lower level, beneath solid rock over 10 m thick (Figure 2.4.).

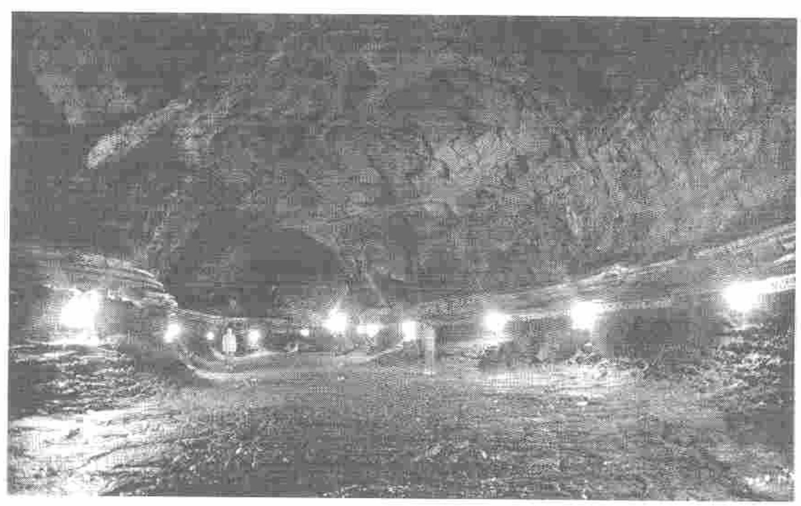

Figure 2.4. The large main tube in the study done by Waltham and Park (2002)

In other region, Sung Gul, the authors pull the readers' attention to a road over a cave. In Cheju Island, the main road over the Sung Gul tube, and some local roads over the tube in different points were studied. The road was a rough track until 1961, when it was paved. Then it was widened into two and finally four lanes in 1998. The cave was not realized until it was found in 1994 during the site investigation for the last phase of road widening. However the diversion of the road was not considered, as since the line was already established, and purely by good luck, the line of the road lay over the most stable part of the cave, where a smooth arch barely 6 – 10 m wide rises 2 m above a clean floor of lava (Figure 2.5.).

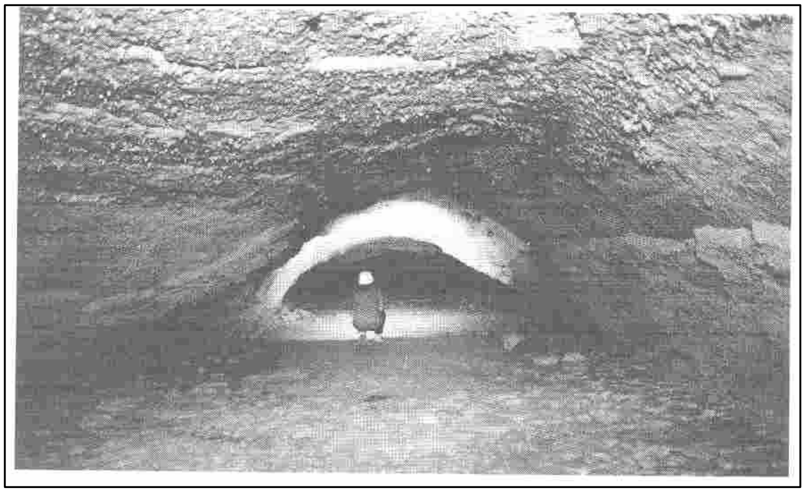

Figure 2.5. A stable arch of lava tube in the study done by Waltham and Park (2002)

The roof shape of the caves at the region of the Sung Gul was investigated by authors. Due to their investigation, most of the roof of the tube is a broad, flat arch, with small glaze structures. The tube is 14 m wide in some sections with an almost flat roof that show no sign of collapse. However the authors observed that some small sections of this tube have some fallen away at its roof (Figure 2.6.).

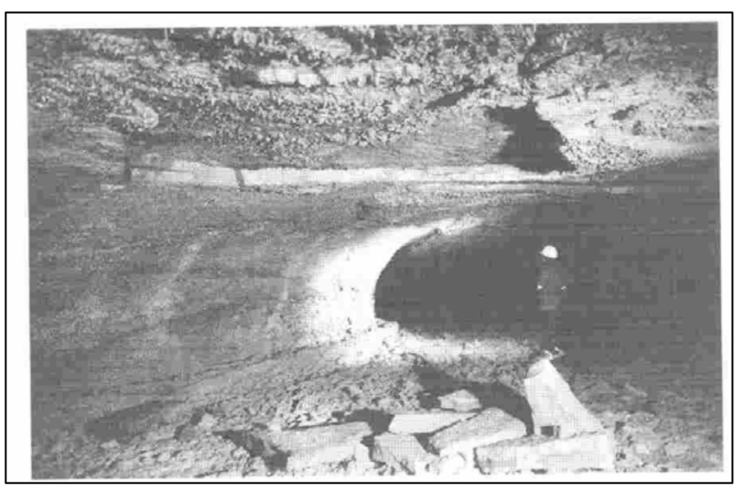

Figure 2.6. Minor breakdown of the roof in a lava tube (Waltham and Park 2002)

The authors advices the direct exploration and mapping of tubes from accessible collapse entrances as the cheapest method of establishing their positions, but the problem is stated as many tubes exist without known accessible entrances.

The authors recommended a simple guide for checking the stability of the lave tube roof. It is the tube width (W) to cover thickness (T) ratio. A ratio of (W/T) > 3 is suggested to be unsafe and prone to failure of the lava tube roof. Finally, they stated that highways and light structures can stand in full safety above the great majority of lava tubes, but heavy structural loadings should only be applied to basalt lava after appropriate investigation of the local ground conditions.

One other study was done by **Waltham and Swift, 2004** about the bearing capacity of rock over mined cavities in Nottingham, UK. It was a similar study, which was done by the same author at the same location in 1993. This study covers a problem that cause a significant geological hazard in Nottingham, UK by hundreds of man-made caves cut in the weak sandstone beneath the city centre.

Stability of the caves has been assessed by a single full-scale loading test (Figure 2.7.), by physical modeling in plaster (Figure 2.8) and by numerical modeling with FLAC (Figure 2.9). The authors make a start with an introduction, which gives information about ground cavities and their potential hazards for many construction projects. At this part, the reader understands the material type of the caves, which is sandstone, the dimension of the caves that most of them are 3 – 5 m wide, and up to 10 m long, and about the history of these caves. Then the authors give details about the strength of the sandstone at the region. The sandstone in which the Nottingham caves have been excavated is a fine-grained material, which the sandstone loses its strength when it is saturated, but recovers when it is subsequently dried. The study concludes that for the typical caves 4m wide, bearing capacity of the rock roof rises from 2 MPa where it is 1m thick to 8 MPa where 3m thick. Some of the results of the study are; stability decreases over wider caves and where the loading pad edge is over the edge of the cave. As solution the author's advice that: Numerical modeling of a very wide cave revealed the failure mechanisms and also showed that an internal support wall increased roof bearing capacity by 50% (Figure 2.10.).

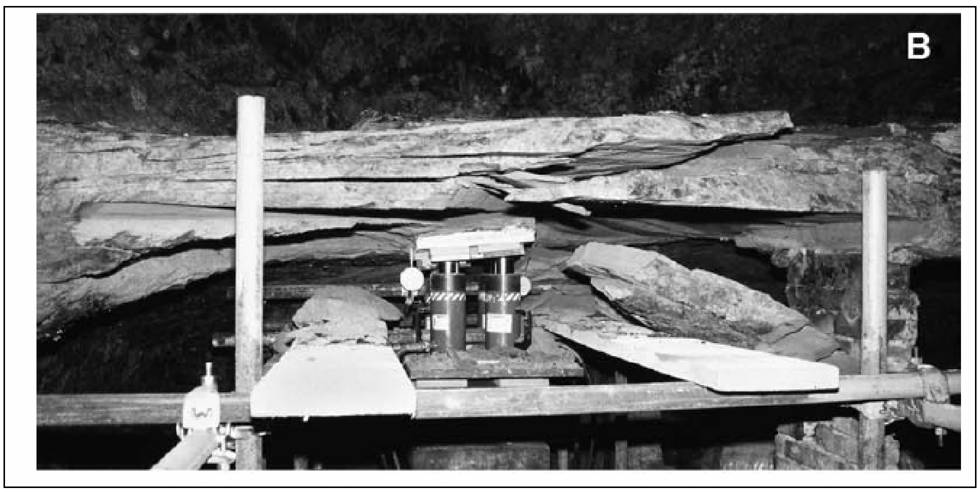

Figure 2.7. (A) Loading Test before applied **(B)** Loading Test after applied

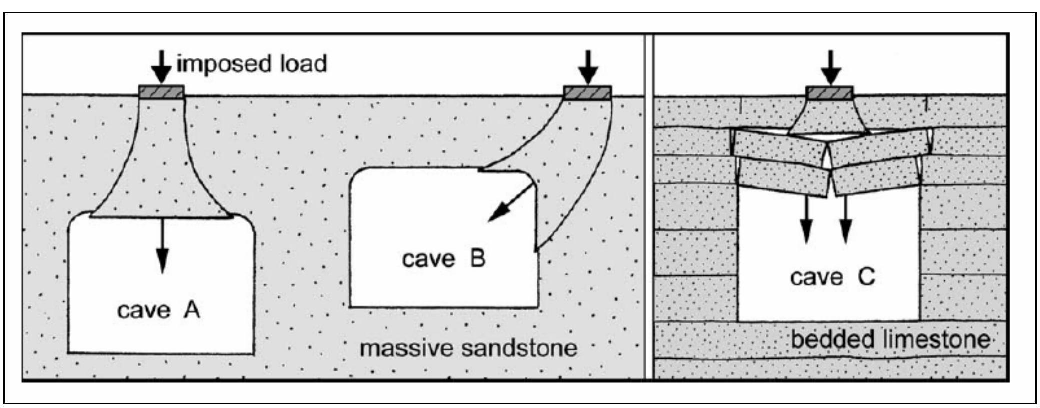

Figure 2.8. Plaster model of a cave in Nottingham (Waltham and Swift, 2004)

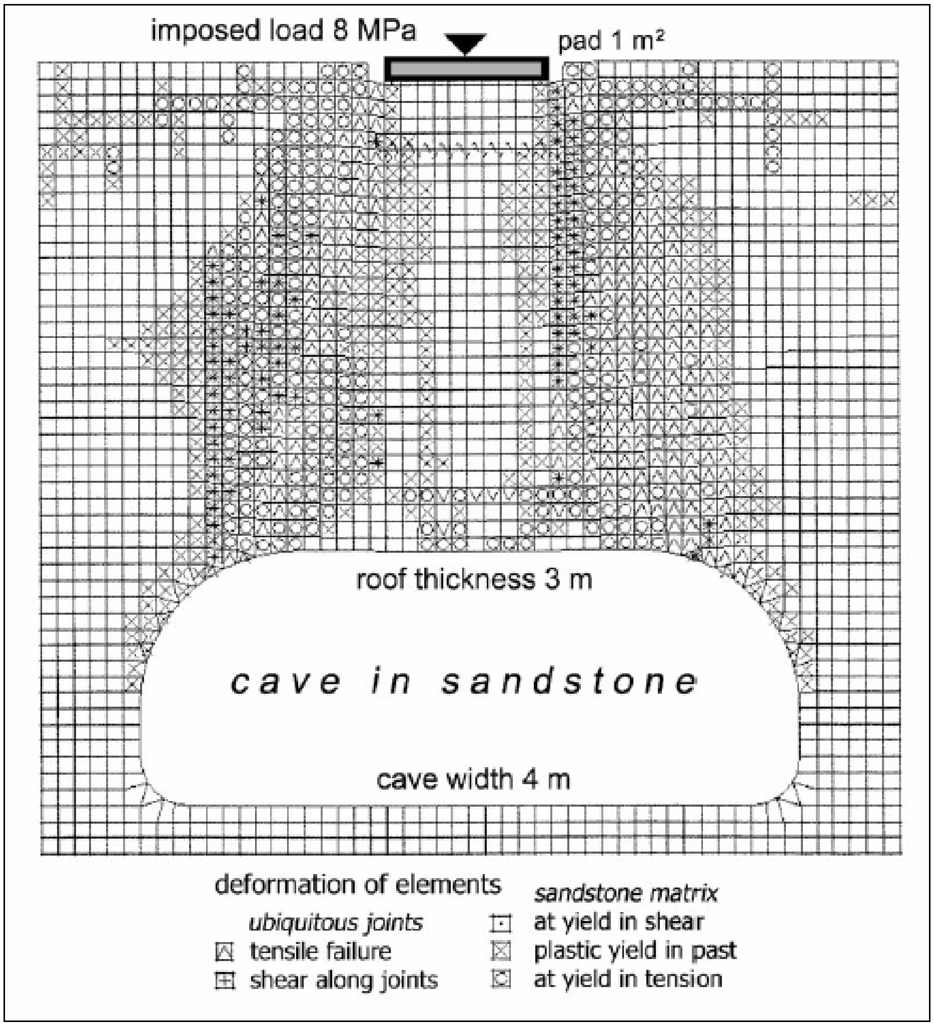

Figure 2.9. Numerical model of a simple plug failure with central loading over a cave roof with FLAC

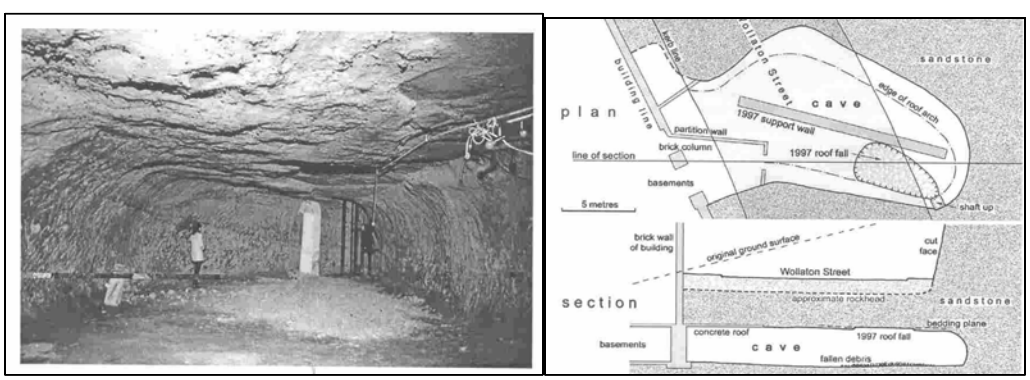

Figure 2.10. A wide cave in sandstone before a central support wall was built within it before a roof fall occurred, and the outline plan of the cave after central support wall was built (Waltham and Swift 2004).

In Gaziantep region, there is another study done by **Güzelbey (2004)** for analysis of the stability of a single cave. At this study, the stability problems of caves were investigated and cave settlements were measured due to the change of cover thickness, modulus of elasticity, and unit weight and water absorption ratios with a finite element software program. The study includes two dimensional models and analysis of a cave with variable cover thickness. It is found that the changes in cover thickness affect vertical displacement and consequently the stability of the cave.

Caves in Gaziantep city center have potential risk to collapse, and cause geological hazards. Therefore this study aims to analyze the caves which have risk to collapse, and help to prevent the potential cave failures in the future.

2.2 Caves in Gaziantep

The caves can be occurred in two ways. One is from natural ways, and the other one is man-made caves. Especially the rocky ground which consists of limestone is suitable to have caves through natural ways or due to the man activities. From natural ways, if precipitation water would meet with carbon dioxide and botanical waste, then the carbonic acids would damage the cave and the gaps would occur in the rocks, and these kinds of caves are generally in deep. Moreover they are not that much dangerous as man-made caves, since the size is generally smaller than man-made ones. However man-made caves are generally closer to the surface, and wider in span, and they generally have high risk of subsidence.

The geological formation in Gaziantep is mainly limestone which covers large area in the city. Limestone is also a good material for construction material. Especially it was the most popular construction material for many years until the arrival of concrete systems. Since it was easy to reach limestone in the region and a good material for construction, the stone mines were opened for supplying dimension stones to be used in the constructions in the half part of twentieth century.

Figure 2.11. A cave with structures above it

These opened stone mines in the later years turned to be used as caves in the region. After the caves were formed, due to some advantages such as no cost for construction or thermal advantage etc., these caves were used by the yarn spinners, or used as workhouse, cold storage or depot, etc. Today some of them are still being used for the same purposes.

Therefore, in Gaziantep around the city center a lot of small and medium size caves are existent (Figure 2.11, 2.12 and 2.16). Within time the caves were continued to be used for different purposes such as housing, work place or storage. Today these caves cause danger for the people living at those regions of Gaziantep due to the risk of subsidence.

Figure 2.12. An abandoned cave with a pillar

The caves of this study are generally situated at the old part of the city. There were fifteen caves that are taken into investigation. Dimensions of the caves were taken from the previous studies.

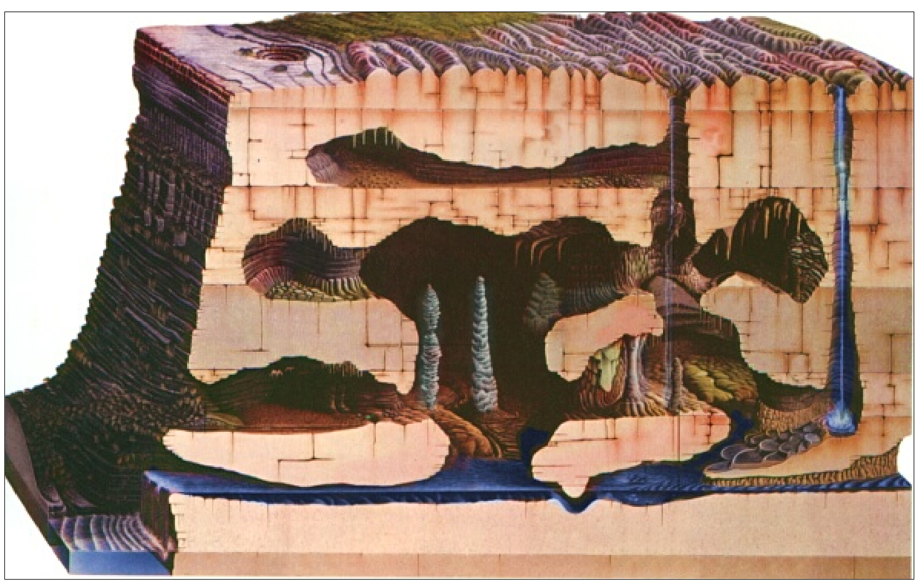

Figure 2.13. The occurrence of a cave from natural ways

The dimensions in width at the caves change from 1.5 m to 33 m. The height of the caves changes from 1.8 m to 14.8 m. The cover thickness of the caves changes from 1m to 10m at the mirror of the cave.

In order to have a better understanding how these caves were occurred, local interviews were held with the people living there for many years.

Figure 2.14. The view of cave at Direkçi Pazarı

Two locals were selected living at the region of Direkçi Pazarı (Figure 2.14.). One is living at that region for more than 50 years, and plus his grandfathers were living in Gaziantep. The other interviewer is living there more than 40 years. From these two interviewers it is understood that the caves are man-made caves in order to supply building material in the past. The rock type of Gaziantep can be easily shaped. This type of rock is soft while cutting from the quarry, and then it becomes harder when it is exposed to the air.

Some of these caves were filled with soil for preventing usage of them, and some of them have been collapsed by the municipality. However most of others are still being used. One of the caves that has the largest opening can be seen in Figure 2.15., which is still in use as a work place.

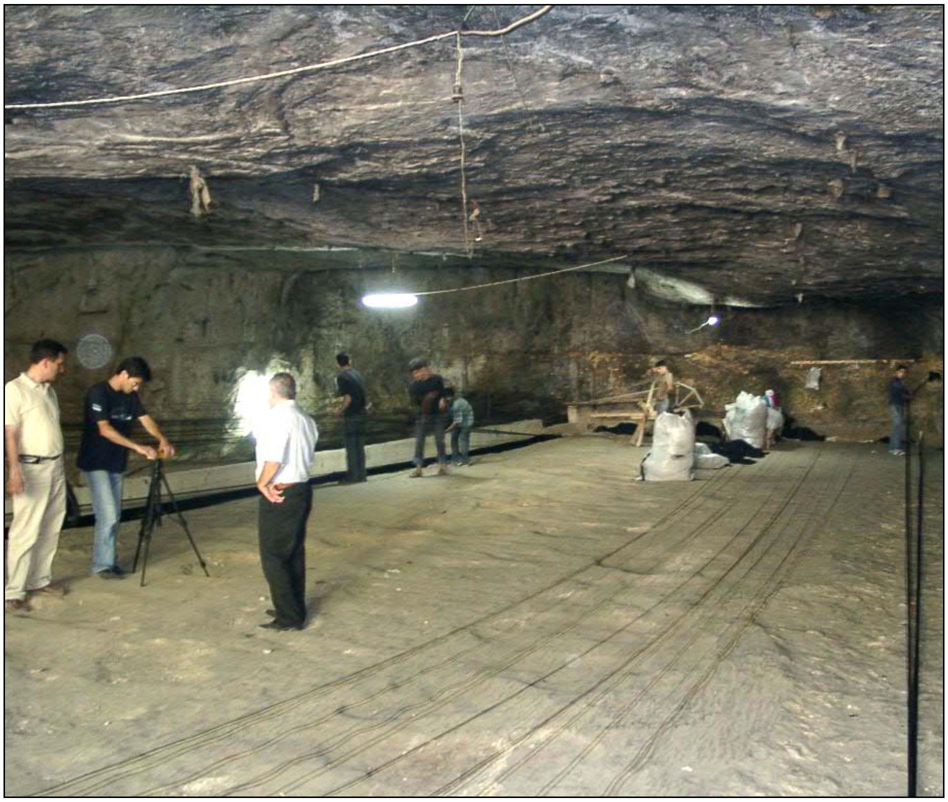

Figure 2.15. A view from a cave called “Sulu Mağara”

Figure 2.16. A view from a cave called “Aydınlar”

Except these caves, people carved some other small caves under their houses for different purposes such as natural cooler, pantry and etc. (Figure 2.17).

Figure 2.17. The view of cave under a house used as storage

2.3 Geology of Gaziantep

A geological map of Gaziantep city prepared by the General Directorate of Mineral Research and Exploration (MTA), Turkey, is shown in Figure 2.18a

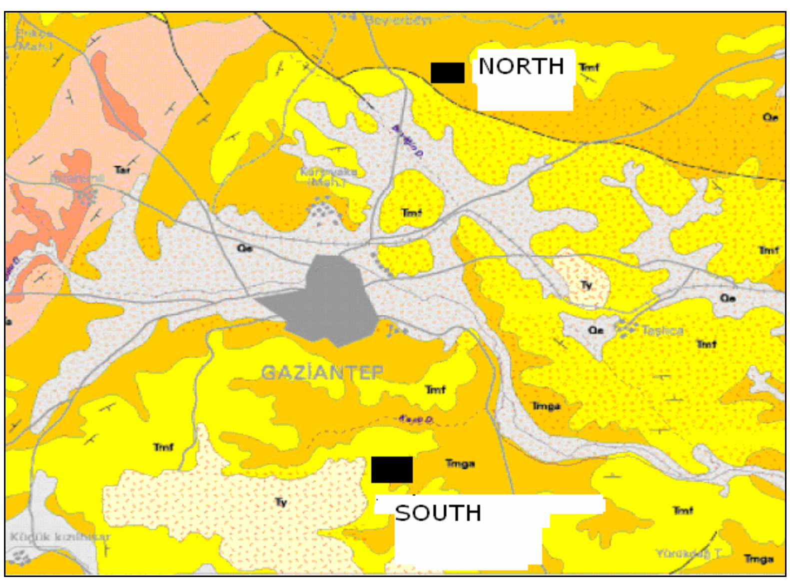

Figure 2. 18a. Geologic map of the Gaziantep **(Terlemez et al., 1997)**

Majority of limestone found in Gaziantep are middle upper Eocene age reefal limestone named as Fırat formation (Tmf) and middle upper Eocene age clayey and chalky limestone named as Gaziantep Formation (Tmga). Thickness of limestone around the region is almost varying from 500 to 1000 m. Gaziantep limestone contains clayey limestone and chalky limestone. Clayey limestone is whitish, grey cream, dirty yellow colored and middle thin layered. Chalky limestone is grey, yellowish grey colored, middle thick layered. In some areas it contains fossils **(Tolun, 1975)**.

Figure 2.18b. Legend **(Terlemez et al., 1997)**

2.4 General Information of Investigated Caves

The previous studies were conducted on most of the caves situated in Gaziantep city region. In order to gain from time, the dataset from previous studies were collected in order to have a better understanding of the geotechnical properties of the rock type of the cave regions, dimensions of the caves and physical properties of the caves and the region. Moreover in order to certify the reliability of the data, some of the caves have been visited and the dataset were collected to check with the previous studies.

The dimensions and the regions of the fifteen selected caves, which are still stable, were given at the Table 2.1.

From the data, it is known that all the caves are at the city center where urban areas were established. The cover thickness of the caves are changing from 1 to 10 meter, where the width of the cave in the span changes from 1.5 to 35 meter, while the height of the cave changes from 1.8 to 15 meter. The depths of the caves are changeable from 3 to 70 meter. Meanwhile the caves are also link to each other, where this information is gathered from the interviews of local people.

The most dangerous caves are the ones with the greater width, height and depth values. That is why the main focus was on the most critical caves, where the site exploration was done in order to see the latest situation of the caves. The first site exploration was done to Cave No: 1, which has the biggest height and width at the span. Due to our observations, inner parts of the caves were collapsed and it is going to be closed by the municipality in the near future.

The second cave, which was investigated, is Cave No: 27 and people are still working in this cave in spite of the risk of collapse. From our investigations, this cave has high risk potential due to some reasons such as the water content of the cave is high, the dimensions of the cave is quite big, the ceiling structure is flat shape, and there are housing on the cave.

Table 2.1.Dimensions and the regions of the caves

Cave no	District	Name of caves	Current status	Cover Thickness (m)	Width (m)	Height (m)	Length (m)
1	İsmet Paşa	Direkçi	Stable	1,8	33	14,8	70,15
2	Kurtuluş	Sumaklı	Stable	7	8,2	2,5	15,5
3	Kurtuluş	Sumaklı	Stable	8	25	6	5,6
4	Kurtuluş	Sumaklı	Stable	4	10	4	3
6	Kılınçoğlu	Kamalı Sk.	Stable	3	6	3,2	18
7	Delbes	Üzümcü	Stable	4	29	7,8	40
13	Hoşgör	Şht. Ahmet Sk.	Stable	2,5	1,5	1,8	3
14	Dumlupınar	Besihane	Stable	1,5	16	8	14
18	Çağlayan	Besni Cad.	Stable	1	15	7	5
19	Çağlayan	Besni Cad.	Stable	2	4	5	15
20	Aydınlar	Mezarlık	Stable	2	8	10	12
21	Aydınlar	Urfayolu	Stable	3,5	25	9	30
22	Umut	Besihane	Stable	10	8	15	18
27	Kılınçoğlu	Sulu	Stable	2	35	5	50
28	Dumlupınar	Boş	Stable	2	15	8	20

Some of the caves were collapsed and some others were closed by municipality. The rest, which is still open, is taken into consideration in this study.

CHAPTER 3

GEOTECHNICAL PARAMETERS AND COMPUTER PROGRAMS

3.1 Introduction

The experimental work is intended for mainly solving the models of the caves with Plaxis V8 2D analysis program, which is working based on finite element method, in order to evaluate the results due to the safety criteria's.

In order to model a cave, and solve it with Plaxis V8, it is essential to know geotechnical parameters of the rock type and the geometry of cave.

The geometry of caves was rather easier to find out compare to finding the geotechnical properties of rocks. There were studies and reports made on these caves before, in order to find physical properties and geometry of caves.

In addition, a site exploration was made to ensure the reliability of the previous reports and studies that were made on these caves. From site exploration some critical caves were selected and the data were collected from these caves to check the data from previous studies. It is found out that both data was corresponding, and previous studies can be used for this study.

After obtaining the geometry and physical properties of caves, it was important to decide which method to use in order to gather the geotechnical properties of the rock.

First of all, the tests that can help to obtain the geotechnical properties of rock were searched. It is found out that the preparation of the rock mass for in-situ tests, such as plate loading, dilatometer, flat jack, etc. is difficult and expensive. Therefore, in-situ tests are almost never done, except for engineering structures having crucial importance. However it is found out that research on empirical equations for determination of stress-strength behavior of a rock mass has been very attractive topic in rock engineering, and numerous empirical equations have been proposed in the literature **(Sönmez and Gökçeoğlu 2006)**.

Also it is difficult to prepare core samples from a rock mass for performing laboratory tests due to the presence of the discontinuities. Since it is very rare to prepare core samples and make in-situ tests on the specimens, and at the same time these tests are expensive, it has been decided to use empirical equations to find geotechnical parameters of rock.

In order to take advantage of empirical equations, a research was made on the empirical equations for finding geotechnical properties of rock. There are many relations between different parameters to find the geotechnical properties of rock. However it was crucial to find the most suitable methods for our case. Therefore the empirical equations for finding unconfined compressive strength from Schmidt Hammer Rebound Values were investigated, which can suit best to this case.

During the research it was noticed that the Schmidt Hammer is widely used for predicting the unconfined compressive strength of rocks. Using the Schmidt Hammer Rebound Values, the unconfined compression strength (UCS) of the limestone was found for each cave.

After finding unconfined compression strength, by using ROCLAB based on Hoek-Brown Criterion, the internal angle of friction (Φ), Young's Modulus (E) and cohesion (c) of limestone for each cave were found.

At this point, the values of unconfined compression strength (UCS), internal angle of friction (Φ), cohesion (c) and Young's Modulus (E) were used in order to make the models and analysis of the cave models to check the stability of them with Plaxis V8 program.

3.1.1 PLAXIS V8 Finite Element Code

Plaxis V8 is a finite element package intended for the two dimensional analysis of deformation and stability in geotechnical engineering. It was first created in 1987 and then developed at Delft University of Technology for complex geotechnical engineering problems based on finite element method by using deformation analysis, stability analysis, behavior analysis depending on time and dynamic analysis. Plaxis V8 is intended to provide a tool for practical analysis to be used by geotechnical engineers who are not necessarily numerical specialists.

The Plaxis V8 program offers a convenient option to create circular and non-circular tunnels using arcs and lines. Meanwhile it is possible to create tunnels without linings, which enable the user to model caves. Fully isoparametric elements are used to model the curved boundaries within the mesh. Various methods have been implemented to analyze the deformations that occur as a result of various methods of tunnel construction **(www.plaxis.nl)**.

There four general usage principles in Plaxis V8, which are input, calculations, output and curves section. At input section, all the geometrical dimensions and the parameters related to the system are entered. The calculations section is the part where the parameters related to the calculation method are entered and the calculations were started. The output section is the place where the analysis results such as deformations, stresses are seen graphically. The curves section can be used for gathering some curves related to the results.

The modeling of the geotechnical structure and the system has to be done accurately, this is very important in order to get the real results from the model. There are two modeling option in Plaxis V8, which are Plain Strain and Axisymmetry modeling options. The default setting of the Model parameter is Plane strain.

A *Plane strain* model is used for geometries with a (more or less) uniform cross section and corresponding stress state and loading scheme over a certain length perpendicular to the cross section (z-direction). Displacements and strains in z-direction are assumed to be zero. However, normal stresses in z-direction are fully taken into account. In this modeling the structure is assumed to have a certain geometry, which lies along on a line and the model is created by taking a section of the whole structure. Slope stability, retaining wall, strip foundation and mat foundation can be a few examples.

An *Axisymmetric* model is used for circular structures with a (more or less) uniform radial cross section and loading scheme around the central axis, where the deformation and stress state are assumed to be identical in any radial direction. Note that for axisymmetric problems the x-coordinate represents the radius and the y-coordinate corresponds to the axial line of symmetry. Negative x-coordinates cannot be used. This model type can be used for the structures, which has symmetry due to an axis.

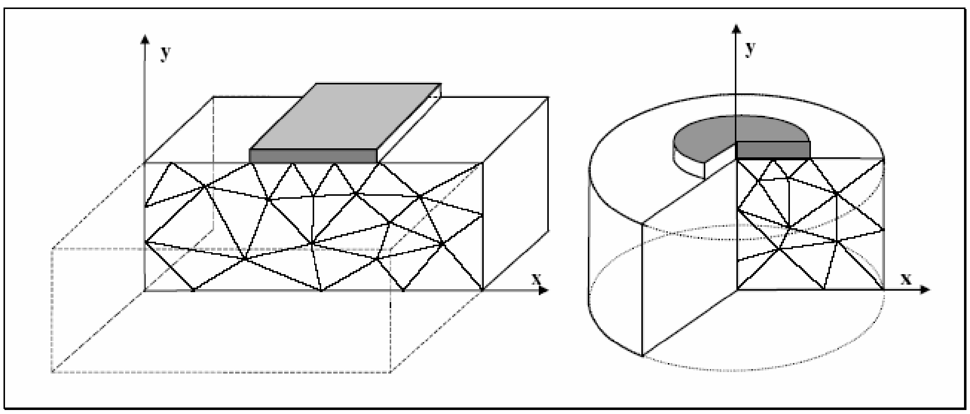

Figure 3.1.Example of a plane strain (left side) and axisymmetric problem

The selection of *Plane strain* or *Axisymmetric* results in a two dimensional finite element model with only two translational degrees of freedom per node (x- and y-direction). In a plane strain analysis, the calculated forces resulting from prescribe displacements represent forces per unit length in the out of plane direction (z-direction, Figure 3.2.). In an axisymmetric analysis, the calculated forces (Force-X, Force-Y) are those that act on the boundary of a circle subtending an angle of 1 radian. In order to obtain the forces corresponding to the complete problem therefore, these forces should be multiplied by a factor of 2π. All other output for axisymmetric problems is given per unit width and not per radian.

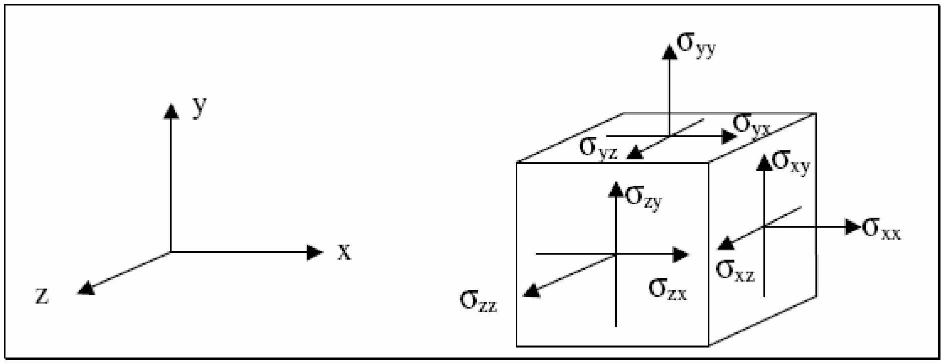

Figure 3.2.Coordinate system and indication of positive stress components

In plane strain models, Force-X and Force- Y are expressed in the unit of force per unit of width in the out-of-plane direction. In axisymmetric models, Force-X and Force-Y are expressed in the unit of force per radian. In order to calculate the total reaction force under a circular footing simulated by prescribed displacements, Force-Y should be multiplied by 2π.

In finite element system, each element can be solved with "6-Node" or "15-Node". These nodes refer to the points within each element. Therefore, if the system is required to be solved with higher accuracy, the "15-Node" will supply better results. However the calculations will take more time than "6-Node".

In Plaxis V8, there are five types of material modeling, which are Linear Elastic, Mohr-Coulomb, Soft Soil Model, Hardening Soil Model and Soft Soil Creep Model. Among these five material models, Mohr-Coulomb model was selected for solving the rock cave models. Mohr-Coulomb model is an elastoplastic soil model, which enables the user to make the calculations quicker. Generally this model is used for measuring the deformations at the geotechnical structure.

The Mohr-Coulomb model requires the following parameters, which are generally familiar to most geotechnical engineers and which were obtained from RocLab.

E:	Young's modulus	[kN/m^2]
Φ:	Friction angle	[°]
c:	Cohesion	[kN/m^2]

Plaxis V8 uses the Young's modulus as the basic stiffness modulus in the elastic model and the Mohr-Coulomb model. A stiffness modulus has the dimension of stress. The values of the stiffness parameter adopted in a calculation require special attention as many geomaterials show a nonlinear behavior from the very beginning of loading. The cohesion strength has the dimension of the stress. The friction angle largely determines the shear strength. For each cave rock, Young's modulus (E), internal angle of friction (Φ), and Cohesion (c) were found by using RocLab computer program. Moreover before finding these parameters with RocLab, the unconfined compressive strength (UCS) of each cave rock were found due to the Schmidt Hammer Rebound Values. Afterwards the model of each cave was created with Plaxis V8 as one model can be seen in Figure 3.3.

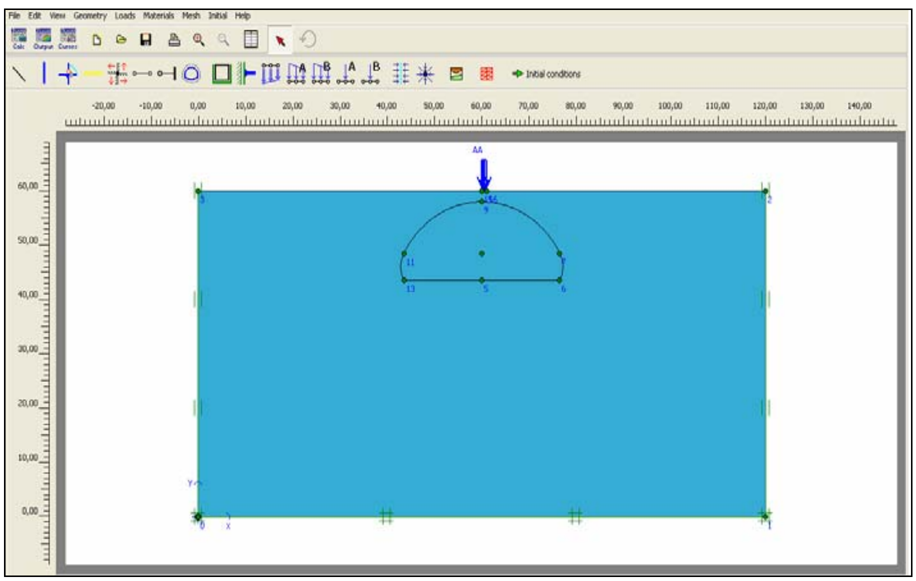

Figure 3.3. A constructed model in Plaxis V8 program which belongs to Cave No:1

In order to solve the systems with finite element method, the system has to be divided into small pieces. These small pieces supply the system to be solved one by one connected to each other. This can be done by generating mesh. In order to analyze the system in details, smaller mesh generations should be used. This will increase the sensitivity of the calculations at that system. There are four different mesh sizes that are coarse, medium, fine and very fine. The studies with Plaxis V8 proved that when global coarseness was decreased, more accurate results were gained. After medium size mesh the results are more or less similar to each other and they are generally very close to real results.

3.1.2 RocLab Software Program

Hoek and Brown (1980) introduced the most popular empirical approach to determine the strength of rock materials and rock masses. The program RocLab provides a simple and intuitive implementation of the Hoek-Brown failure criterion, allowing users to easily obtain reliable estimates of rock mass properties, and to visualize the effects of changing rock mass parameters, on the failure envelopes.

One of the major obstacles which is encountered in the field of numerical modeling for rock mechanics, is the problem of data input for rock mass properties. The usefulness of elaborate constitutive models, and powerful numerical analysis programs, is greatly limited, if the analyst does not have reliable input data for rock mass properties. The latest version of the Hoek-Brown failure criterion, in conjunction with its implementation in the software program RocLab, goes a long way toward remedying this situation.

Hoek et al. (1992), **Hoek (1994)** and **Hoek et al. (1995)** introduced Geological Strength Index (GSI). This index was subsequently extended for weak rock masses in a series of papers by **Hoek et al. (1998)**, **Hoek and Marinos (2000), Marinos and Hoek (2000)** and **Marinos (2001)**.

As a result the idea behind of using ROCLAB is that this computer program would be very helpful in order to predict the geotechnical properties such as internal angle of friction, cohesion and Young's Modulus of rock mass without doing difficult and expensive in-situ tests.

3.2 Finding UCS from Schmidt Hammer Rebound Values

The Schmidt Hammer Rebound Values have been conducted with a previous study (unpublished report, 2005). From this report the Schmidt Hammer Rebound Values are driven for each cave.

The Schmidt Hammer was developed in 1948 for non-destructive testing of concrete hardness **Cargill and Shakoor (1990)**, and was later used to estimate rock strength **(Israely 1973)**. The Schmidt hammer provides a quick and inexpensive measure of surface hardness that is widely used for estimating the mechanical properties of rock material **(Aydın and Basu 2005)**. Such fast, non-destructive and in situ evaluations of rock mechanical parameters reduce the expenses for sample collection and laboratory testing. Consequently, the mechanical parameters can be determined in dense arrays of field measurements that reflect the real inherent inhomogeneity of rock masses **(Katz et al. 1999)**.

That is why in this research Schmidt Hammer Rebound Values were used for predicting the unconfined compressive strength (UCS), which is one of the mechanical properties of rock.

Previous studies have charted a large number of empirical relationships between rebound values and UCS of various rocks. These relationships are expressed by power, exponential or linear functions. In a number of these functions, rebound value (the main independent variable) is multiplied with dry density (introduced as a second variable) in an effort to improve the correlations **(Aydın and Basu 2005)**.

Use of additional variables (e.g., density, porosity, ultrasonic velocity) should be avoided in establishing empirical correlations for practical use unless their roles are complementary and significant and can be clearly explained **(Aydın and Basu 2005)**. Because of this reason, the formulation with only one variable was chosen, which Schmidt Hammer Rebound Value is. Among all those empirical relationships, the best suited relationship was selected for our case. This relation is derived for limestone by **Katz et al. (2000)**.

$$\sigma_{ucs} = 2.21 * e^{(0.07 * R_N)} \tag{3.1}$$

where σ_{ucs} is unconfined compression strength of rock and R_N is the Schmidt Hammer Rebound Value of N-type.

For each cave the equation (3.1) was used for finding unconfined compressive strength due to Schmidt Hammer Rebound Value.

The Schmidt Hammer Rebound Values, which were obtained from previous studies, are L type values. Therefore the first thing to do was to convert these L type values into the N type values.

$$R_N = 1.0646 * R_L + 6.3673 \qquad (3.2)$$

The standard L-and N-type Schmidt hammers are built to generate different levels of impact energy 0.735 and 2.207 Nm, respectively. ISRM (1978a) only endorsed the use of the L hammer for testing rocks, while ASTM (2001) did not specify the hammer type **(Aydın and Basu 2005)**. However the relations between L and N type of Schmidt Hammer Rebound Values are important because of driving the UCS from Schmidt Hammer Rebound Values with formulas, which certainly depends on the type of the value. It was found that a very good correlation exists between L and N hammer rebound values **(Aydın and Basu 2005).** The Schmidt Hammer Rebound Values are L type of values, which are conducted on the caves, and these values are used for predicting the unconfined compressive strength.

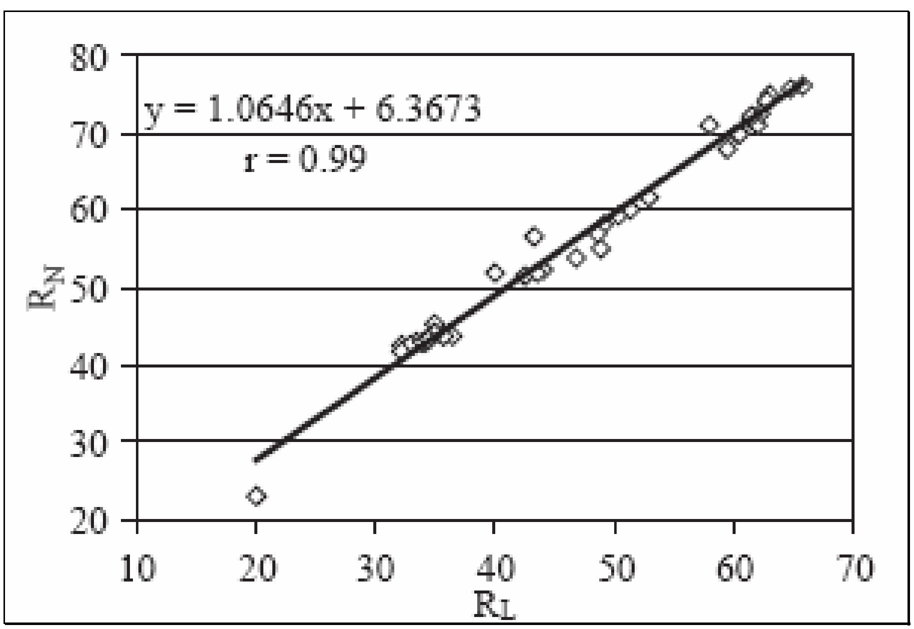

Figure 3.4. Relations between L and N hammer rebound values

After converting the L-type Schmidt Hammer Rebound Values into N-type Values, the unconfined compressive strength of each cave rock was found with the formulation given in (3.2). The results can be seen at the Table 3.1.

Table 3.1.Unconfined Compression Strength due to Schmidt Hammer Rebound Values

Cave No	District	Name of caves	Schmidt Hammer Rebound Values (L Type)	Schmidt Hammer Rebound Values (N Type)	Unconfined Compression Strength (MPa)
1	İsmet Paşa	Direkçi	17.90	25.42	13.10
2	Kurtuluş	Sumaklı	19.20	26.81	14.43
3	Kurtuluş	Sumaklı	19.50	27.13	14.76
4	Kurtuluş	Sumaklı	19.00	26.59	14.22
6	Kılınçoğlu	Kamalı Sk.	13.00	20.21	9.09
7	Delbes	Üzümcü	21.40	29.15	17.00
13	Hoşgör	Şht. Ahmet Sk.	16.30	23.72	11.63
14	Dumlupınar	Besihane	11.60	18.72	8.19
18	Çağlayan	Besni Cad.	14.10	21.38	9.87
19	Çağlayan	Besni Cad.	21.90	29.68	17.65
20	Aydınlar	Mezarlık	15.20	22.55	10.71
21	Aydınlar	Urfayolu	13.80	21.06	9.65
22	Umut	Besihane	13.50	20.74	9.44
27	Kılınçoğlu	Sulu	16.85	24.31	12.12
28	Dumlupınar	Boş	11.90	19.04	8.38

3.3 Determination of Strength Parameters of Cave Rock Using ROCLAB

The Generalized Hoek-Brown strength parameters of a rock mass can be determined based on the following input data by ROCLAB program; unconfined compressive strength of intact rock, The intact rock parameter, the geological strength index (GSI) and the disturbance factor.

When it is wanted to select a parameter or input, a table or chart will appear, allowing the user to determine a suitable value for the desired parameter.

Once the unconfined compressive strength of each cave is determined by using Schmidt Hammer Rebound Values, and the physical properties of caves were observed by site exploration and from previous studies, the desired output parameters, internal angle of friction (Φ), cohesion (c) and Young's Modulus (E), were calculated for each cave with RocLab.

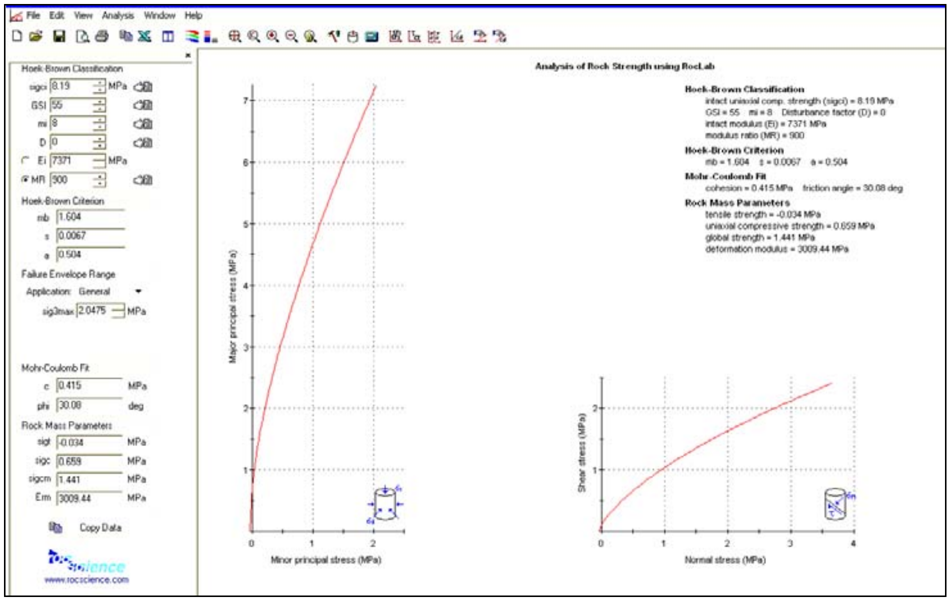

Figure 3.5. The view of RocLab used for input and output data

The primary means of user interaction with RocLab, is with the sidebar data input area, shown in Figure 3.5. The sidebar is used for data input, and also for display of calculated output parameters.

The geological strength index (GSI) is a system of rock-mass characterization that has been developed in engineering rock mechanics to meet the need for reliable input data, particularly those related to rock-mass properties required as inputs into numerical analysis or closed form solutions for designing tunnels, slopes or foundations in rocks. The geological character of rock material, together with the visual assessment of the mass it forms, is used as a direct input to the selection of parameters relevant for the prediction of rock-mass strength and deformability. This approach enables a rock mass to be considered as a mechanical continuum without losing the influence geology has on its mechanical properties. It also provides a field method for characterizing difficult-to-describe rock masses **(Marinos et al. 2005)**.

GSI and its applications are in use for a decade with its variations in quantitative characterization of rock mass.

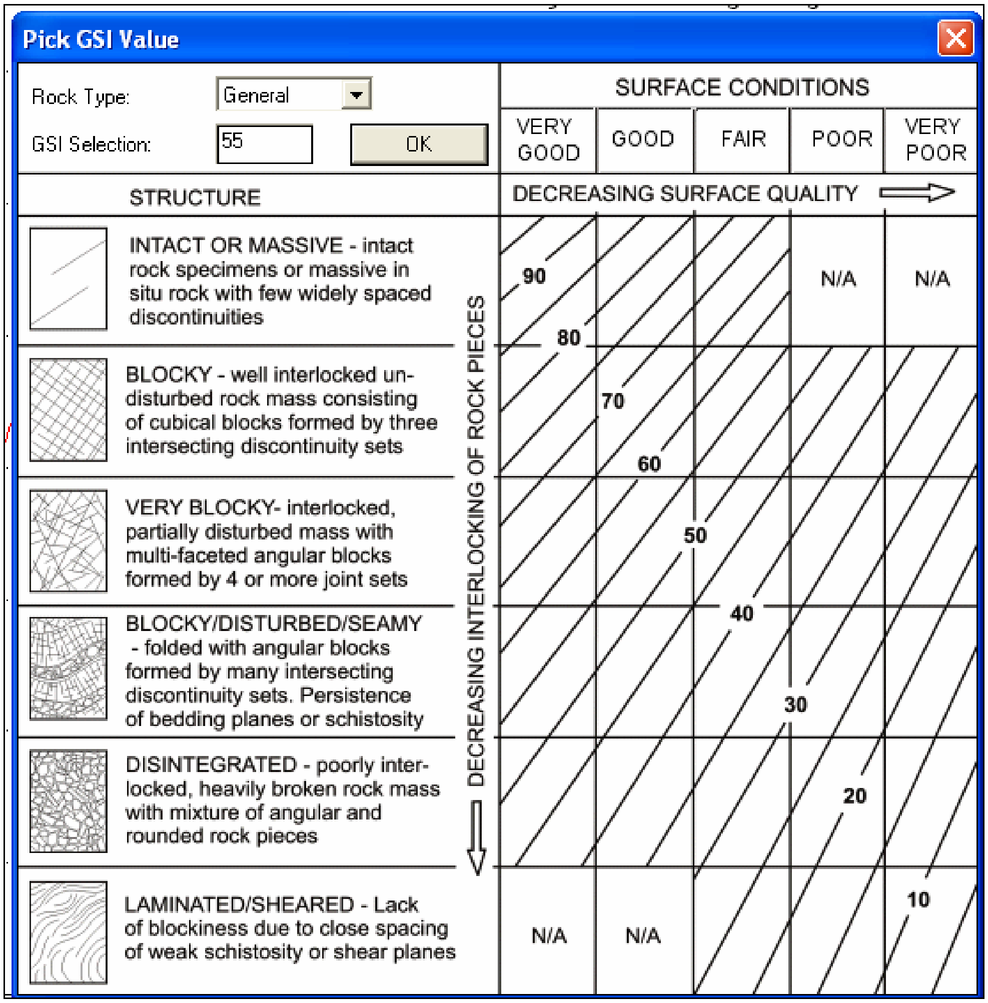

Figure 3.6. GSI Chart

The disturbance factor (D) is a factor which depends upon the degree of disturbance to which the rock mass has been subjected by blast damage and stress relaxation. It varies from 0 for undisturbed in situ rock masses to 1 for very disturbed rock masses.

CHAPTER 4

NUMERICAL MODELING

4.1 Introduction

A plastic model described as the Mohr-Coulomb model was selected from those available in Plaxis V8 to describe the limestone behavior in this study. This Mohr-Coulomb model represents a 'first-order' approximation of soil or rock behavior. It is recommended to use this model for a first analysis of the problem considered.

The Mohr-Coulomb model may be used to compute realistic support pressures for tunnel faces, and it may also be used to calculate a safety factor by 'phi-c reduction' approach.

Since this method was the best suit for this problem in cave rock analysis among other models, the Mohr-Coulomb model was selected in Plaxis V8. Also it was possible to find a safety factor with this model, and it was crucial to find a safety factor for each cave in this study. Therefore Mohr-Coulomb model was preferred.

The Mohr-Coulomb model requires the following parameters, which are generally familiar to most geotechnical engineers and which were obtained from RocLab. These parameters with their standard units are listed:

E:	Young's modulus	[kN/m^2]
Φ:	Friction angle	[°]
c:	Cohesion	[kN/m^2]

Plaxis V8 uses the Young's modulus as the basic stiffness modulus in the elastic model and the Mohr-Coulomb model. A stiffness modulus has the dimension of stress. The values of the stiffness parameter adopted in a calculation require special attention as many geomaterials show a nonlinear behavior from the very beginning of loading. The cohesion strength has the dimension of the stress. The friction angle largely determines the shear strength.

Besides the model parameters mentioned above, initial soil conditions play an essential role in most soil deformation problems. Initial horizontal soil stresses have to be generated by selecting proper K_0-values. This initial horizontal soil stresses are created due to the internal angle of friction. In each model, the internal angle of friction was selected for that rock type and initial horizontal stresses was generated at the analysis of each cave.

The analyses were carried out using a plane strain model. Although, geometric dimensions of the analyzed caves are not perfectly fits the plane strain conditions, it models caves better than the axisymmetric model that is given in Plaxis V8.

For deformation problems two types of boundary conditions exist: Prescribed displacements and prescribed forces (loads). In principle, all boundaries must have one boundary condition in each direction. That is to say, when no explicit boundary condition is given to a certain boundary (a free boundary), the natural condition applies, which is a prescribed force equal to zero and a free displacement. To avoid the situation where the displacements of the geometry are undetermined, some points of the geometry must have prescribed displacements. The simplest form of a prescribed displacement is a fixity (zero displacement), but non-zero prescribed displacements may also be given.

Therefore boundary conditions were used at the models of the caves in this study. In Plaxis V8, boundary conditions are generated automatically; it generates full fixity at the base of the geometry and smooth conditions at the vertical sides.

Five different mesh densities are available in Plaxis V8 ranging from very coarse, involving approximately 48 elements, to very fine, involving up to 1000 elements. In this study fine mesh size was selected for all the analysis. The coarse mesh is the default option in Plaxis V8. However in order to provide a greater accuracy, the fine size mesh generation was used. The very fine mesh size was not selected in order to gain from time and gain optimum performance from the calculations.

During the generation of the mesh, 15-node triangular elements were selected in preference to the alternative 6-noded versions in order to provide greater accuracy in the determination of stresses. The type of element for structures and interfaces is automatically taken to be compatible with the basic type of soil element.

Plaxis V8 incorporates a fully automatic mesh generation procedure, in which the geometry is divided into elements of the basic element type, and compatible structural elements.

Although the caves are symmetric in analysis, full geometry was analyzed. The loading was applied at 1 m wide as distributed load. The load is applied beginning from the right side of the axis at the same point for each cave.

In order to analyze the caves, the models are needed to be constructed for each cave. The dimensions and the pictures of each cave were taken out and investigated from previous studies and some published data. Moreover, some critical caves were investigated on site. Afterwards, the models were constructed using Plaxis V8 program.

The caves were modeled using Plaxis V8 and solved with the program in order to find the displacements of the caves and Factor of Safety against failure for each cave. Output results of the analyzed caves from Plaxis V8 are given below. Four outputs were given for each cave. Two of them are for deformed shape and deformation, and the other two figures belong to relative shear stress values. The relative shear stress option gives an indication of the proximity of the stress point to the failure envelope. The relative shear stress, τ_{rel} , is defined as:

$$\tau_{rel} = \tau / \tau_{max} \qquad (4.1)$$

where τ is the value of shear stress (i.e. radius of the Mohr stress circle). The parameter τ_{max} is the maximum value of shear stress for the case where the Mohr's circle is expanded to touch the Coulomb failure envelope keeping the intermediate principal stress constant.

The classical approach used in designing engineering structures is to consider the relationship between the capacity c (strength or resisting force) of the element, and the demand D (stress or disturbing force). The Factor of Safety of the structure is defined as F = C/D and failure is assumed to occur when F is less than unity.

In structural design, the safety factor is usually defined as the ratio of the collapse load to the working load. For soil structures, however, this definition is not always useful. For embankments, for example, most of the loading is caused by soil weight and an increase in soil weight would not necessarily lead to collapse. Indeed, a slope of purely frictional soil will fail in a test in which the self weight of the soil is increased (like in a centrifuge test). A more appropriate definition of the safety factor is therefore:

$$\textit{Safety Factor} = \frac{S \ \max imum\ available}{S\ needed\ \ for\ equilibrium} \tag{4.2}$$

Where S represents the shear strength. The ratio of the true strength to the computed minimum strength required for equilibrium is the safety factor that is conventionally used in soil mechanics. By introducing the standard coulomb condition, the safety factor is obtained:

$$\textit{Safety Factor} = \frac{C - \sigma_N * \tan \Phi}{Cr - \sigma_N * \tan \Phi r} \tag{4.3}$$

Where c (cohesion) and Φ (internal angle of friction) are the input parameters and σ_N is the actual normal stress component. The parameters c_r and Φ_r are reduced strength parameters that are just large enough to maintain equilibrium. The principle described above is the basis of the method of Phi-c-reduction that can be used in

Plaxis V8 to calculate a global safety factor. In this approach the cohesion and the tangent of the friction angle are reduced in the same proportion:

$$\frac{C}{Cr} = \frac{\tan \Phi}{\tan \Phi r} = \Sigma Msf \qquad (4.4)$$

The reduction of strength parameters is controlled by the total multiplier ΣMsf. This parameter is increased in a step-by-step procedure until failure occurs. The safety factor is defined as the value of ΣMsf at failure, provided that at failure a more or less constant value is obtained for a number of successive load steps.

As a convergence criterion, Plaxis V8 employs the nodal unbalanced force – the sum of forces acting on a node from its neighboring elements; at a node in equilibrium, these forces sum to zero.

Before solving the models with Plaxis V8 program, properties of limestone required for the modeling were obtained from in-situ testing, published data, and previous studies. The tensile strength for limestone was assumed to be zero. The compressive strengths were driven from Schmidt Hammer Rebound Values of each cave rock.

All loads have been applied to a square foundation pad of $1m^2$, just beginning from the right side of the axis of the cave origin.

4.2 Results of Analysis

Table 4.1. Input and Output Summary of Cave No:1

CAVE NO:1, DİREKÇİ PAZARI, DISTRICT: İSMET PAŞA		
Width = 33m	Height = 14.80m	Depth = 70.15m

Cover Thickness:	1.8 m
Unconfined Compressive Strength:	13.10 MPa
Cohesion (c):	0.664 MPa
Young's Modulus (E) :	4.81 GPa
Internal Angle of Friction (Φ) :	30.08
Extreme Total Displacement :	6.17 mm
Extreme Relative Shear Stress :	0.80
Factor of Safety (FS) :	3.14

Output results obtained from the analysis of Cave No: 1 is shown in Figure 4.1a to Figure 4.1d. As it can be seen in Figure 4.1b, the maximum deflection is 6.17 mm, which occurs under the loading area. The results also show that the maximum vertical displacements occur under the loaded area and the maximum horizontal displacement occurs both at the ground level towards the loading and at the cave walls close to the base of the cave. The maximum vertical displacement is 6 times higher than the maximum horizontal displacement. There is also a slightly heave at the base of the cave.

The extreme relative shear stress with loading is 0.80, while it is 0.58 without loading that indicates the loading adds extra stresses on the cave (Figure 4.1c, d). Without loading, the extreme relative shear stresses concentrate at the walls of the cave near the base and at the axis close to surface. However, when the load is applied, the maximum relative shear stresses concentrate more under the loaded area. The extreme relative shear stress has not reached to 1.00 at any point and does not yield a shear failure line.

The calculated factor of safety (FS) against failure is 3.14.

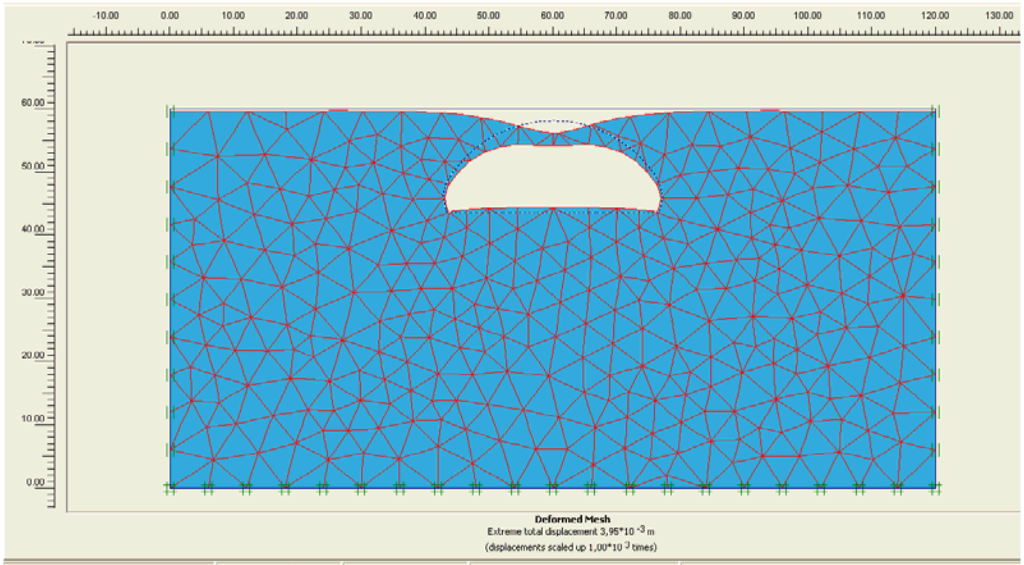

Figure 4.1a. Cave No: 1 Extreme Total Displacement and Deformed Shape Without Loading

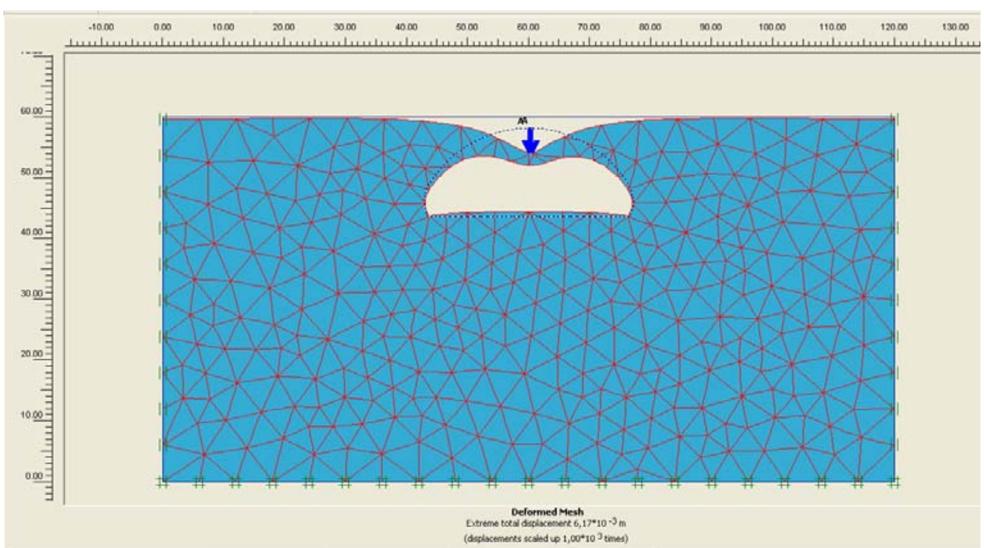

Figure 4.1b. Cave No: 1 Extreme Total Displacement and Deformed Shape With Loading

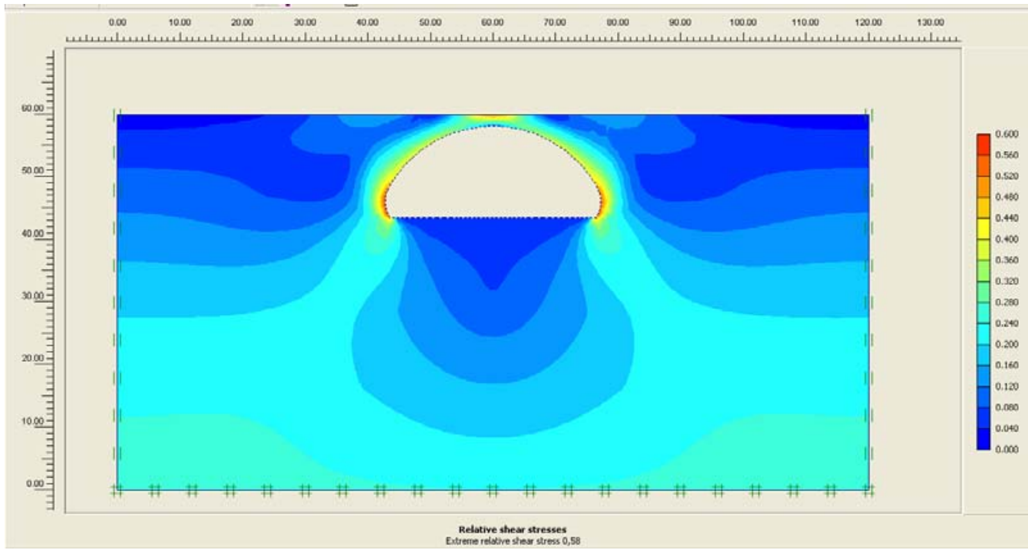

Figure 4.1c. Cave No: 1 Relative Shear Stress Without Loading

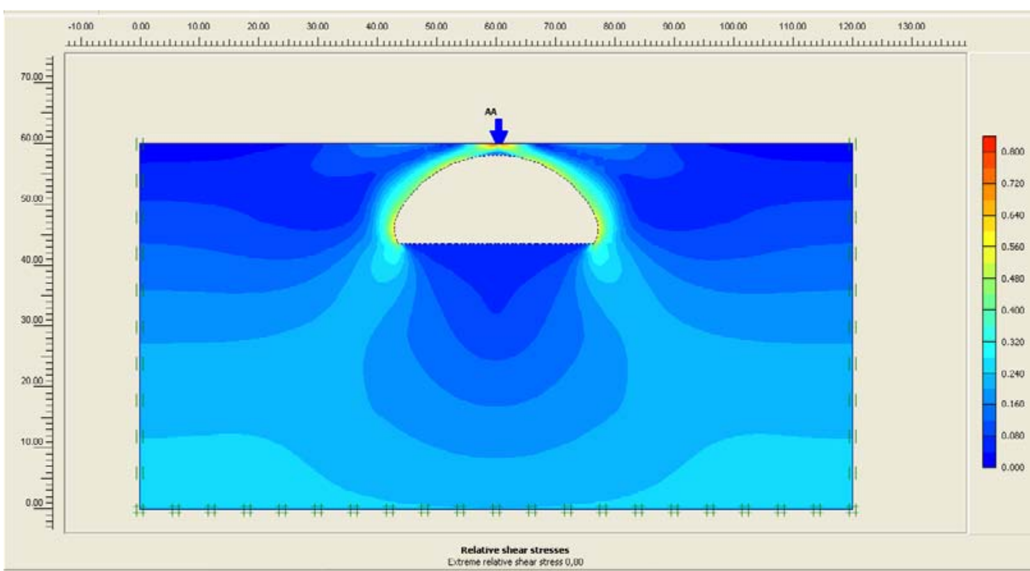

Figure 4.1d. Cave No: 1 Relative Shear Stress With Loading

Table 4.2. Input and Output Summary of Cave No:2

CAVE NO:2, SUMAKLI, DISTRICT: KURTULUŞ		
Width = 8.20m	Height = 2.50m	Depth = 15.50m
Cover Thickness:	7 m	
Unconfined Compressive Strength:	14.43 MPa	
Cohesion (c):	0.732 MPa	
Young's Modulus (E) :	5.30 GPa	
Internal Angle of Friction (Φ) :	30.08	
Extreme Total Displacement :	0.29 mm	
Extreme Relative Shear Stress :	0.78	
Factor of Safety (FS) :	9.21	

Output results obtained from the analysis of Cave No:2 is shown in Figure 4.2a to Figure 4.2d. As it can be seen at Figure 4.2b., the maximum deflection is 0.29 mm, which occurs under the loading area. The output results show that the maximum vertical displacements occur at the middle point of cave where the height of the cave is maximum. The maximum horizontal displacement occurs at the ground level towards the loading, and under the cave to the other side of the loading due to the cave axis. The maximum vertical displacement is 5 times higher than the maximum horizontal displacement. There is also a slightly heave at the base of the cave.

The extreme relative shear stress with loading is 0.78, while it is 0.74 without loading, which indicates that the loading does not add much extra stresses on the cave (Figure 4.2c, d). Without loading the extreme relative stresses concentrate at the corners of the cave close to the base. Under the loading condition, the relative shear stress distribution is seen similar to the unloading condition. At the axis of the cave, the relative shear stress almost does not occur under and above the cave. The extreme relative shear stress is not higher than 1.00 and does not yield a failure line. Therefore the model showed that there is no shear failure occurs at this cave.

The calculated factor of safety (FS) against failure is 9.21.

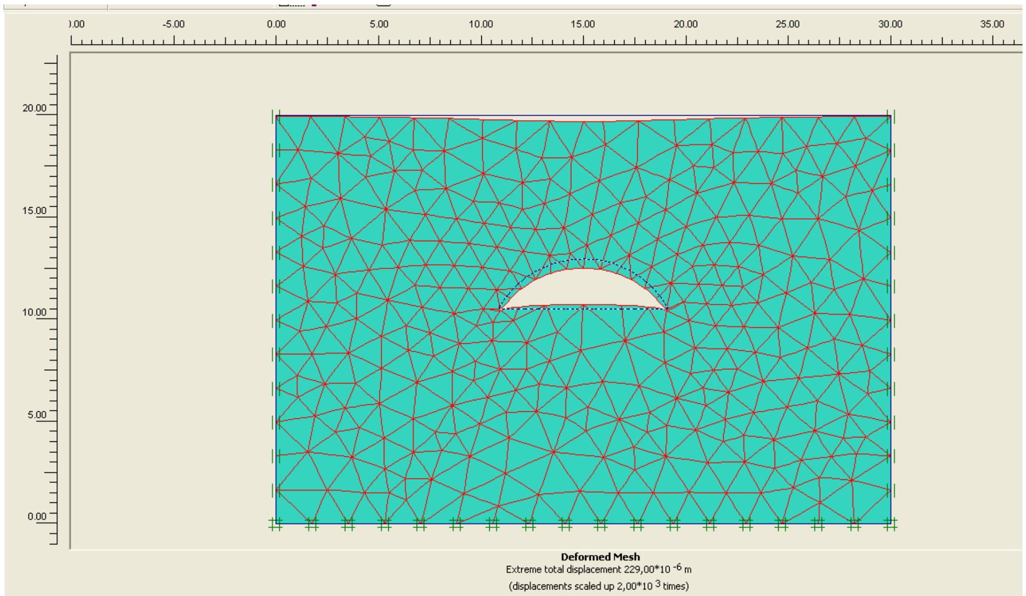

Figure 4.2a. Cave No: 2 Extreme Total Displacement and Deformed Shape Without Loading

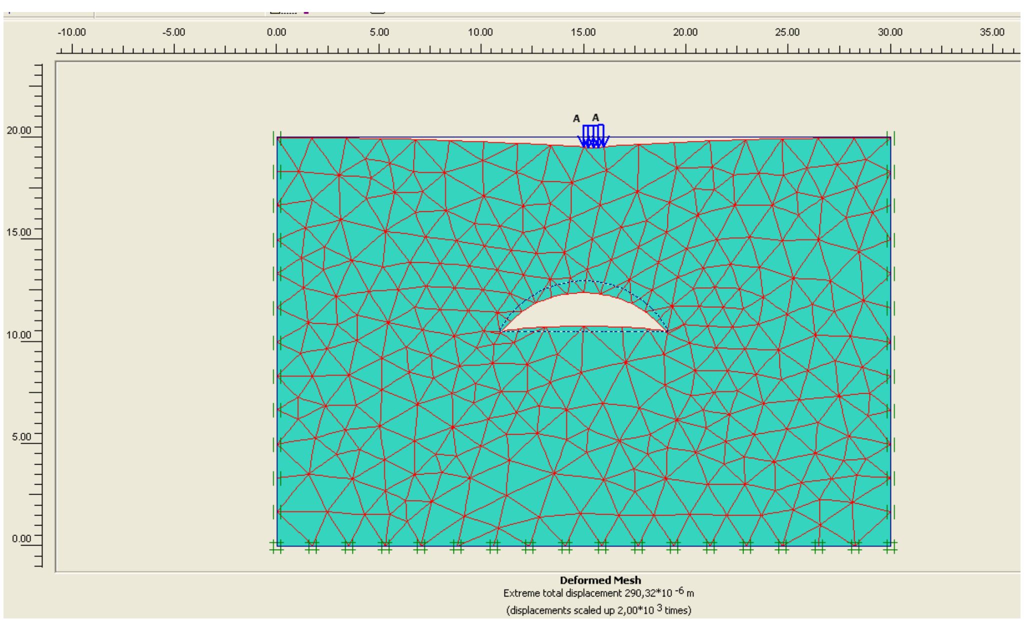

Figure 4.2b. Cave No: 2 Extreme Total Displacement and Deformed Shape With Loading

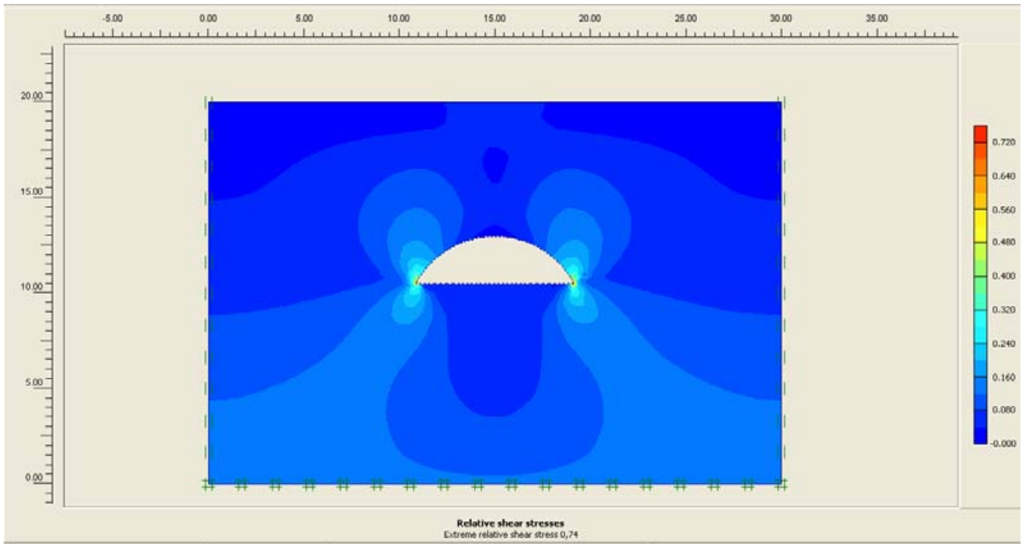

Figure 4.2c. Cave No: 2 Relative Shear Stress Without Loading

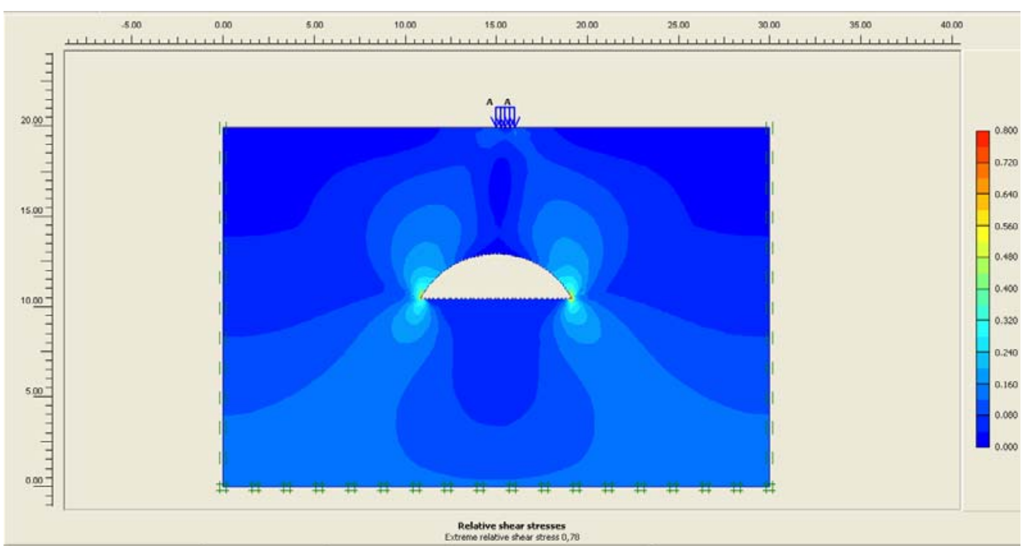

Figure 4.2d. Cave No: 2 Relative Shear Stress With Loading

Table 4.3. Input and Output Summary of Cave No:3

CAVE NO:3, SUMAKLI, DISTRICT: KURTULUŞ		
Width = 25m	Height = 6m	Depth = 5.6m
Cover Thickness:	8 m	
Unconfined Compressive Strength:	14.76 MPa	
Cohesion (c):	0.749 MPa	
Young's Modulus (E) :	5.42 GPa	
Internal Angle of Friction (Φ) :	30.08	
Extreme Total Displacement :	2.35 mm	
Extreme Relative Shear Stress :	0.85	
Factor of Safety (FS) :	4.32	

Output results obtained from the analysis of Cave No: 3 are shown in Figure 4.3a to Figure 4.3d. As it can be seen at Figure 4.3b, the maximum deflection is 2.35 mm, which occurs under the load. The output results show that the maximum vertical displacements occur around the axis of cave under the loading area. Meanwhile the maximum horizontal displacement occurs at the ground level towards the loading. The maximum vertical displacement is 4 times higher than the maximum horizontal displacement. There is also a slightly heave at the base of the cave.

The extreme relative shear stress with loading is 0.88, while it is 0.85 without loading, which indicates that the loading does not add much extra stresses on the cave (Figure 4.1c, d). Without loading the extreme relative stresses concentrate at the corners of the cave close to the base. Under the loading condition, the relative shear stress distribution is seen similar to the unloading condition. At the axis of the cave, the relative shear stress almost does not occur under the cave. The extreme relative shear stress does not yield a failure line. Therefore the model showed that there is no shear failure occurs at this cave.

The factor of safety against failure was calculated and it is 4.32.

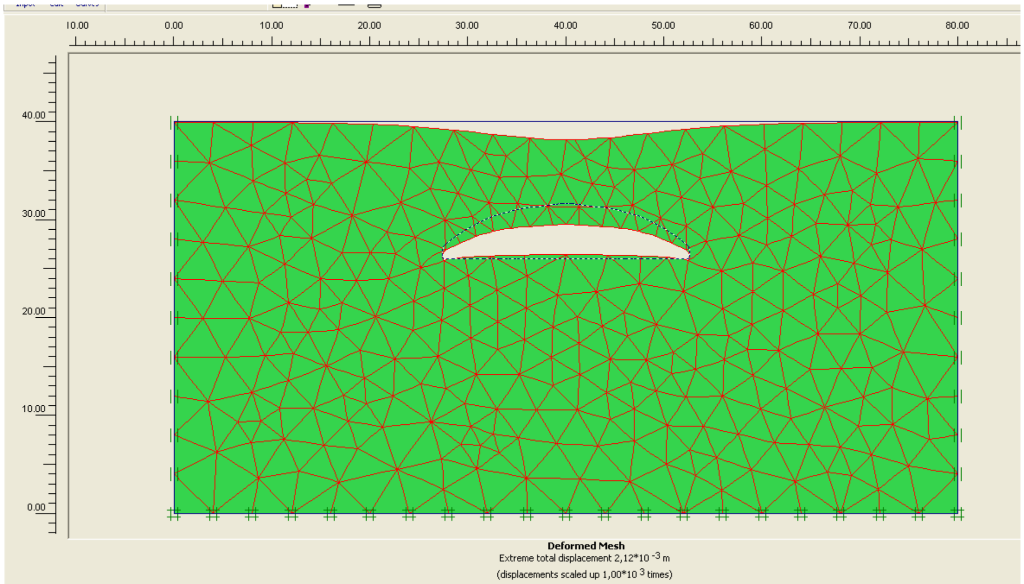

Figure 4.3a. Cave No: 3 Extreme Total Displacement and Deformed Shape Without Loading

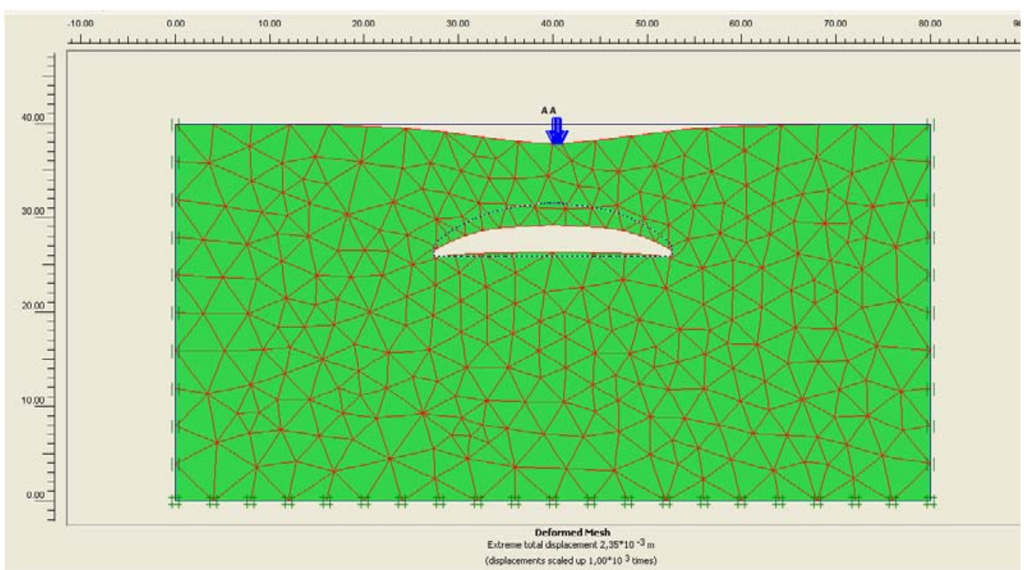

Figure 4.3b. Cave No: 3 Extreme Total Displacement and Deformed Shape With Loading

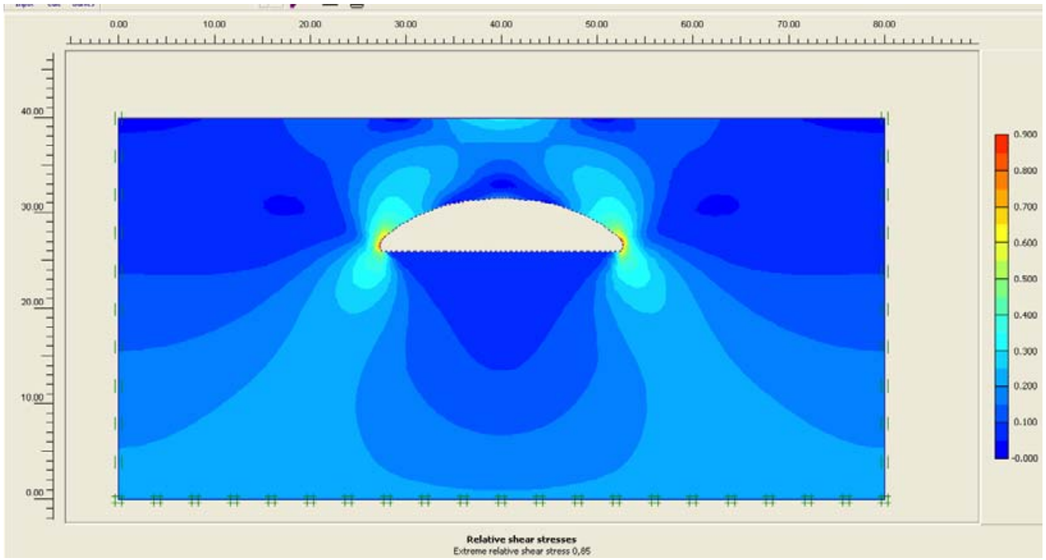

Figure 4.3c. Cave No: 3 Relative Shear Stress Without Loading

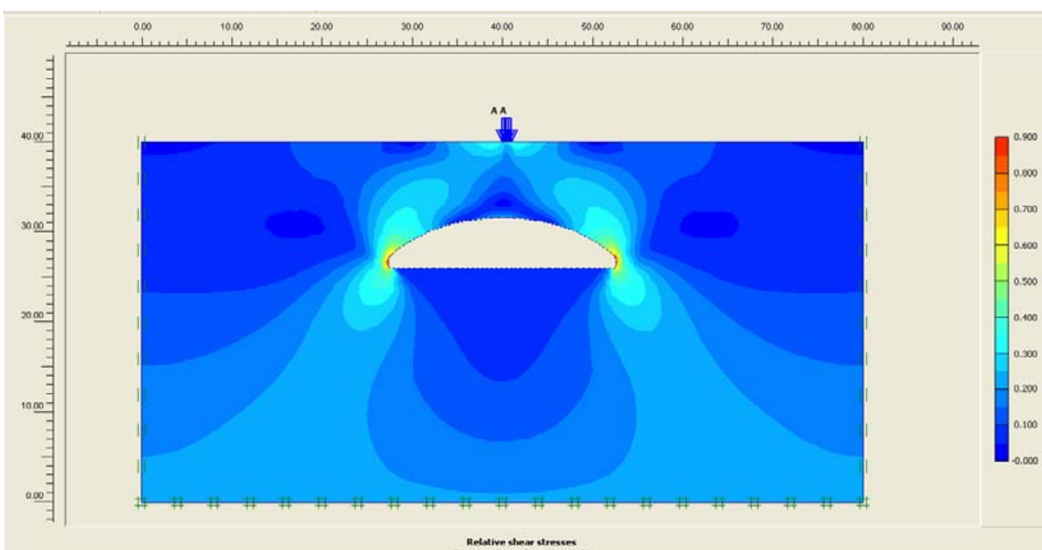

Figure 4.3d. Cave No: 3 Relative Shear Stress With Loading

Table 4.4. Input and Output Summary of Cave No:4

CAVE NO:4, SUMAKLI, DISTRICT: KURTULUŞ		
Width = 10m	Height = 4m	Depth = 3m
Cover Thickness:	4 m	
Unconfined Compressive Strength:	14.22 MPa	
Cohesion (c):	0.721 MPa	
Young's Modulus (E) :	5.23 GPa	
Internal Angle of Friction (Φ) :	30.08	
Extreme Total Displacement :	0.48 mm	
Extreme Relative Shear Stress :	0.45	
Factor of Safety (FS) :	8.02	

Output results obtained from the analysis of Cave No: 4 are shown in Figure 4.4a to d. As it can be seen at Figure 4.4b, the maximum deflection is 0.48 mm, which occurs under the load. The results show that the maximum vertical displacements occur at under the loaded area. The maximum horizontal displacement occurs at the ground level towards the loading. The horizontal displacement is almost zero around the walls of the cave. The maximum vertical displacement is 4.5 times higher than the maximum horizontal displacement. There is also a slightly heave at the base of the cave.

The extreme relative shear stress with loading is 0.45, while it is 0.41 without loading, which indicates that the loading does not add much extra stresses on the cave. Without loading the extreme relative stresses concentrate at the corners of the cave close to the base. Under the loading condition, the relative shear stress distribution is seen similar to the unloading condition. The extreme relative shear stress does not yield a failure line for the cave. Therefore the model showed that there is no shear failure occurs at this cave.

The factor of safety against failure was calculated and it is 8.02

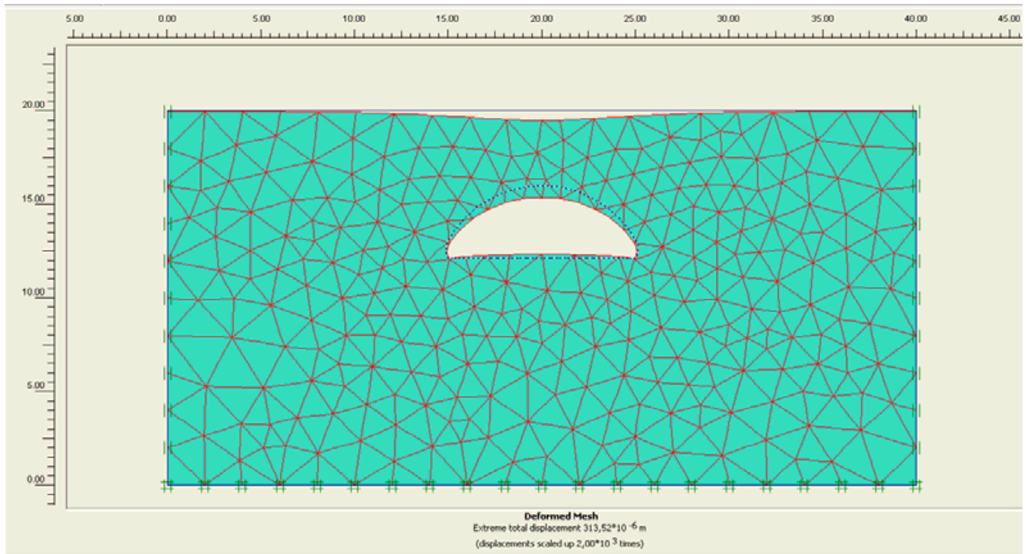

Figure 4.4a. Cave No: 4 Extreme Total Displacement and Deformed Shape Without Loading

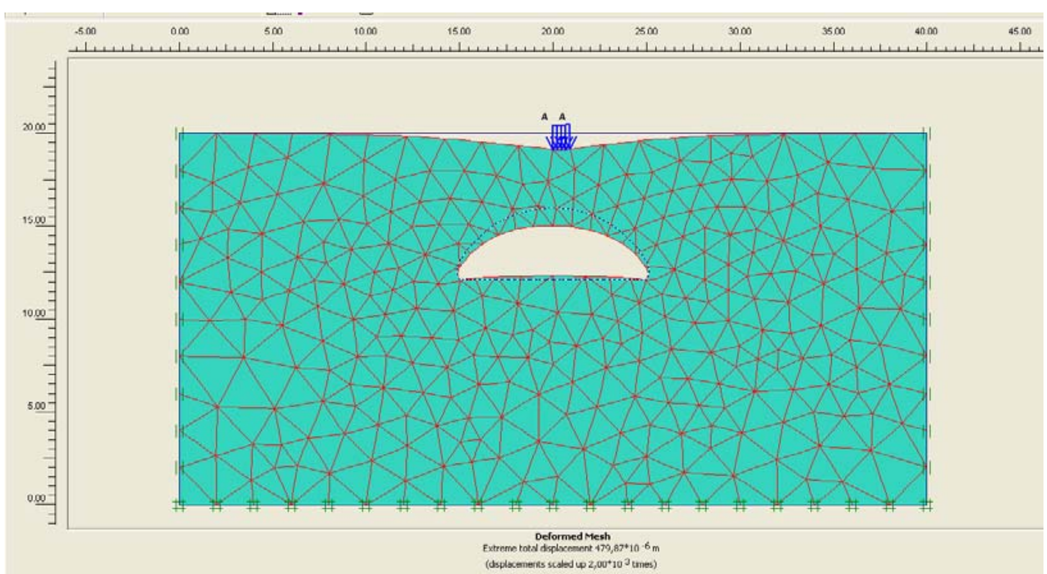

Figure 4.4b. Cave No: 4 Extreme Total Displacement and Deformed Shape With Loading

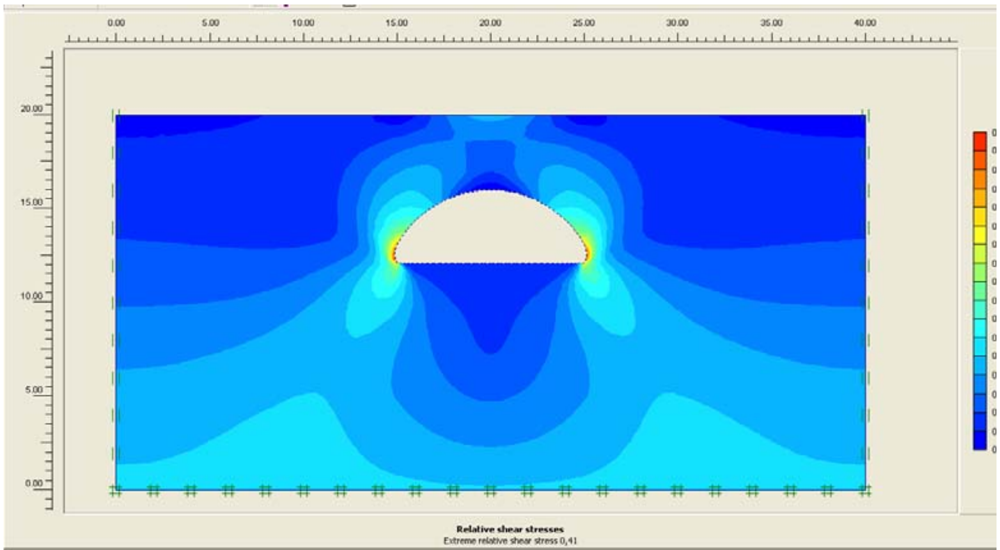

Figure 4.4c. Cave No: 4 Relative Shear Stress Without Loading

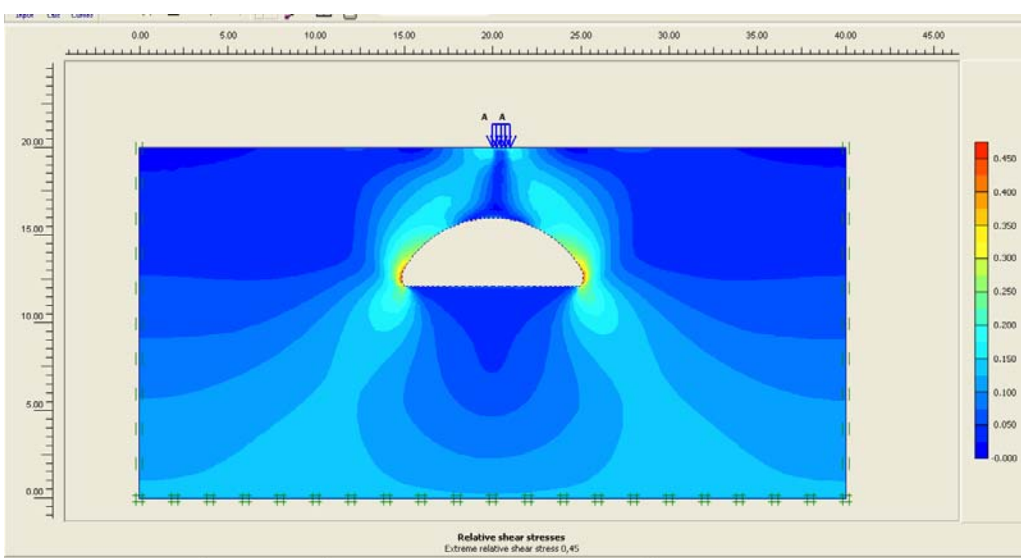

Figure 4.4d. Cave No: 4 Relative Shear Stress With Loading

Table 4.5. Input and Output Summary of Cave No:6

CAVE NO:6, KAMALI, DISTRICT: KILINÇOĞLU		
Width = 6m	Height = 3.2m	Depth = 18m
Cover Thickness:	3m	
Unconfined Compressive Strength:	9.09 MPa	
Cohesion (c):	0.461 MPa	
Young's Modulus (E) :	3.34 GPa	
Internal Angle of Friction (Φ) :	30.08	
Extreme Total Displacement :	0.53 mm	
Extreme Relative Shear Stress :	0.45	
Factor of Safety (FS) :	5.32	

Output results obtained from the analysis of Cave No: 6 are shown in Figure 4.5a to Figure 4.5d. The maximum deflection is 0.53 mm, which occurs under the load (Figure 4.5b). The output results prove that the maximum vertical displacements occur under the loaded area. The maximum horizontal displacement occurs at the ground level towards the loading, and slightly on the walls of the cave. The maximum vertical displacement is 4.5 times higher than the maximum horizontal displacement. There is also a slightly heave at the base of the cave.

The extreme relative shear stress with loading is 0.45, while it is 0.31 without loading, which indicates that the loading adds some extra stresses on the cave (Figure 4.5c, d). Without loading the extreme relative stresses concentrate towards the walls of the cave. Under the loading condition, the relative shear stress distribution is seen similar to the unloading condition. Nevertheless under loading condition, the relative shear stress distribution starts to concentrate towards the loading. The extreme relative shear stress does not yield a failure line for the cave. For that reason the model showed that there is no shear failure occurs at this cave.

The factor of safety against failure was calculated and it is 5.32.

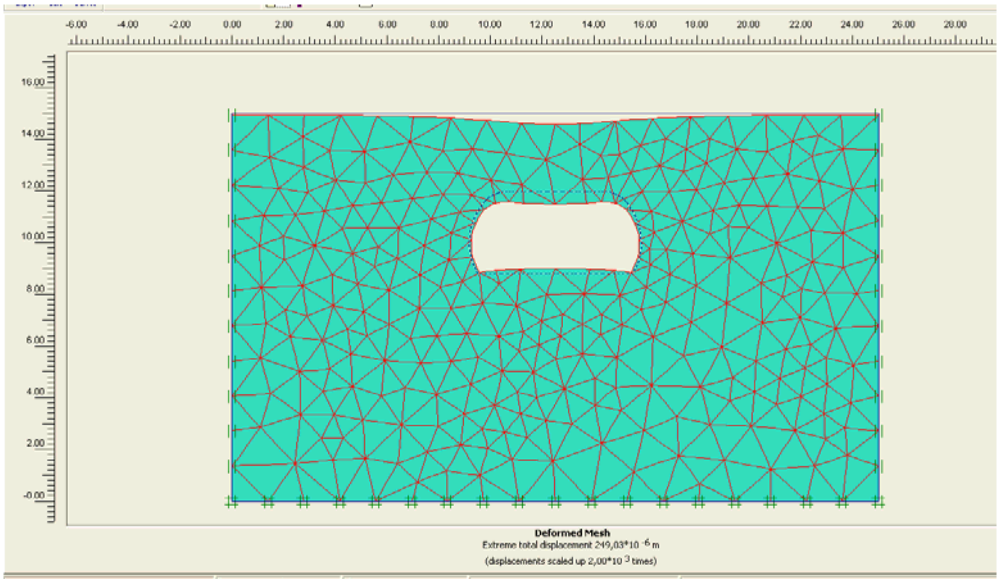

Figure 4.5a. Cave No: 6 Extreme Total Displacement and Deformed Shape Without Loading

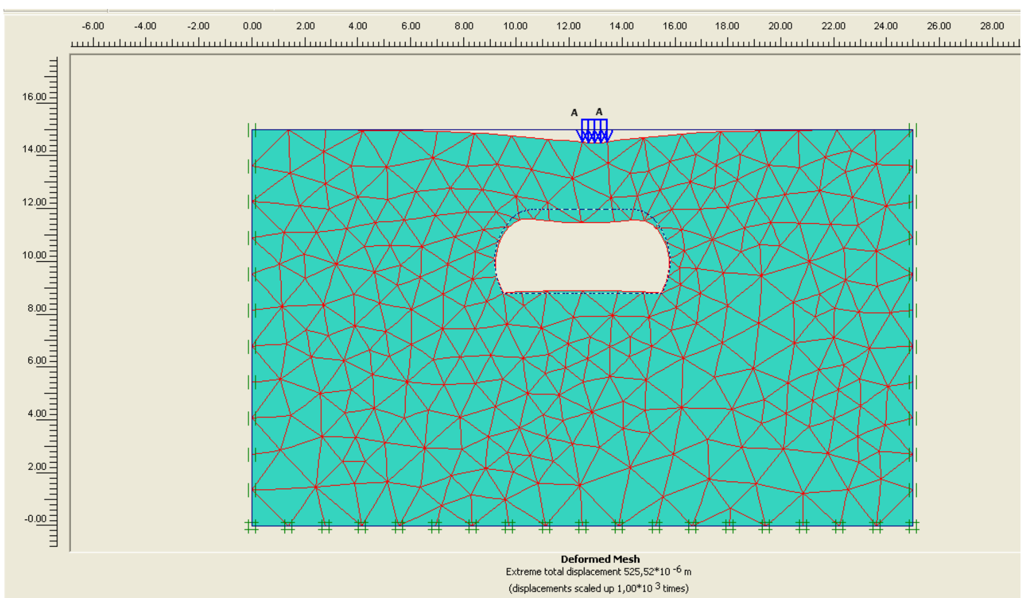

Figure 4.5b. Cave No: 6 Extreme Total Displacement and Deformed Shape With Loading

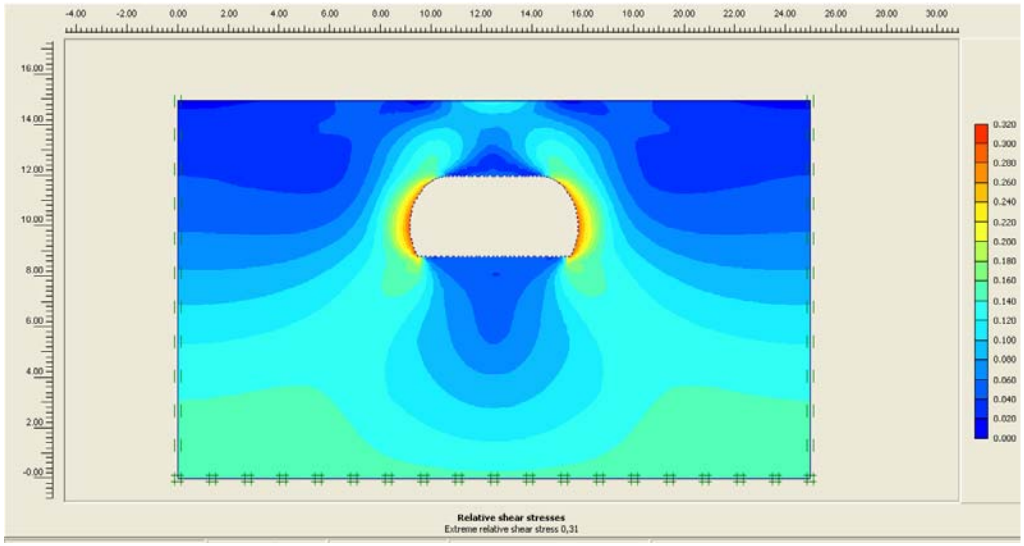

Figure 4.5c. Cave No: 6 Relative Shear Stress Without Loading

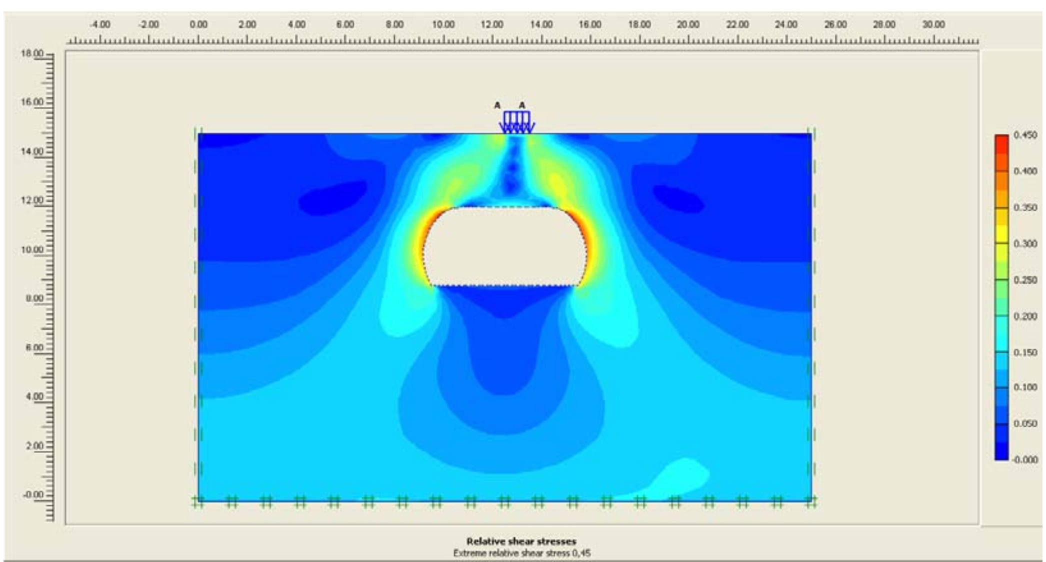

Figure 4.5d. Cave No: 6 Relative Shear Stress With Loading

Table 4.6. Input and Output Summary of Cave No:7

CAVE NO:7, ÜZÜMCÜ, DISTRICT: DELBES		
Width = 29m	Height = 7.5m	Depth = 40m
Cover Thickness:	4m	
Unconfined Compressive Strength:	17 MPa	
Cohesion (c):	0.862 MPa	
Young's Modulus (E) :	6.25 GPa	
Internal Angle of Friction (Φ) :	30.08	
Extreme Total Displacement :	3.03 mm	
Extreme Relative Shear Stress :	0.52	
Factor of Safety (FS) :	4.21	

Output results obtained from the analysis of Cave No: 7 are shown in Figure 4.6a to Figure 4.6d. As it can be seen at Figure 4.6b., the maximum deflection is 3.03 mm, which occurs under the loading area. The output results explain that the maximum vertical displacements occur under the loading area and the maximum horizontal displacement occurs at the ground level towards the loading, and there is almost no horizontal displacement at cave walls. The maximum vertical displacement is 4.5 times higher than the maximum horizontal displacement. There is also a very small heave occurs at the base of the cave.

The extreme relative shear stress with loading is 0.52, while it is 0.47 without loading, which indicates that the loading adds some extra stresses on the cave (Figure 4.6c, d). Without loading the extreme relative stresses concentrate towards the walls of the cave, and at the middle point of the cave close to the surface. Under the loading condition, the relative shear stress concentrations are similar to unloading condition. The extreme relative shear stress has not reached to 1.00 at any point and does not yield a failure line. So that there is no shear failure occurs at this cave.

The factor of safety against failure was calculated and it is 4.21.

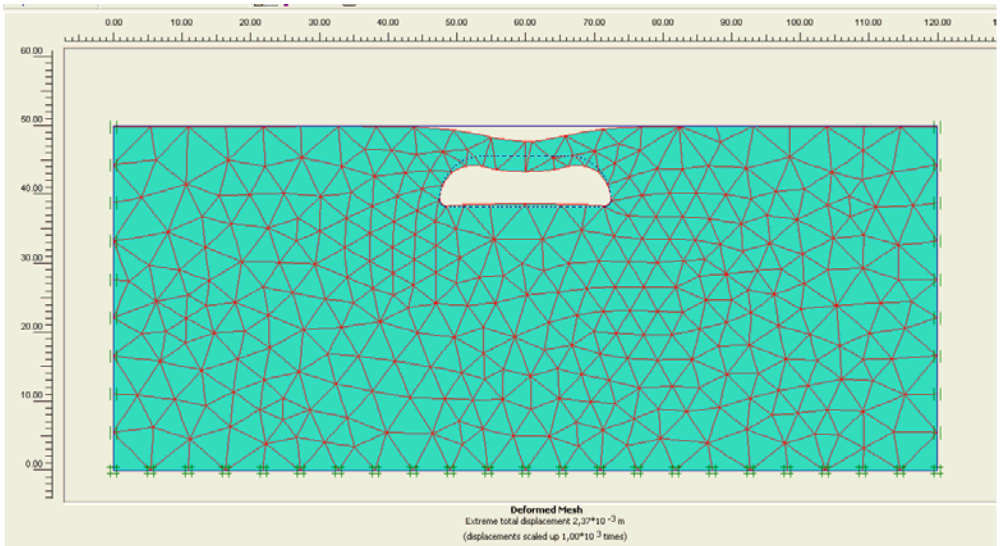

Figure 4.6a. Cave No: 7 Extreme Total Displacement and Deformed Shape Without Loading

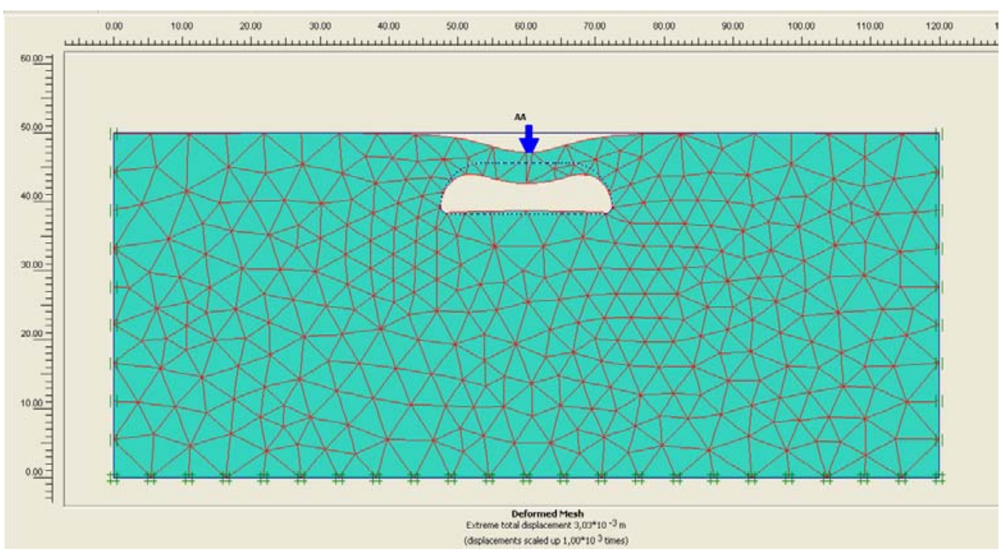

Figure 4.6b. Cave No: 7 Extreme Total Displacement and Deformed Shape With Loading

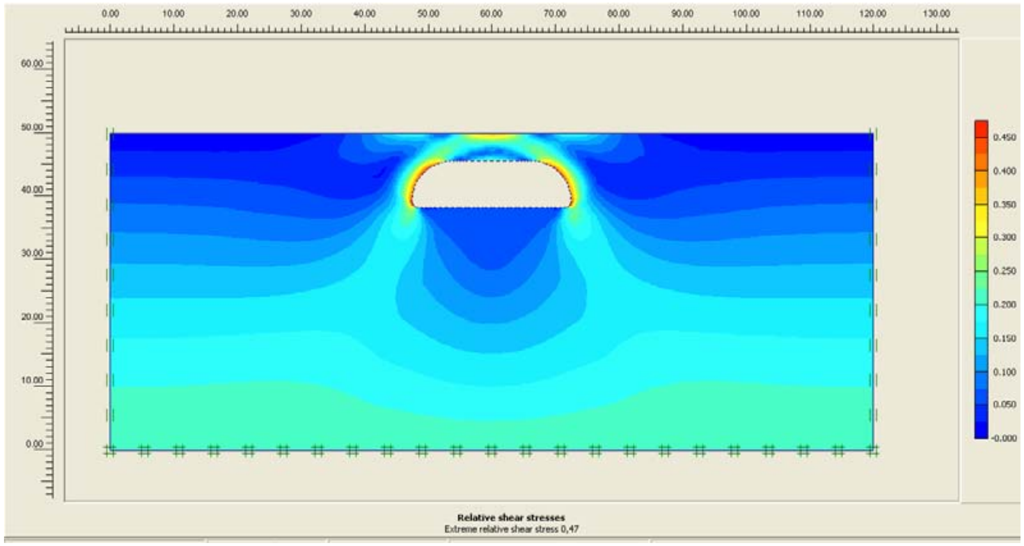

Figure 4.6c. Cave No: 7 Relative Shear Stress Without Loading

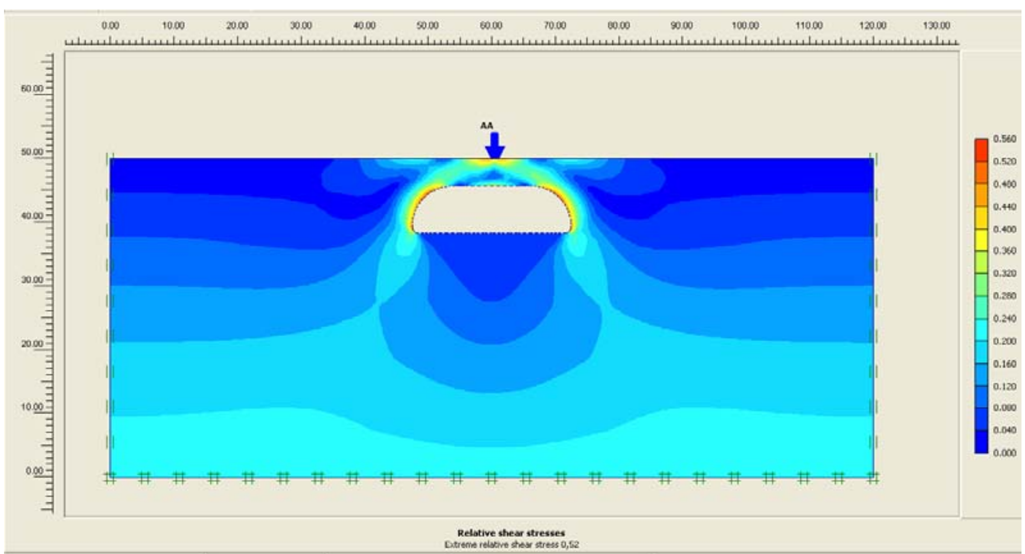

Figure 4.6d. Cave No: 7 Relative Shear Stress With Loading

Table 4.7. Input and Output Summary of Cave No:13

CAVE NO:13, ŞEHİT AHMET SK., DISTRICT: HOŞGÖR		
Width = 1.5m	Height = 1.8m	Depth = 3m
Cover Thickness:	2.5m	
Unconfined Compressive Strength:	11.63 MPa	
Cohesion (c):	0.590 MPa	
Young's Modulus (E) :	4.27 GPa	
Internal Angle of Friction (Φ) :	30.08	
Extreme Total Displacement :	0.11 mm	
Extreme Relative Shear Stress :	0.26	
Factor of Safety (FS) :	9.95	

Results obtained from the analysis of Cave No: 13 are shown in Figure 4.7a to Figure 4.7d. As it can be seen at Figure 4.7b., the maximum deflection is 0.11 mm, which occurs under the load. The results prove that the maximum vertical displacements occur just under the loading, and around the cave the vertical displacement is getting smaller. The maximum horizontal displacement occurs more on the loading side of the cave walls. The maximum vertical displacement is 6 times higher than the maximum horizontal displacement. The heave at the base of the cave is very small.

The extreme relative shear stress with loading is 0.26, while it is 0.19 without loading, which indicates that the loading adds extra stresses on the cave. Without loading the extreme relative stresses concentrate at the walls of the cave close to the base of the cave. Under the loading condition, the maximum relative shear stresses concentrate towards the walls of cave and under the loading close to the surface. The extreme relative shear stress is not higher than 1.00 at any point and does not yield a failure line for the cave to fail. Consequently the model showed that there is no shear failure occurs at this cave.

The factor of safety against failure was calculated and it is 9.95.

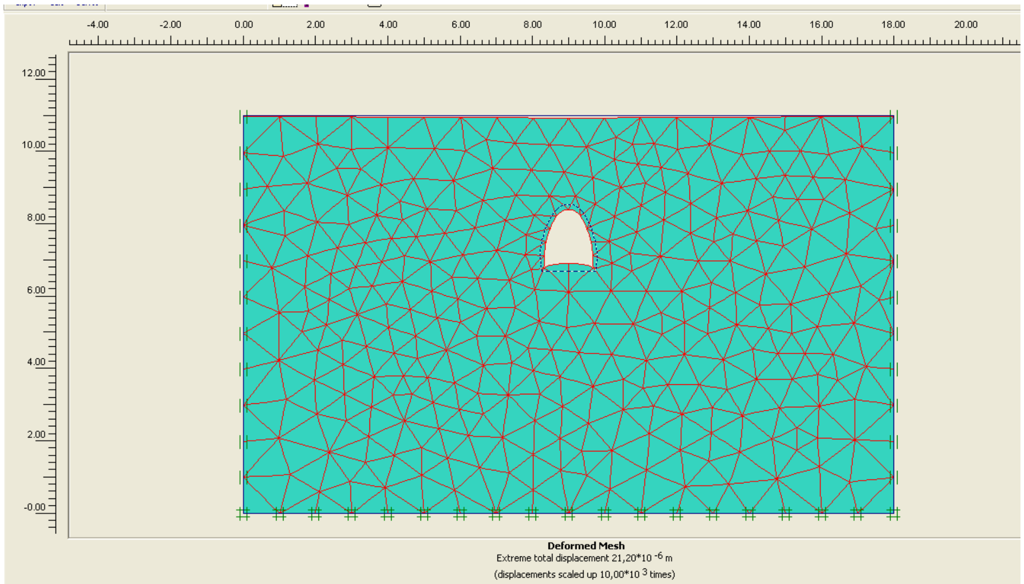

Figure 4.7a. Cave No: 13 Extreme Total Displacement and Deformed Shape Without Loading

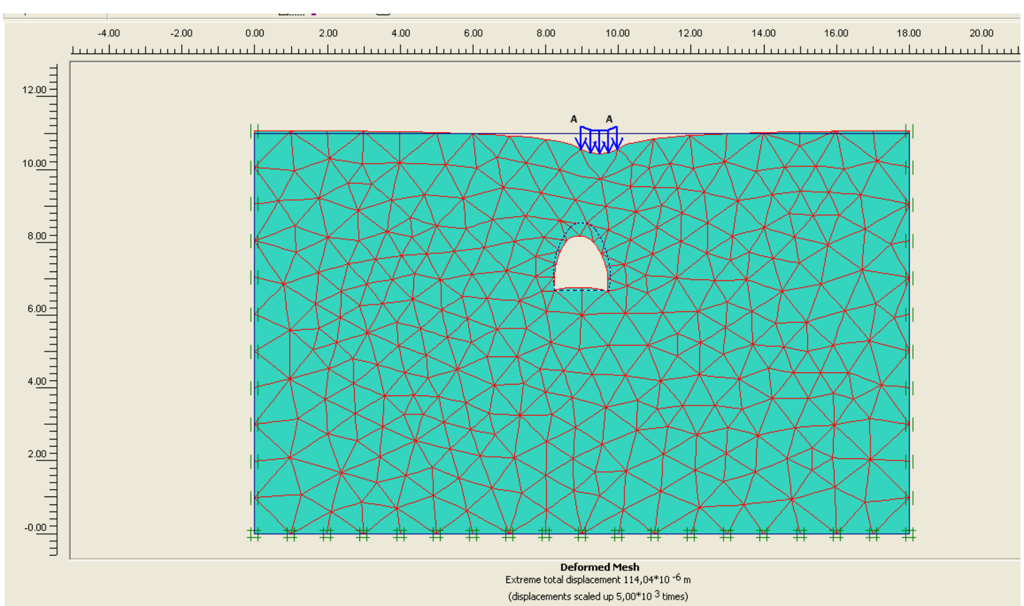

Figure 4.7b. Cave No: 13 Extreme Total Displacement and Deformed Shape With Loading

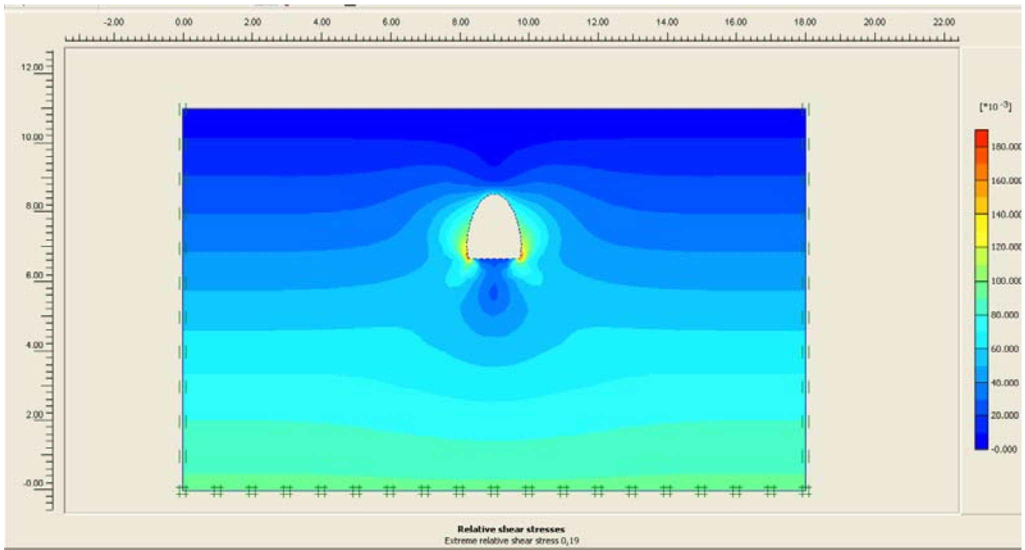

Figure 4.7c. Cave No: 13 Relative Shear Stress Without Loading

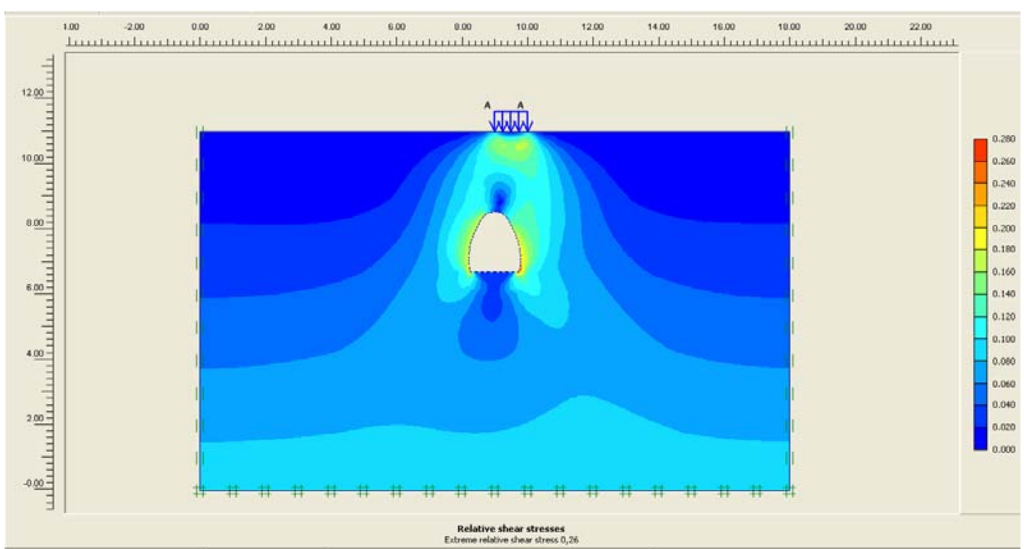

Figure 4.7d. Cave No: 13 Relative Shear Stress With Loading

Table 4.8. Input and Output Summary of Cave No:14

CAVE NO:14, BESİHANE, DISTRICT: DUMLUPINAR		
Width = 16m	Height = 8m	Depth = 14m
Cover Thickness:	1.5m	
Unconfined Compressive Strength:	8.19 MPa	
Cohesion (c):	0.415 MPa	
Young's Modulus (E) :	3.01 GPa	
Internal Angle of Friction (Φ) :	30.08	
Extreme Total Displacement :	6.91 mm	
Extreme Relative Shear Stress :	1	
Factor of Safety (FS) :	1.83	

Results obtained from the analysis of Cave No: 14 are shown in Figure 4.8a to Figure 4.8d. As it can be seen at Figure 4.8b., the maximum deflection is 6.91 mm, which occurs under the load. The output results demonstrate that the maximum vertical displacements occur under the loaded area and the maximum horizontal displacement occurs at the ground level towards the loading. Nearly no displacement occurs at the walls and the base of the cave. The maximum vertical displacement is almost 6 times higher than the maximum horizontal displacement. Generally the displacements occur only at the cover layer of the cave.

The extreme relative shear stress with loading is 1.00, while it is 0.62 without loading, which indicates that the loading adds a lot of extra stresses on the cave. Without loading the extreme relative stresses concentrate at the walls of the cave, and at the middle point of the cave close to the surface. Similarly under the loading condition, the maximum relative shear stresses concentrate at the walls of the cave and under the loading with larger stresses. This extra stresses cause the extreme relative shear stress to reach 1.00 at the shoulders of the cave and just under the loading, but no failure line occurs at the cave that can cause shear failure of the cave.

The factor of safety against failure was calculated and it is 1.83.

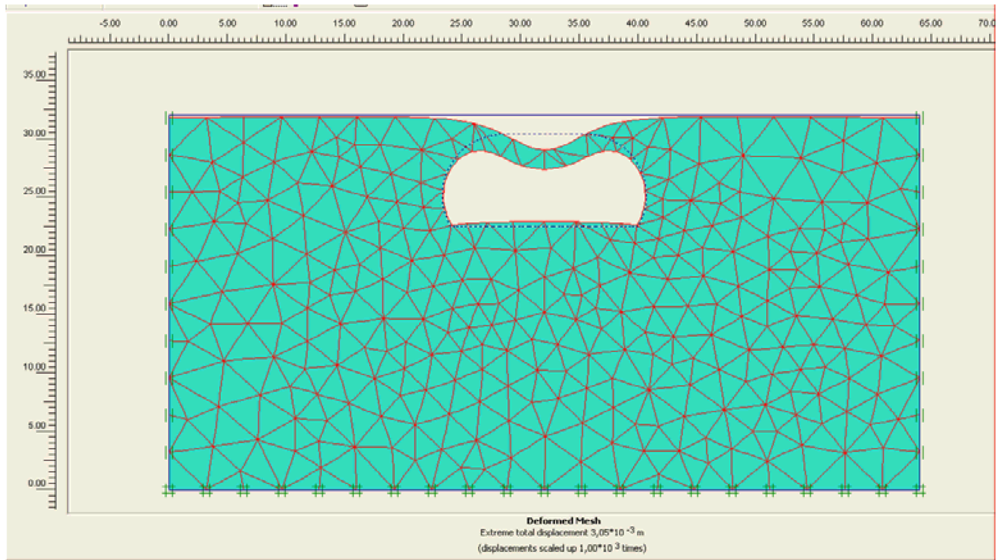

Figure 4.8a. Cave No: 14 Extreme Total Displacement and Deformed Shape Without Loading

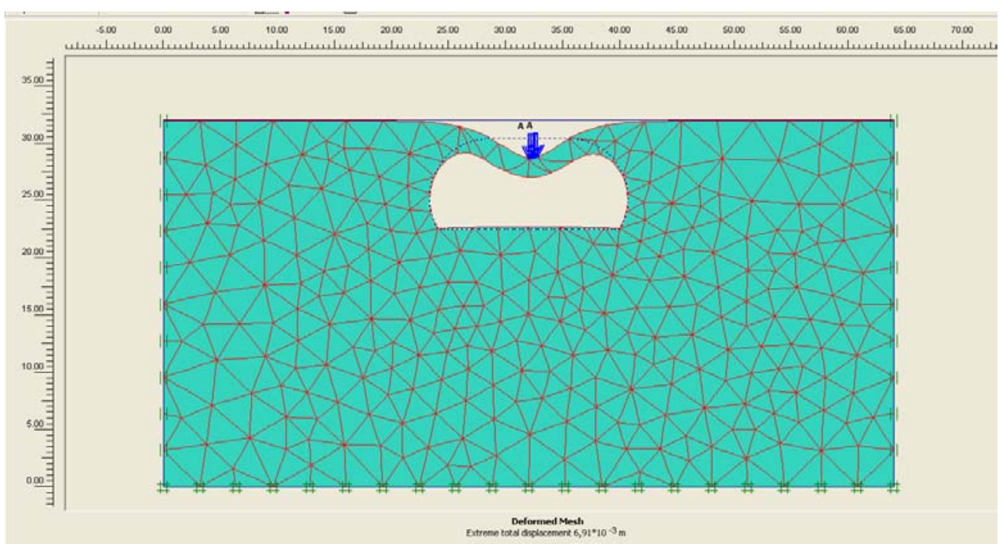

Figure 4.8b. Cave No: 14 Extreme Total Displacement and Deformed Shape With Loading

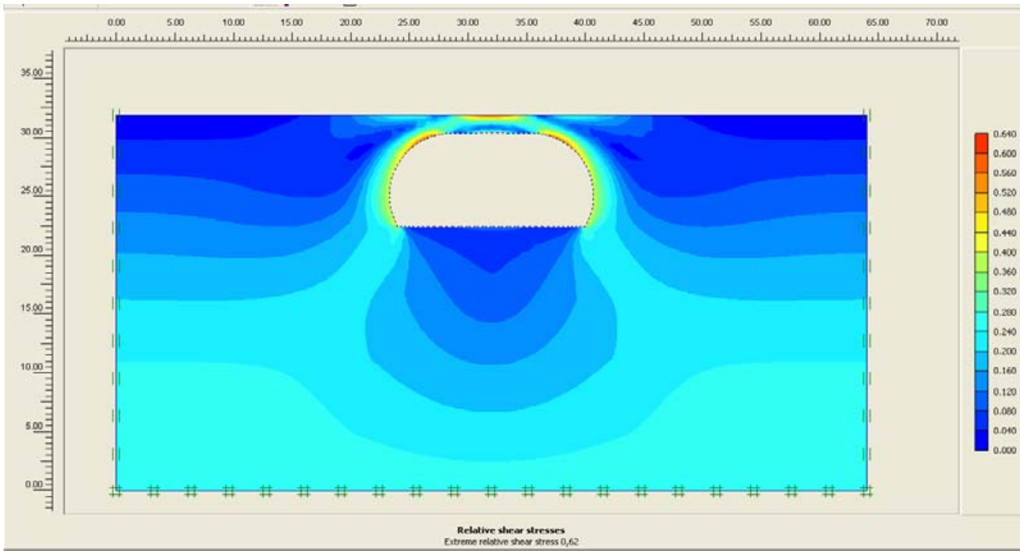

Figure 4.8c. Cave No: 14 Relative Shear Stress Without Loading

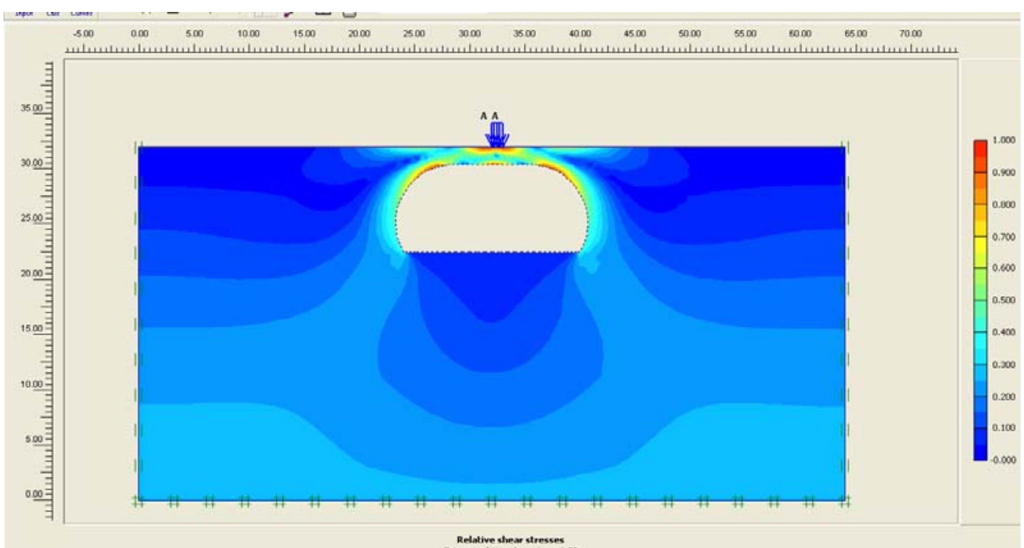

Figure 4.8d. Cave No: 14 Relative Shear Stress With Loading

Table 4.9. Input and Output Summary of Cave No:18

CAVE NO:18, BESNİ CAD., DISTRICT: ÇAĞLAYAN		
Width = 15m	Height = 7m	Depth = 5m
Cover Thickness:	1m	
Unconfined Compressive Strength:	9.87 MPa	
Cohesion (c):	0.501 MPa	
Young's Modulus (E) :	3.63 GPa	
Internal Angle of Friction (Φ) :	30.08	
Extreme Total Displacement :	3.47 mm	
Extreme Relative Shear Stress :	0.94	
Factor of Safety (FS) :	2.52	

Results obtained from the analysis of Cave No: 18 are shown in Figure 4.9a to Figure 4.9d. As it can be seen at Figure 4.9b., the maximum deflection is 3.47 mm, which occurs under the load. The output results show that the maximum vertical displacements occur at the middle point of cave under the loading and the maximum horizontal displacement occurs above the cave roof towards the loading, and slightly on the walls of the cave. The maximum vertical displacement is almost 6 times higher than the maximum horizontal displacement. There is also a slightly heave at the base of the cave.

The extreme relative shear stress with loading is 0.94, while it is 0.39 without loading, which indicates that the loading adds a lot of extra stresses on the cave (Figure 4.9c, d). Without loading the extreme relative stresses concentrate at the just under the loading and at the walls of the cave close to the base of the cave, which the stress concentration decreases towards the roof of the cave. However under the loading condition, the maximum relative shear stresses concentrate more under the loading close to the surface. The extreme relative shear stress has not reached to 1.00 at any point and does not yield a failure line. As a result there is no shear failure.

The factor of safety against failure was calculated and it is 2.52.

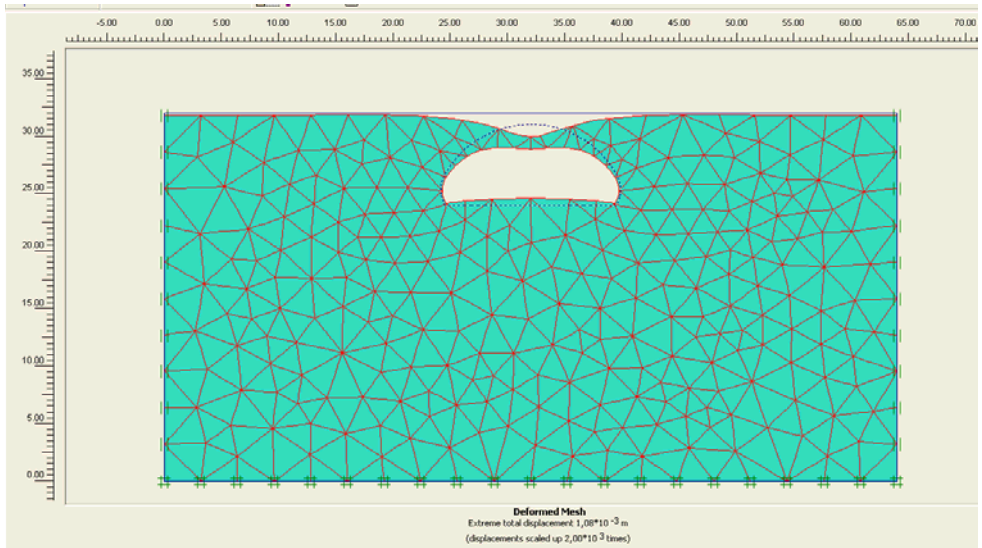

Figure 4.9a. Cave No: 18 Extreme Total Displacement and Deformed Shape Without Loading

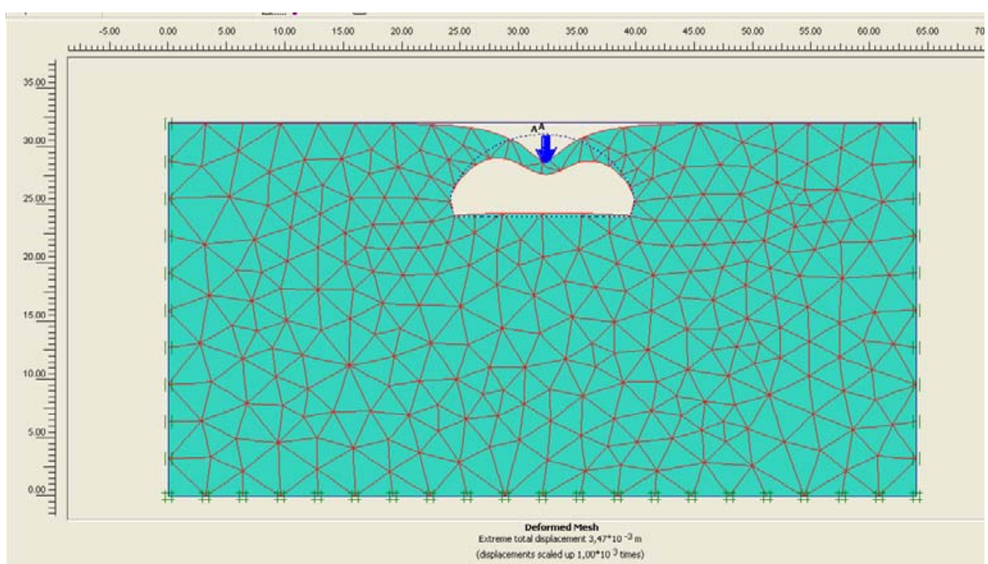

Figure 4.9b. Cave No: 18 Extreme Total Displacement and Deformed Shape With Loading

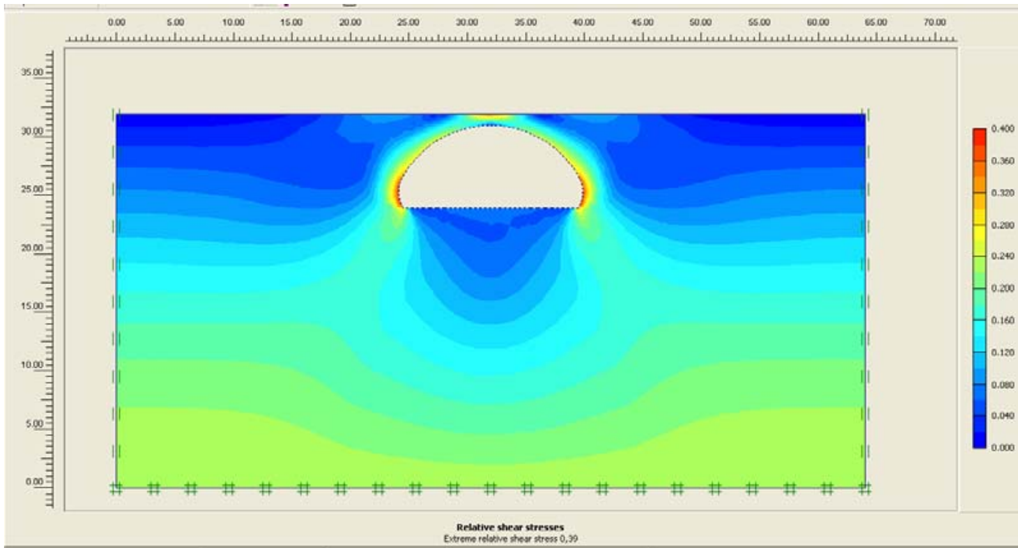

Figure 4.9c. Cave No: 18 Relative Shear Stress Without Loading

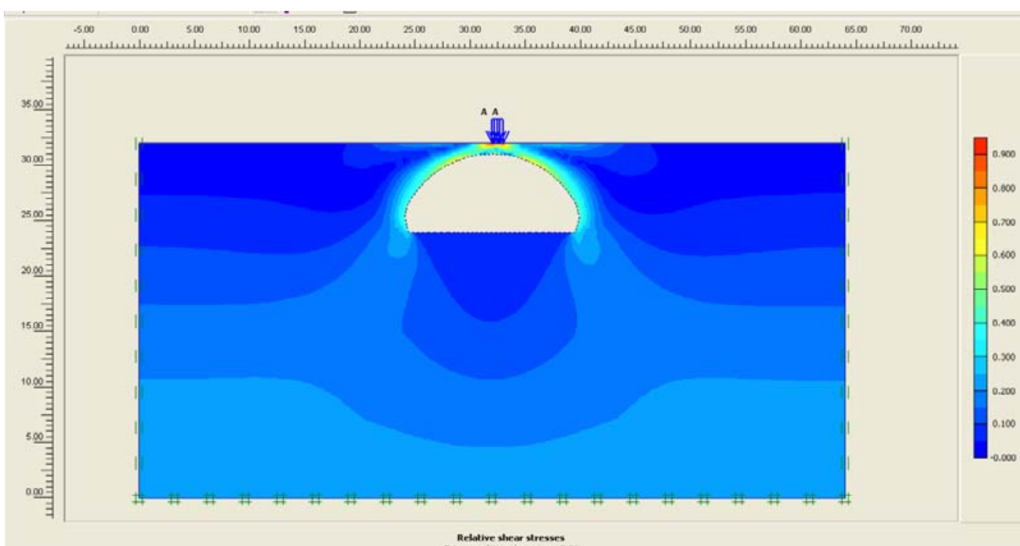

Figure 4.9d. Cave No: 18 Relative Shear Stress With Loading

Table 4.10. Input and Output Summary of Cave No:19

CAVE NO:19, BESNİ CAD., DISTRICT: ÇAĞLAYAN		
Width = 4m	Height = 6m	Depth = 15m
Cover Thickness:	2m	
Unconfined Compressive Strength:	17.65 MPa	
Cohesion (c):	0.895 MPa	
Young's Modulus (E) :	6.49 GPa	
Internal Angle of Friction (Φ) :	30.08	
Extreme Total Displacement :	0.59 mm	
Extreme Relative Shear Stress :	0.38	
Factor of Safety (FS) :	6.35	

Results obtained from the analysis of Cave No: 19 are shown in Figure 4.10a to Figure 4.10d. As it can be seen at Figure 4.10b., the maximum deflection is 0.59 mm, which occurs under the load. The output results show that the maximum vertical displacements occur at the roof of cave under the loading area. The maximum horizontal displacement occurs at the ground level towards the loading and at the shoulders of the cave. The maximum vertical displacement is 4.5 times higher than the maximum horizontal displacement. There is also a heave at the base of the cave.

The extreme relative shear stress with loading is 0.38, while it is 0.17 without loading, which indicates that the loading adds extra stresses on the cave. Without loading the extreme relative stresses concentrate at the walls of the cave. However under the loading condition, the maximum relative shear stresses concentrate at the corners of the cave where the walls and the roof meet, and also under the loading close to surface. The extreme relative shear stress is not higher than 1.00 at any point and does not yield a failure line for the cave to fail. Therefore the model showed that there is no shear failure occurs at this cave. Because of the shape, the stress changes are different for this cave than the others

The calculated factor of safety against failure is 6.35.

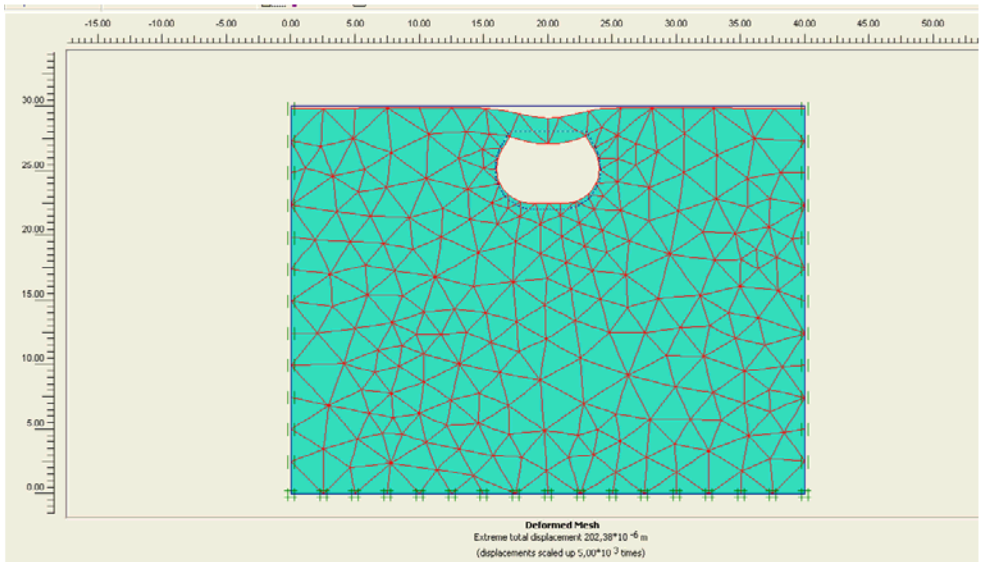

Figure 4.10a. Cave No: 19 Extreme Total Displacement and Deformed Shape Without Loading

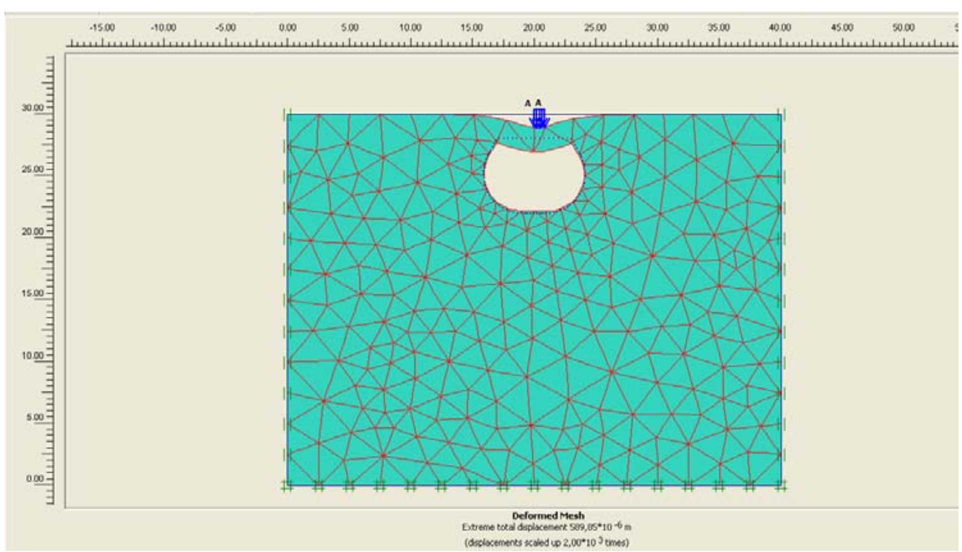

Figure 4.10b. Cave No: 19 Extreme Total Displacement and Deformed Shape With Loading

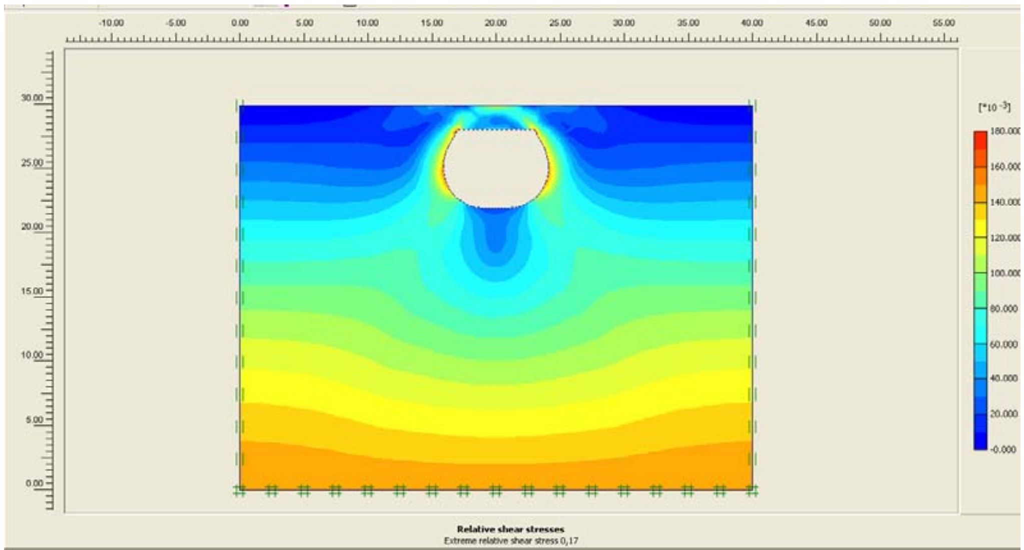

Figure 4.10c. Cave No: 19 Relative Shear Stress Without Loading

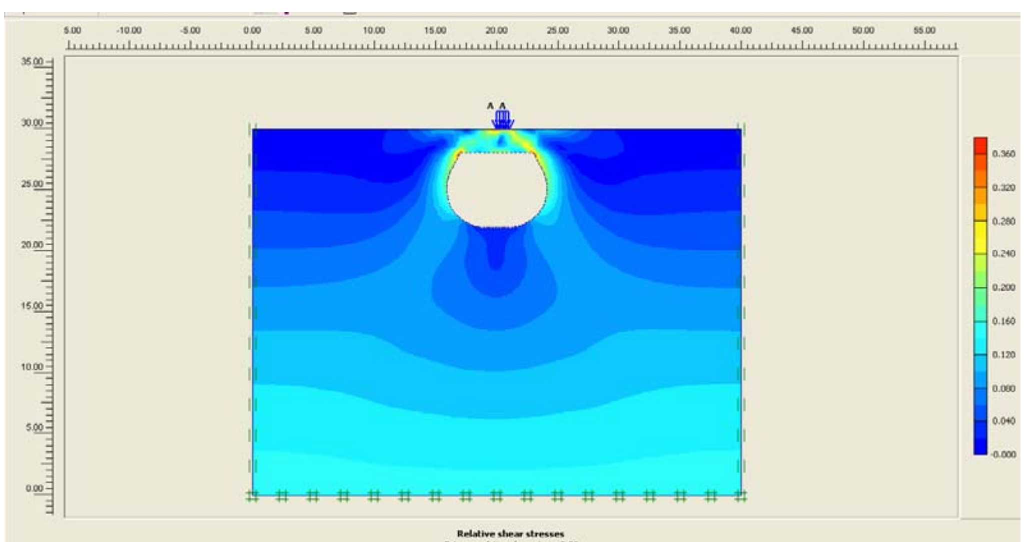

Figure 4.10d. Cave No: 19 Relative Shear Stress With Loading

Table 4.11. Input and Output Summary of Cave No:20

CAVE NO:20, MEZARLIK., DISTRICT: AYDINLAR		
Width = 8m	Height = 10m	Depth = 12m
Cover Thickness:	2m	
Unconfined Compressive Strength:	10.71 MPa	
Cohesion (c):	0.543 MPa	
Young's Modulus (E) :	3.94 GPa	
Internal Angle of Friction (Φ) :	30.08	
Extreme Total Displacement :	1.55 mm	
Extreme Relative Shear Stress :	0.57	
Factor of Safety (FS) :	3.48	

Results obtained from the analysis of Cave No: 20 are shown in Figure 4.11a to in Figure 4.11d. As it can be seen at Figure 4.11b., the maximum deflection is 1.55 mm, which occurs under the load. The output results show that the maximum vertical displacements occur under the loading area. The maximum horizontal displacement occurs at the ground level towards the loading, and towards the cave wall. The maximum vertical displacement is 4.5 times higher than the maximum horizontal displacement. There is also a slightly heave at the base of the cave.

The extreme relative shear stress with loading is 0.57, while it is 0.43 without loading, which indicates that the loading adds some extra stresses on the cave (Figure 4.11c, d). Without loading the extreme relative stresses concentrate at the corners of the cave close to the base of the cave, and some at the shoulders of the cave. However under the loading condition, the maximum relative shear stresses concentrate more at the shoulders of the cave, and under the loading close to the surface. The extreme relative shear stress is not higher than 1.00 at any point and does not yield a failure line for the cave to fail. Therefore the model showed that there is no shear failure occurs at this cave.

The factor of safety against failure was calculated and it is 3.48.

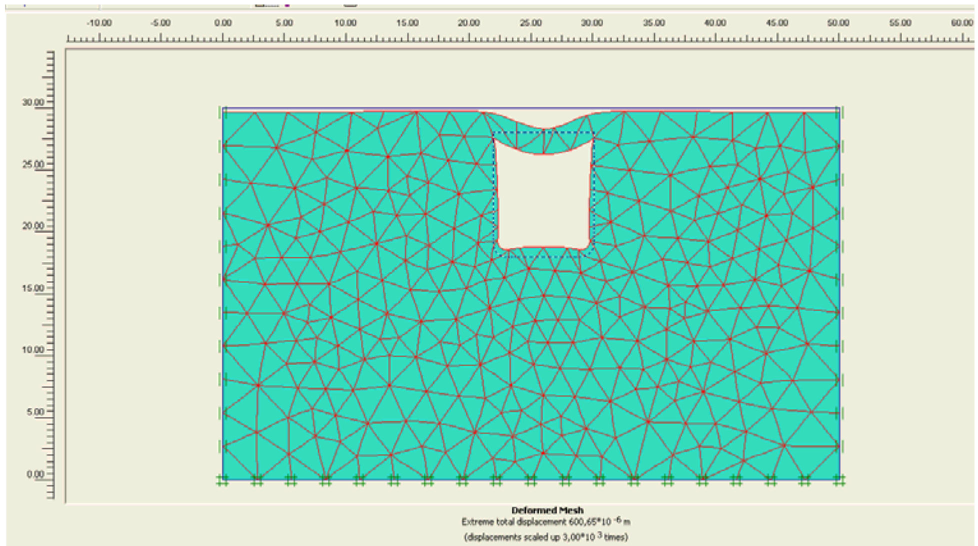

Figure 4.11a. Cave No: 20 Extreme Total Displacement and Deformed Shape Without Loading

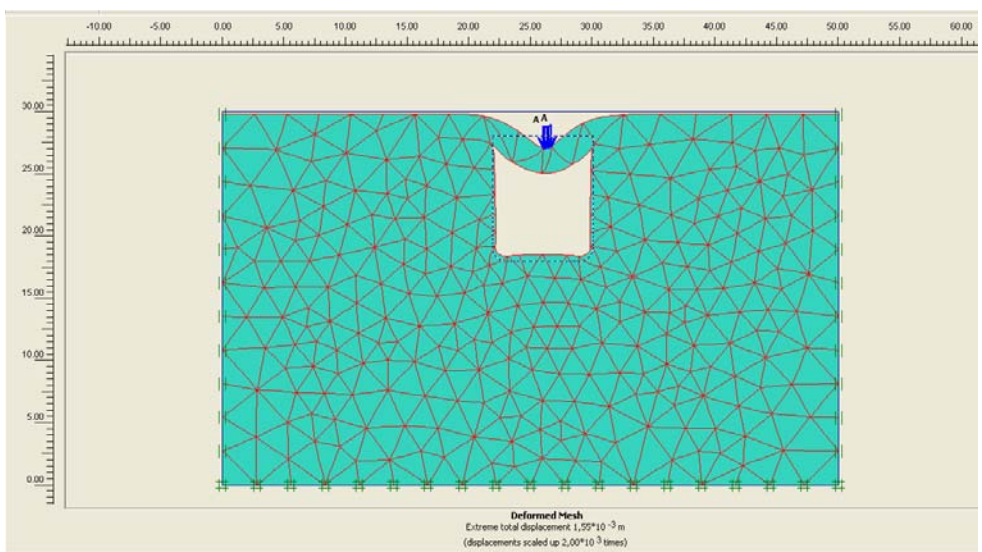

Figure 4.11b. Cave No: 20 Extreme Total Displacement and Deformed Shape With Loading

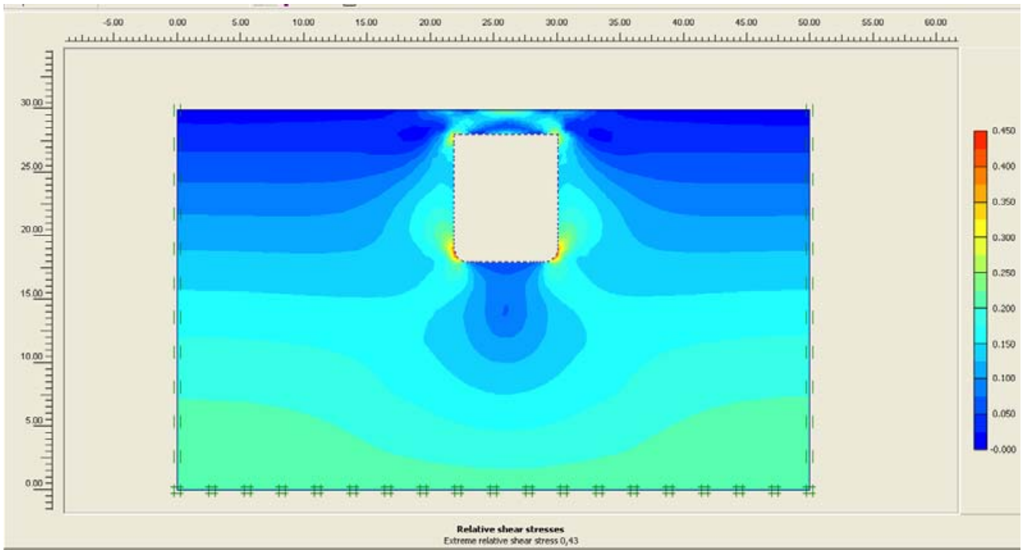

Figure 4.11c. Cave No: 20 Relative Shear Stress Without Loading

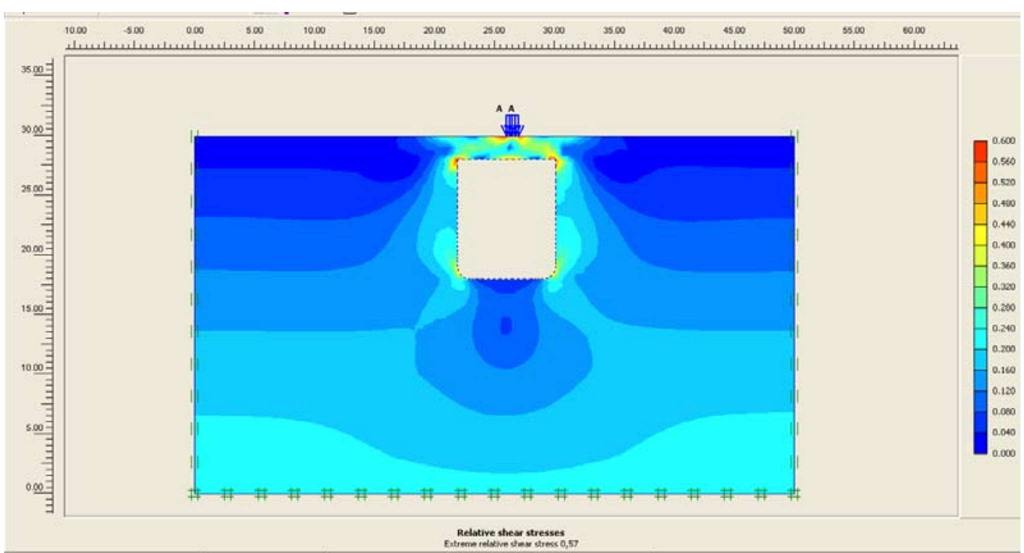

Figure 4.11d. Cave No: 20 Relative Shear Stress With Loading

Table 4.12. Input and Output Summary of Cave No:21

<table>
<tr><th colspan="3">CAVE NO:21, URFA YOLU, DISTRICT: AYDINLAR</th></tr>
<tr><td>Width = 25m</td><td>Height = 9m</td><td>Depth = 30m</td></tr>
<tr><td colspan="2">Cover Thickness:</td><td>3.5m</td></tr>
<tr><td colspan="2">Unconfined Compressive Strength:</td><td>9.65 MPa</td></tr>
<tr><td colspan="2">Cohesion (c):</td><td>0.489 MPa</td></tr>
<tr><td colspan="2">Young's Modulus (E) :</td><td>3.55 GPa</td></tr>
<tr><td colspan="2">Internal Angle of Friction (Φ) :</td><td>30.08</td></tr>
<tr><td colspan="2">Extreme Total Displacement :</td><td>5.71 mm</td></tr>
<tr><td colspan="2">Extreme Relative Shear Stress :</td><td>0.77</td></tr>
<tr><td colspan="2">Factor of Safety (FS) :</td><td>2.65</td></tr>
</table>

Results obtained from the analysis of Cave No: 21 are shown in Figure 4.12a to Figure 4.12d. As it can be seen at Figure 4.12b., the maximum deflection is 5.71 mm, which occurs under the loading area. The output results show that the maximum vertical displacements occur at the middle point of cave under the loading. Meanwhile the maximum horizontal displacement occurs at the ground level towards the loading, and just a little bit at the cave walls close to the basement of the cave. The maximum vertical displacement is 5 times higher than the maximum horizontal displacement. There is also a slightly heave at the basement of the cave.

The extreme relative shear stress with loading is 0.77, while it is 0.65 without loading, which indicates that the loading adds some extra stresses on the cave (Figure 4.12c, d). Without loading the extreme relative stresses concentrate towards the walls of the cave, and at the middle point of the cave close to the surface, but at the roof there is not much relative stress occurrence. Under the loading condition, the maximum relative shear stresses concentration is very similar to unloading condition. The extreme relative shear stress does not yield failure line. No shear failure occurs.

The factor of safety against failure was calculated and it is 2.65.

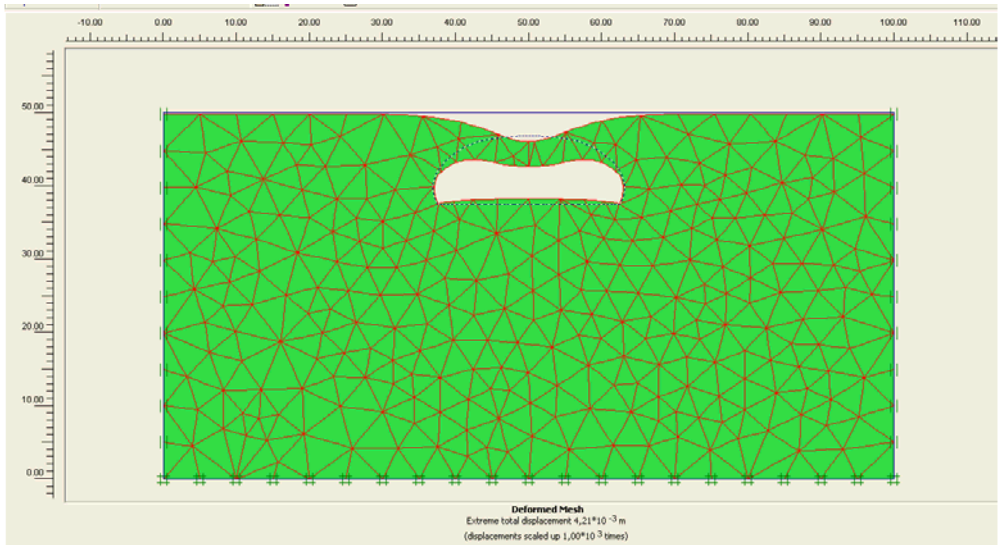

Figure 4.12a. Cave No: 21 Extreme Total Displacement and Deformed Shape Without Loading

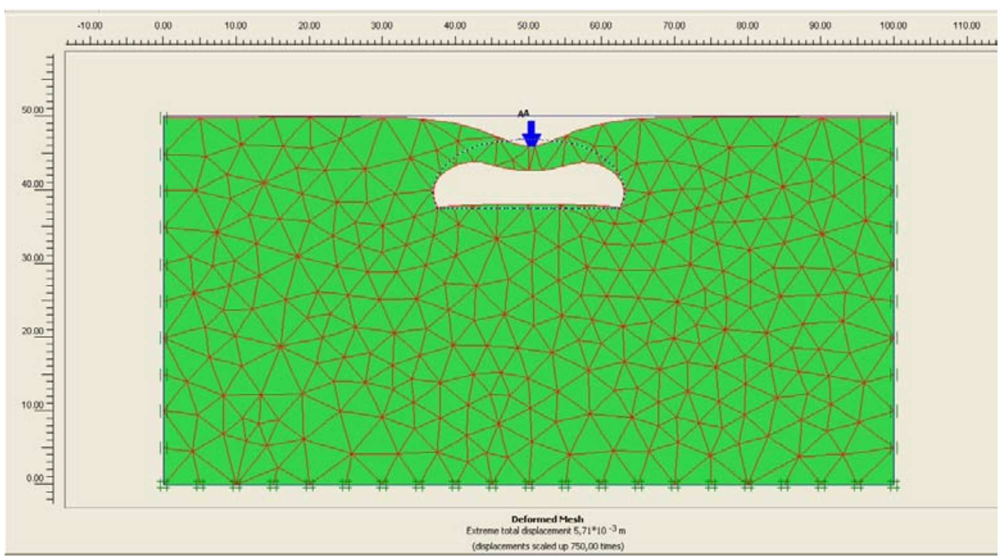

Figure 4.12b. Cave No: 21 Extreme Total Displacement and Deformed Shape With Loading

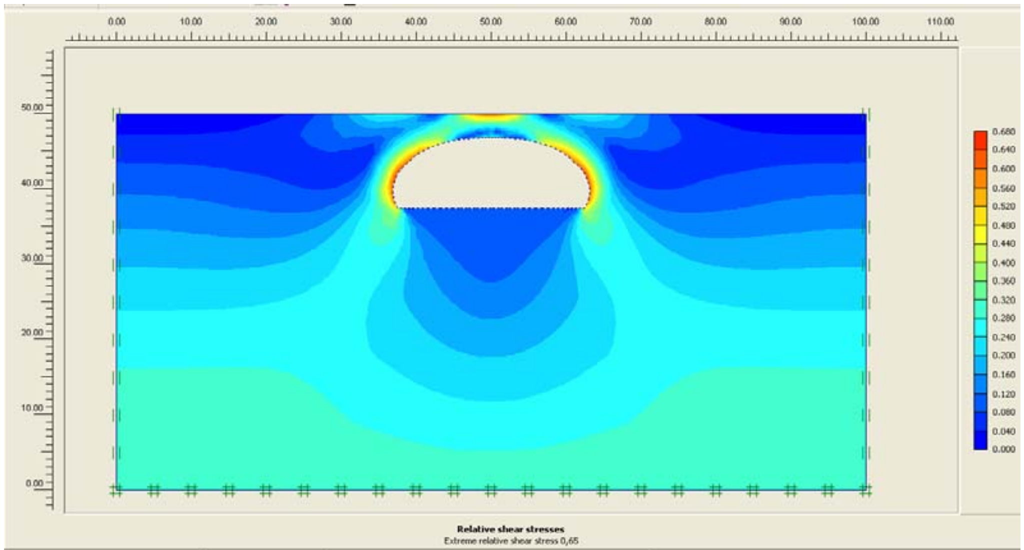

Figure 4.12c. Cave No: 21 Relative Shear Stress Without Loading

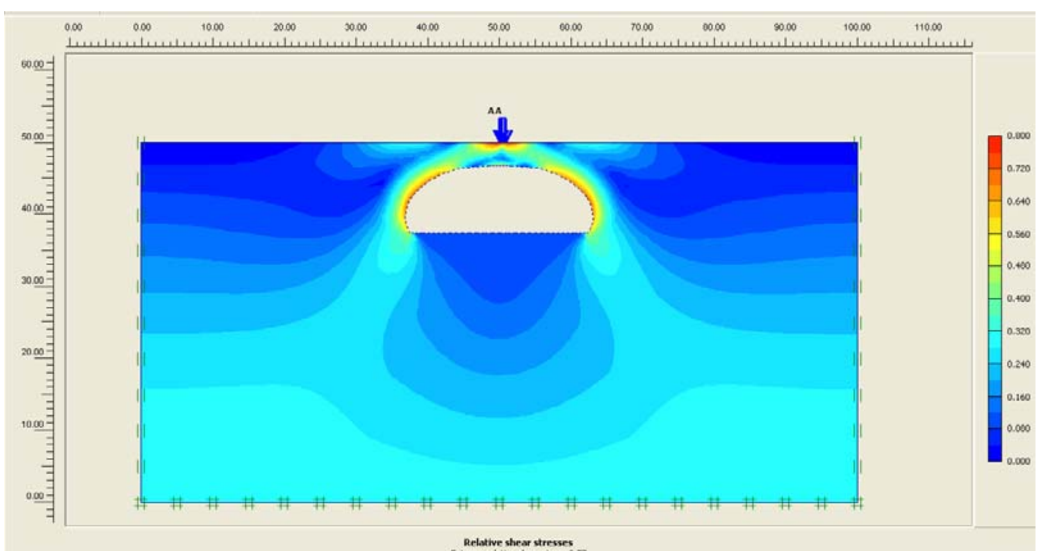

Figure 4.12d. Cave No: 21 Relative Shear Stress With Loading

Table 4.13. Input and Output Summary of Cave No:22

CAVE NO:22, BESİHANE, DISTRICT: UMUT		
Width = 8m	Height = 15m	Depth = 18m
Cover Thickness:	10m	
Unconfined Compressive Strength:	9.44 MPa	
Cohesion (c):	0.479 MPa	
Young's Modulus (E) :	3.47 GPa	
Internal Angle of Friction (Φ) :	30.08	
Extreme Total Displacement :	1.75 mm	
Extreme Relative Shear Stress :	0.68	
Factor of Safety (FS) :	3.92	

Results obtained from the analysis of Cave No: 22 are shown in Figure 4.13a to Figure 4.13d. As it can be seen at Figure 4.13b, the maximum deflection is 1.75 mm, which occurs under the loading area. The results show that the maximum vertical displacements occur towards the roof of cave under the loading. The maximum horizontal displacement occurs at the ground level towards the loading, towards the cave walls and under the base of the cave. The maximum vertical displacement is 4.5 times higher than the maximum horizontal displacement. There is a considerable heave at the base of the cave.

The extreme relative shear stress with loading is 0.68, while it is 0.58 without loading, which indicates that the loading adds some extra stresses on the cave (Figure 4.13c, d). Without loading the extreme relative stresses concentrate towards the walls of the cave. Under the loading condition, the maximum relative shear stress distribution occurs similarly to the unloading condition. The extreme relative shear stress is not higher than 1.00 at any point and does not yield a failure line for the cave to fail. Therefore the model showed that there is no shear failure occurs at this cave.

The factor of safety against failure was calculated and it is 3.92.

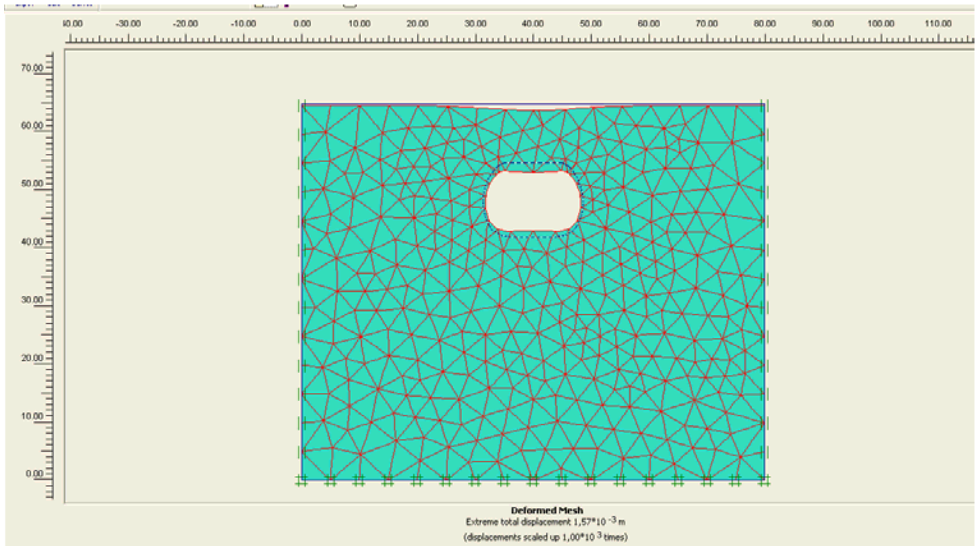

Figure 4.13a. Cave No: 22 Extreme Total Displacement and Deformed Shape Without Loading

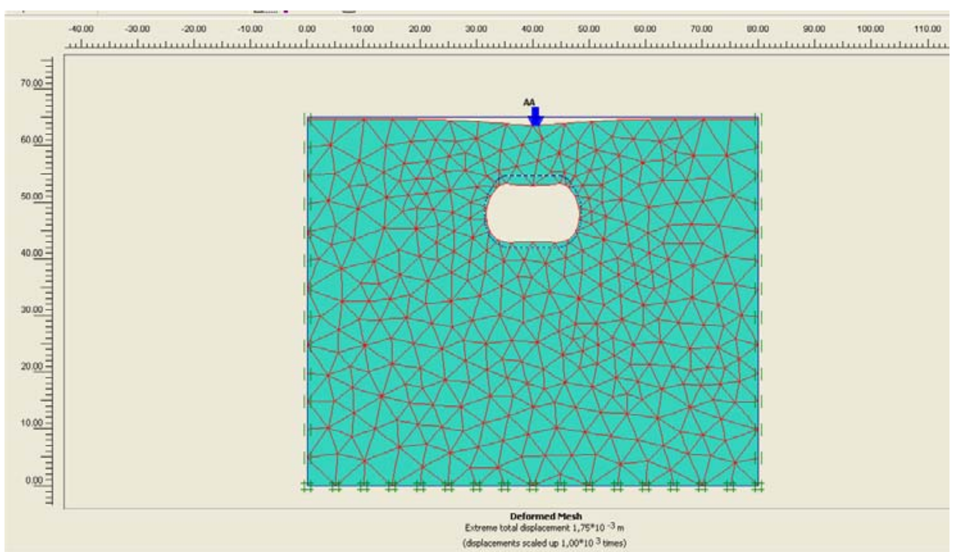

Figure 4.13b. Cave No: 22 Extreme Total Displacement and Deformed Shape With Loading

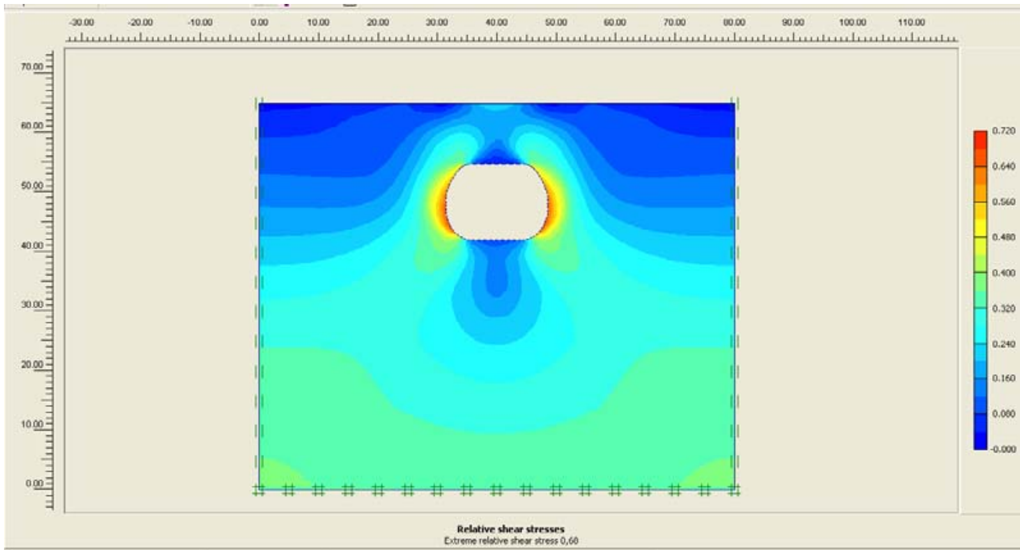

Figure 4.13c. Cave No: 22 Relative Shear Stress Without Loading

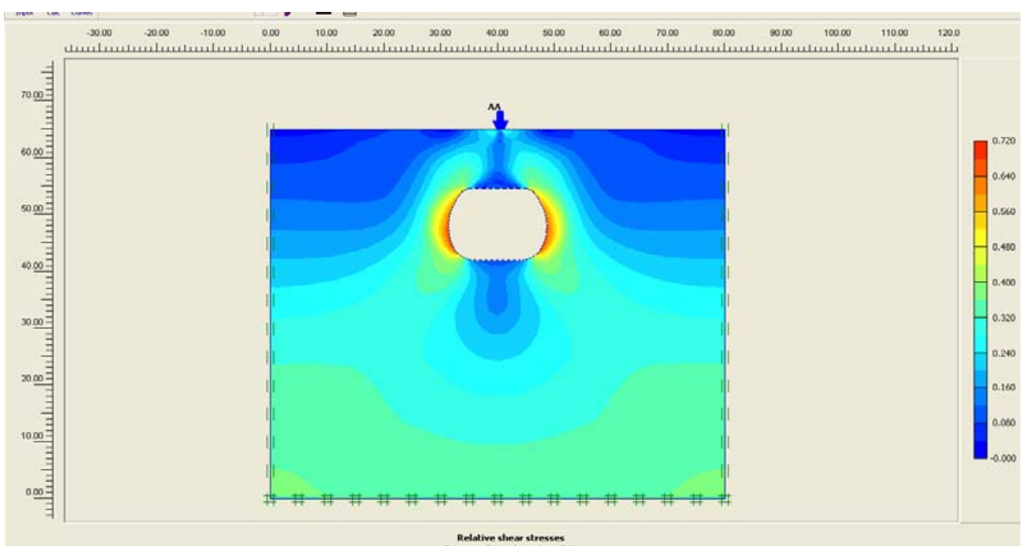

Figure 4.13d. Cave No: 21 Relative Shear Stress With Loading

Table 4.14. Input and Output Summary of Cave No:27

CAVE NO:27, SULU, DISTRICT: KILINÇOĞLU		
Width = 35m	Height = 5m	Depth = 50m
Cover Thickness:	2m	
Unconfined Compressive Strength:	12.12 MPa	
Cohesion (c):	0.615 MPa	
Young's Modulus (E) :	4.45 GPa	
Internal Angle of Friction (Φ) :	30.08	
Extreme Total Displacement :	15,07 mm	
Extreme Relative Shear Stress :	1	
Factor of Safety (FS) :	1.80	

Results obtained from the analysis of Cave No: 27 are shown in Figure 4.14a to Figure 4.14d. As it can be seen at Figure 4.14b., the maximum deflection is 15.07 mm occurs under the loading area. The output results show that the maximum vertical displacements occur towards the cave roof under the loading. The maximum horizontal displacement occurs at the ground level towards the loading and at the cave roof towards to the cave walls. The maximum vertical displacement is 6 times higher than the maximum horizontal displacement. No heave occurs at the base of this cave.

The extreme relative shear stress with loading is 1.00, while it is 0.98 without loading, which indicates that the loading adds extra stresses on the cave. Without loading the extreme relative stresses concentrate at the shoulders of the cave and at the middle point of the cave close to the surface. Under the loading condition, the maximum relative shear stress distribution occurs similarly to the unloading condition with more stress concentration. This extra stresses cause the extreme relative shear stress to reach 1.00 at the cave shoulders and under the loading. However no failure line can be seen. Therefore no shear failure occurs at this cave.

The factor of safety against failure was calculated and it is 1.80.

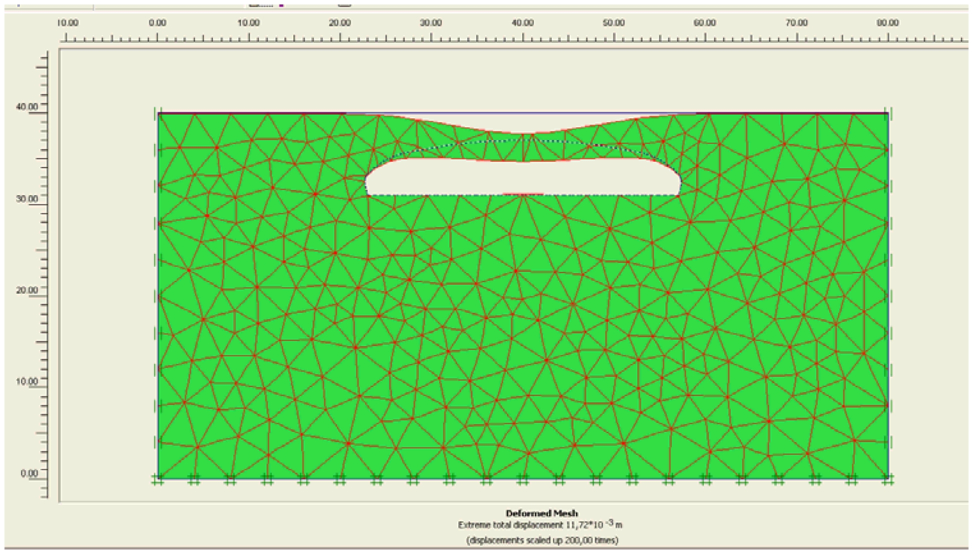

Figure 4.14a. Cave No: 27 Extreme Total Displacement and Deformed Shape Without Loading

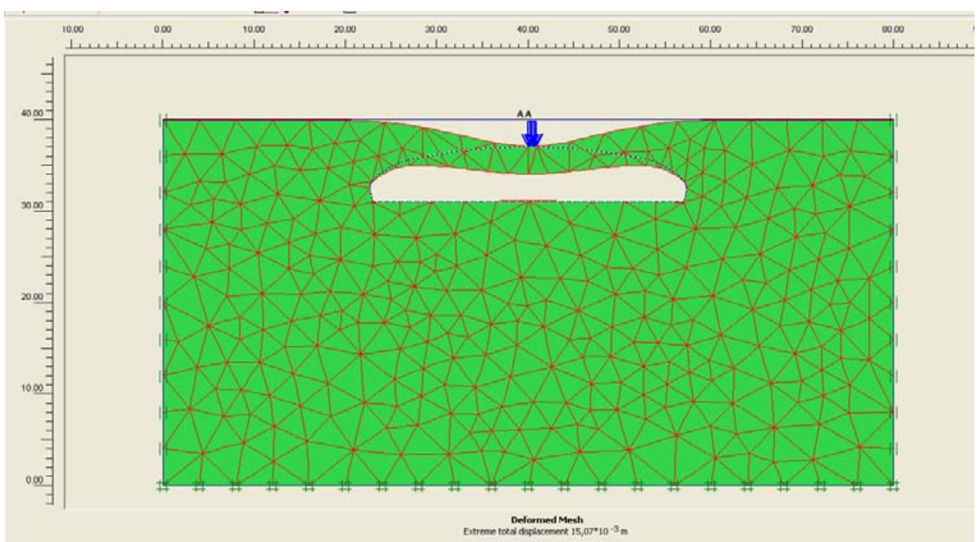

Figure 4.14b. Cave No: 27 Extreme Total Displacement and Deformed Shape With Loading

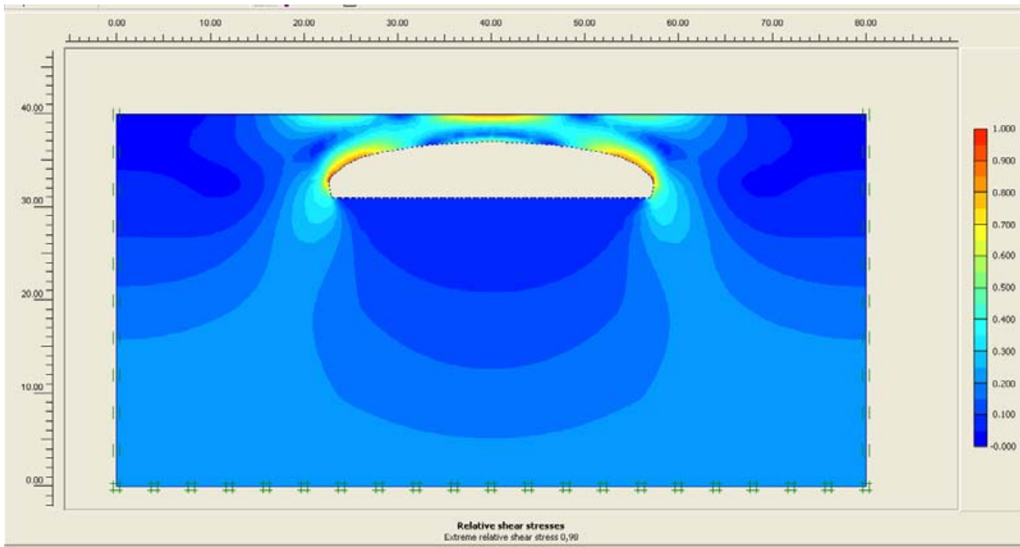

Figure 4.14c. Cave No: 27 Relative Shear Stress Without Loading

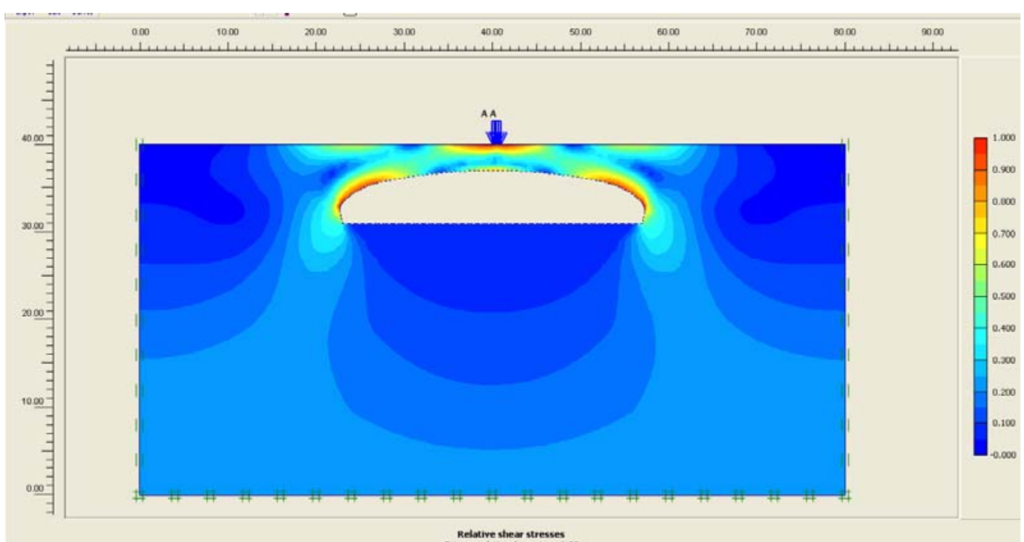

Figure 4.14d. Cave No: 27 Relative Shear Stress With Loading

Table 4.15. Input and Output Summary of Cave No:28

CAVE NO:28, XXXX, DISTRICT: DUMLUPINAR		
Width = 15m	Height = 8m	Depth = 20m
Cover Thickness:	2m	
Unconfined Compressive Strength:	8.38 MPa	
Cohesion (c):	0.425 MPa	
Young's Modulus (E) :	3.08 GPa	
Internal Angle of Friction (Φ) :	30.08	
Extreme Total Displacement :	2.36 mm	
Extreme Relative Shear Stress :	0.75	
Factor of Safety (FS) :	3.02	

Results obtained from the analysis of Cave No: 28 are shown in Figure 4.15a to Figure 4.15d. As it can be seen at Figure 4.15b., the maximum deflection is 2.36 mm, which occurs under the loading area. The output results show that the maximum vertical displacements occur at the middle point of cave under the loading. The maximum horizontal displacement occurs at the ground level towards the loading, and slightly at the cave walls close to the base of the cave. The maximum vertical displacement is 4.5 times higher than the maximum horizontal displacement. There is a slightly heave at the base of the cave.

The extreme relative shear stress with loading is 0.75, while it is 0.47 without loading, which indicates that the loading adds extra stresses on the cave (Figure 4.15c, d). Without loading the extreme relative stresses concentrate towards the walls of the cave, and at the middle point of the cave close to the surface. However under the loading condition, the relative shear stresses concentrate more to the shoulders of the cave and under the loading close to the surface. The extreme relative shear stress has not reached to 1.00 at any point and does not yield a shear failure

The factor of safety against failure was calculated and it is 3.02.

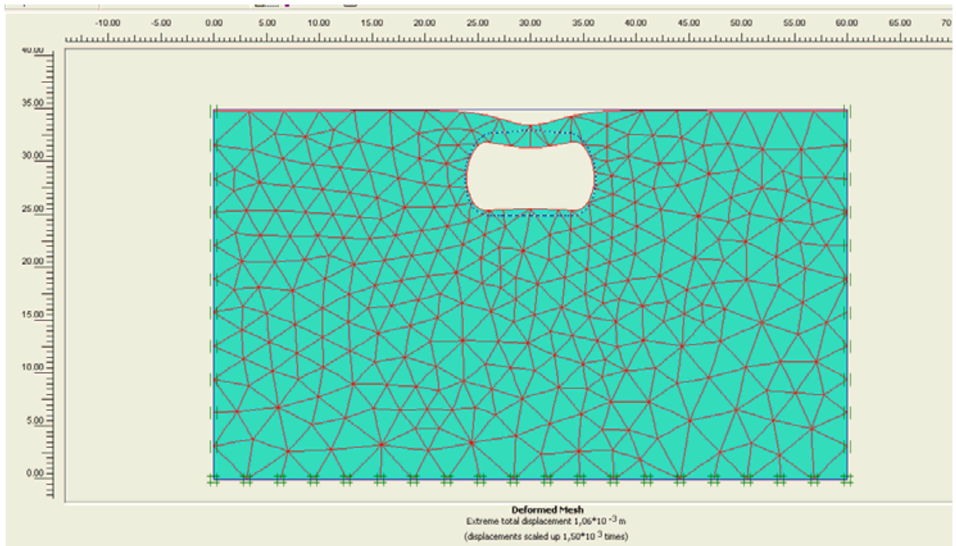

Figure 4.15a. Cave No: 28 Extreme Total Displacement and Deformed Shape Without Loading

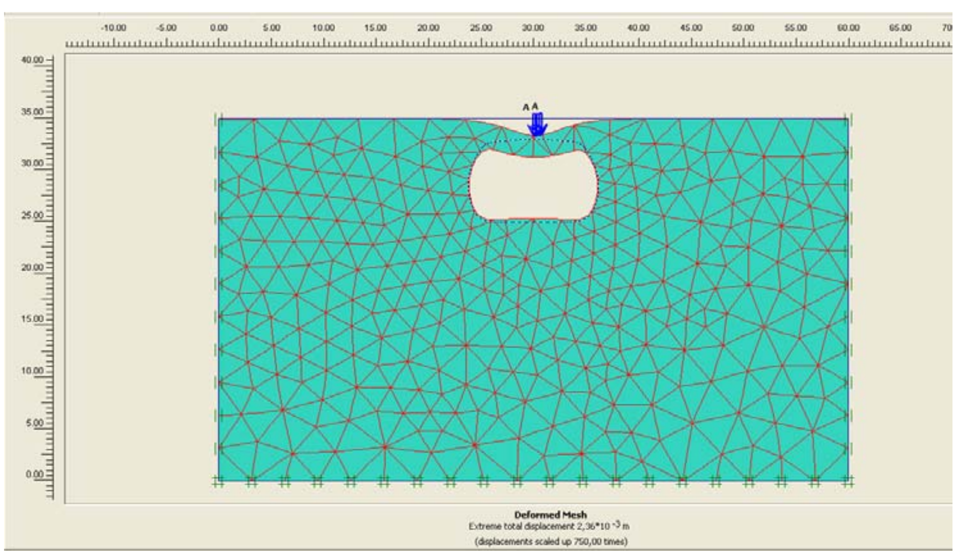

Figure 4.15b. Cave No: 28 Extreme Total Displacement and Deformed Shape With Loading

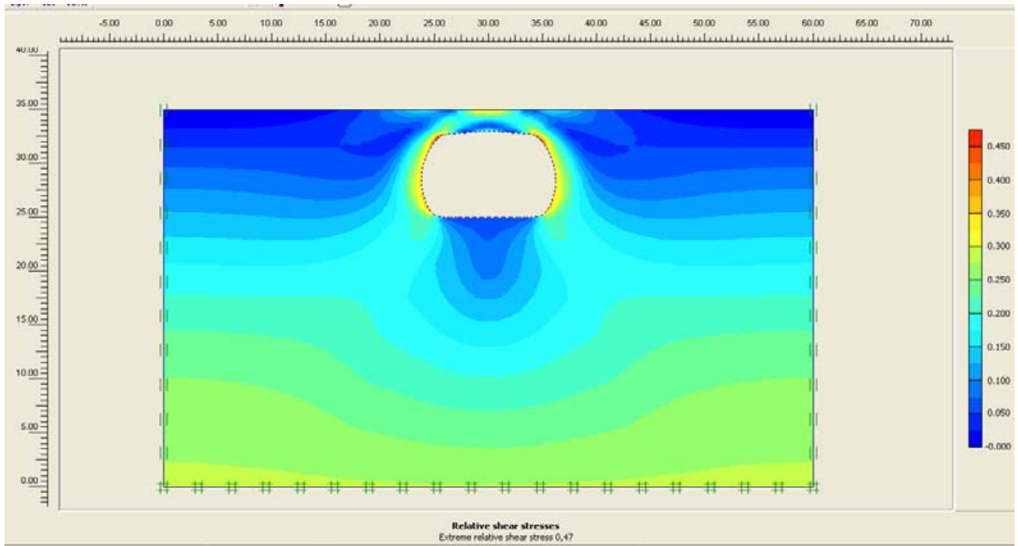

Figure 4.15c. Cave No: 28 Relative Shear Stress Without Loading

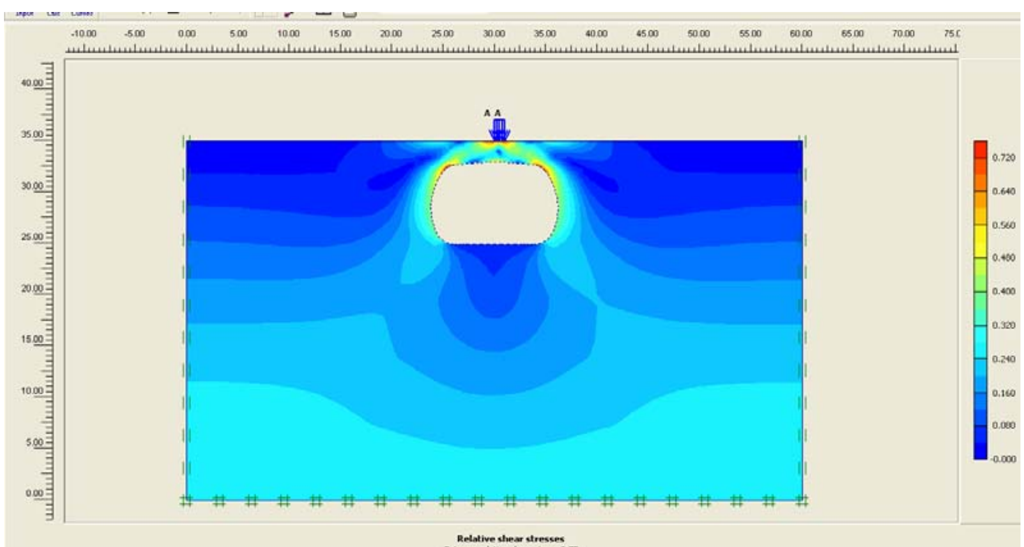

Figure 4.15d. Cave No: 28 Relative Shear Stress With Loading

4.3. Discussion

4.3.1. Effect of Cover Thickness and Width on Cave Stability

Waltham and Swift (2004) studied the effect of cover thickness on the stability of cave excavated in sandstone in Nottingham. They performed a plate load test on a roof of a cave and made an experiment in the laboratory to investigate the stability of the roof of the cave. They concluded that the most important factor in defining the stability of a loaded foundation pad directly over a cave is the thickness of rock that remains to form the roof. They found that when the cover thickness increases, the stability of the cave also increases. For 4 m wide cave, bearing capacity of the rock roof rises from 2 MPa where it is 1m thick to 8 MPa where 3m thick. It is also suggested as an engineering guideline that cover thickness should exceed 50% of cave width would appear to be reasonable for most construction projects on typical Karstic limestone.

Waltham and Park (2002) reported the existence of 59 lava tubes with a total length of 42 km in Cheju Island, South Korea. They discussed three different causes of the tube roof failure. These are collapse of the thin roof during the flow of lava, minor earthquakes that are common on active volcanoes, and weathering and weakening of the thin arches above the lava tubes. The authors proposed microgravity survey as the most useful method to determine the location of lava tubes during subsurface investigation. In this study, a simple guide is recommended for checking the stability of the lava tube roof. It is the tube width (W) to cover thickness (T) ratio. A ratio of $(W/T) < 3/1$ is suggested against safety of the lava tube roof failure.

Güzelbey (2004) investigated the stability problems of caves and cave settlements with a finite element software program. The study includes two dimensional model and analysis of the cave with variable cover thickness. The author found that the changes in cover thickness affect vertical displacement and consequently the stability of the cave.

In Table 4.16, factor of safety of the inspected caves in Gaziantep were calculated and risk conditions of the caves were given.

Table 4.16 Factor of Safety of the caves in Gaziantep

Cave no	District	Name of caves	Current status	Cover Thickness (m)	Width (m)	Height (m)	Length (m)	Factor of Safety
1	İsmet Paşa	Direkçi	Stable	1,8	33	14,8	70,15	3,14
2	Kurtuluş	Sumaklı	Stable	7	8,2	2,5	15,5	9,21
3	Kurtuluş	Sumaklı	Stable	8	25	6	5,6	4,32
4	Kurtuluş	Sumaklı	Stable	4	10	4	3	8,02
6	Kilinçoğlu	Kamalı Sk.	Stable	3	6	3,2	18	5,32
7	Delbes	Üzümcü	Stable	4	29	7,8	40	4,21
13	Hoşgör	Şht. Ahmet Sk.	Stable	2,5	1,5	1,8	3	9,95
14	Dumlupınar	Besihane	Stable	1,5	16	8	14	1,83
18	Çağlayan	Besni Cad.	Stable	1	15	7	5	2,52
19	Çağlayan	Besni Cad.	Stable	2	4	5	15	6,35
20	Aydınlar	Mezarlık	Stable	2	8	10	12	3,48
21	Aydınlar	Urfayolu	Stable	3,5	25	9	30	2,65
22	Umut	Besihane	Stable	10	8	15	18	3,92
27	Kilinçoğlu	Sulu	Stable	2	35	5	50	1,8
28	Dumlupınar	Boş	Stable	2	15	8	20	3,02

A ratio of (W/T) < 3/1 is suggested by Waltham and Park (2002) for the caves to be stable. When the stability of caves are checked from their W/T ratios, the caves 2, 3, 4, 6, 13, 19 and 22 seem to be safe. On the other hand, caves 1, 7, 14, 18, 20, 21, 27, and 28 are not safe according to this criteria.

According to You et al. (2005) during tunnel excavation, factor of safety is taken as 1.5 for long term stability. Moreover some interviews were held with professionals working in the industry of tunnel analysis. From those interviews, one of the interviewers, Tahir Kımıldar * , Vice General Manager of Tunnel Section in STFA Group, specified that the factor of safety for the tunnel design stability is taken as 1.5 for most of the projects which he had worked. In this analysis, all the calculated FS are greater than 1.5. These results support present state of the caves, since the caves are still stable.

*Personal interview with Tahir Kımıldar, Vice General Manager of Tunnel Section in STFA Group

Stability ratio suggested by Waltham and Park (2002) seems to work for some caves 2, 3, 4, 6, 13, 19 and 22. However for some caves which have higher W/T ratio than 3/1, this criteria does not work. This may be due to some factors such as strength of the rock, roof shape of the cave, and selected factor of safety. Stability can be attributed to the high compressive strength of limestone. Since the compressive strength of the limestone in Gaziantep ranged from 3.76 to 49.79 MPa **(Marangoz 2005)**, some of the limestone might have a very high compressive strength values. Waltham and Park (2002) did not mention about which factor of safety they have chosen for the criteria of W/T < 3/1. Therefore, it can be also explained with the chosen factor of safety number why W/T < 3/1 criteria is not sufficient for some caves.

Waltham and Swift (2004) explained that the choice of a guideline relating safe cover thickness to cave width is dependent on the factor of safety required. However, Waltham and Park (2002) has not specified any number for safety factor when they are finding W/T ratio. Most probably Waltham and Park (2002) have taken a high safety factor in their study when they find the W/T ratio as 3/1. Therefore, W/T ratio depends on the chosen number of safety factor. This study indicated that they have most probably taken FS around 4.00, for the W/T < 3.

While authors were suggesting W/T < 3, they did not mention about the shape of the roof (flat or arch). The analysis showed that roof shape has a great effect on the stability of the cave. Therefore, W/T ratio should be used with taking the other parameters into account.

Generally speaking, when the W/T ratio is increasing, which indicates that the stability of cave is decreasing, the factor of safety is also decreasing. This correspondence has some exceptions in this study such as Cave No:22 or Cave No: 1.

When Cave No:22 is taken into consideration, it can be seen that this cave has a low W/T ratio. However in spite of its low W/T ratio, its factor of safety is not that much high compare to other caves. This may be explained due to some facts at this cave. First of all due to a high cover thickness which is 10 m, the overburden pressure above this cave is much higher than the other caves. Therefore this extra loading on the cave affects the stability of the cave in a negative way. The other reason for low factor of safety could be the shape of the cave. The flat roof caves are less stable compare to arch roof caves. Hence this is the other factor that causes the cave to have a smaller factor of safety number. Moreover this cave has a low strength compare to other caves.

When Cave No:1 was investigated, even though this cave has the highest W/T ratio, its factor of safety is not small (FS = 3.14). This may be explained with roof shape of the cave, which is arch. Due to its arch shape and small overburden pressure, it can resist more stress, and therefore it stays stable. Also the strength of the rock is high compared to the other caves, which can also be accepted as an advantage for the stability of the cave. Due to these reasons, the factor of safety of this cave is higher than expected.

Other findings from this study can also be explained as: when the cover thickness increases, the maximum displacement and extreme relative shear stress decreases while the factor of safety of the cave increases. All the test results indicate that the stability of the cave is increased when the cover thickness of the cave is increased for the shallow depth caves. This was observed at the cave 2, 4, 6, 13, 22.

CHAPTER 5

CONCLUSIONS AND FUTURE WORKS

5.1 Conclusions

In this study, stability analysis of the fifteen existing caves in Gaziantep city center was investigated. Geometric dimensions of the caves and some geotechnical properties of the cave rock were taken from the previous studies. The caves were modeled in plane strain condition. Although, geometric dimensions of the analyzed caves are not perfectly fits the plane strain condition, it is the best alternative provided in Plaxis V8 program. Shear strength parameters (internal angle of friction and cohesion) and elastic properties (modulus of elasticity and Poisson's ratio) of the cave rocks were calculated using RocLab program. Stress analysis with and without loading were carried out and factor of safety against failure for each cave was calculated. All the conclusions are valid under studied conditions.

Following conclusions were drawn from the results of the analysis;

a. Minimum factor of safety against failure is 1.8 and maximum factor of safety is 9.9. These are all greater than 1.5, which indicates that all the investigated caves are safe against failure under studied conditions. Cave with the largest width has the smallest factor of safety that is 1.80. The cave with the smallest dimensions has the maximum factor of safety number that is 9.95.

b. When the cover thickness is decreased the stability of the cave rock is decreased. Among the investigated caves, the ones with thinner cover thickness such as Cave No:1 and Cave No:18 have smaller factor of safety and higher displacement values. From the results of the analyses, it can be seen that the caves with greater cover thickness and smaller width such as Cave No:2 and Cave No:13 are more stable.

c. The width of the cave plays an important role in its stability. It is found that when the width of the cave is increased the stability of the cave decreased. Furthermore, the width is also an important effect together with the cover thickness at the stability of caves. That is why, when the cover thickness get thinner, and the width gets higher, the stability of the cave can decrease dramatically.

d. When the roof shape of the cave is flat, stress concentrations occurs at the corners, and displacements at the mid span of the roof get higher. Meanwhile, the factor of safety against failure of the cave is decreasing. Some of the caves such as Cave No 3, 6, 7, 14, 19, 20, 21, 27 and 28 were analyzed with flat roof and arch roof. All the results indicate that the factor of safety is lower and the displacement is higher at the flat roof cave compare to arch roof cave. Therefore it can be concluded that, the arch roof cave is more stable than the flat roof cave under same conditions.

e. Under the applied load, the stability of the caves is decreasing since the factor of safety is decreasing and the extreme relative shear stress and maximum displacement are increasing. Stress analysis with and without loading shows the fact that under loading condition, especially with thinner cave roof, more relative shear stress occurs, the maximum displacements increase and factor of safety decreases. As a result, if the cave gets extra loads on its roof, the stability of the cave decreases. This result can be seen at all caves. Some caves have less effect of loading due to the their cover thickness and some have more effect of loading due to thin layer of cover thickness.

5.2 Future Work

Further investigation of this study could be the analysis of caves under different magnitude of load and loading combinations. The ultimate loading that yield the system to failure can be studied for each cave.

REFERENCES

Altanhan, H. (2002). "*Geotechnical properties of carbonic rocks occurring in Gaziantep- Şanlıurfa region."* M.Sc.Thesis in Civil Engineering, University of Gaziantep.

Aydin A. and Basu A. (2005), The Schmidt hammer in rock material characterization, Department of Earth Sciences, The University of Hong Kong, *Engineering Geology* 81 (2005) 1–14.

Bieniawski Z.T. Rock Mechanics Design in Mining and Tunneling, pp. 97-133. Balkema, Rotterdam (1984).

Cargill JS and Shakoor A. (1990), Evaluation of empirical methods for measuring the uniaxial compressive strength of rock. International Rock Mech Min Sci & Geomech Abstr 1990; 27:495-503.

Çanakcı H.,(Accepted on: 8 May, 2007), "Collapse of caves at shallow depth in Gaziantep city center, Turkey: a case study" *Environmental Geology,* 10.1007/s000254-007-0802-y.

De Freitas, (1979). *A Geology for Engineers.* 6th edition Formerly Reader in Engineering Geology, Imperial College of Science and Technology, London Lecturer in Engineering Geology, Imperial College of Science and Technology, London. pp. 130 – 131, 148 – 149. 171 – 173, 189 – 191.

Güzelbey B. (July 2004), *The finite element analysis of foundation of a structure of a constructed over sinkhole*, M.Sc. thesis submitted to school of natural and applied science, University of Gaziantep.

Hoek, E. 1994. Strength of rock and rock masses, *ISRM News Journal*, 2, 4-16.

Hoek E and Brown ET., 1980 *"Underground excavations in rock"* The Institution of Mining Metallurgy, London, 527.

Hoek E. and Diederichs M.S., February 2006 "Empirical estimation of rock mass modulus" *International Journal of Rock Mechanics and Mining Sciences* Volume 43, Issue 2, 203-215.

Hoek E., Kaiser P.K. and Bawden W.F. 1995. Support of underground excavations in hard rock. Rotterdam, Balkema.

Hoek E., Marinos P. and Benissi M. 1998. Applicability of the Geological Strength Index (GSI) classification for very weak and sheared rock masses. The case of the Athens Schist Formation. Bull. Engg. Geol. Env. 57(2), 151-160.

Hoek, E., Wood D. and Shah S. 1992. A modified Hoek-Brown criterion for jointed rock masses. Proc. Rock Characterization, Symp. Int. Soc. Rock Mech.: Eurock '92, (ed. J.A. Hudson), 209-214. London, Brit. Geotech. Soc.

Israely AA. Study of the engineering-geological characteristics of the bedrock in the Jerusalem area; Geological map, scale 1:100000 (in Hebrew). MSc Thesis, The Hebrew University Jerusalem, 1973.

Katz O, Reches Z, Lyakhovsky V, Baer G. Rock damage at the proximity of small faults: Field measurements of elastic wave velocity and elastic rebound. In: AGU 1999 Spring Meeting, EOS, Transaction, American Geophysical Union, 1999.

Katz O, Reches Z, Rogiers J.C., Evaluation of mechanical rock properties using a Schmidt Hammer, International Journal of Rock Mechanics and Mining Sciences. 37 (2000) 723-728.

Marangoz L. (2005), Correlation of geotechnical properties of limestone with ultrasonic pulse velocity in Gaziantep region. M.Sc. thesis submitted to school of natural and applied science, University of Gaziantep.

Marinos P and Hoek E. 2000. GSI – A geologically friendly tool for rock mass strength estimation. Proc. GeoEng2000 Conference, Melbourne Hoek, E. and Marinos, P. 2000. Predicting Tunnel Squeezing. Tunnels and Tunnelling International. Part 1 – November 2000, Part 2 – December, 2000.

Marinos P. and Hoek E. 2001. – Estimating the geotechnical properties of heterogeneous rock masses such as flysch. Accepted for publication in the Bulletin of the International Association of Engineering Geologists.

Marinos V., Marinos P., Hoek E., "The geological strength index: applications and limitations", *Building Engineering and Geolology Environment* (2005) 64: 55–65 DOI 10.1007/s10064-004-0270-5.

Sonmez H. and Gokceoglu C, (June, 2006) "Discussion of the paper by E. Hoek and M.S. Diederichs Empirical estimation of rock mass modulus" *International Journal of Rock Mechanics and Mining Sciences*, Volume 43, Issue 4, 671-676.

Terlemez I., Şentürk K., Sümengen M., Oral A. (1997), Türkiye jeoloji haritaları. No: 45 Jeoloji Etütleri Dairesi, Ankara.

Tolun N, (1975) Maden Tetkik ve Arama Enstitüsü Genel Müdürlüğü, Türkiye Jeoloji Haritası, Hatay. MTA Enstitüsü Yayınları, Ankara.

Waltham A.C., Park H.D. (2002, 18 January)., "Roads over lava tubes in Cheju Island, South Korea*" Engineering Geology*, 66 (2002) 53-64.

Waltham A.C., Swift G.M., (2004, 17 June) *"*Bearing capacity of rock over mined cavities in Nottingham", *Engineering Geology*, 75 (2004) 15-31.

You K., Park Y. And Lee J.S., (10 May, 2005), “Risk analysis for determination of a tunnel support pattern” *Tunneling and Underground Space Technology* 20 (2005) 479–486.

References from Electronic Sources:

General Information of Gap Provinces - Gaziantep:
http://www.gap.gov.tr/English/Ggbilgi/gantep.html

General Information about Plaxis V8, 2D Program:
http://www.plaxis.nl/index.php?cat=productinfo&mouse=Plaxis%20V8